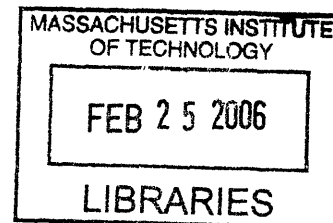


**EGF Receptor-mediated Fibroblast Signaling and Motility:
Role Of Nanoscale Spatial Ligand Organization**

By

Llewellyn B. Richardson III



B.S., Chemical Engineering, Virginia Polytechnic Institute and State University, 1999

SUBMITTED TO THE DEPARTMENT OF CHEMICAL ENGINEERING
IN PARTIAL FULFILLMENT OF THE REQUIREMENTS FOR THE DEGREE OF

Doctor of Philosophy in Chemical Engineering

at the

Massachusetts Institute of Technology

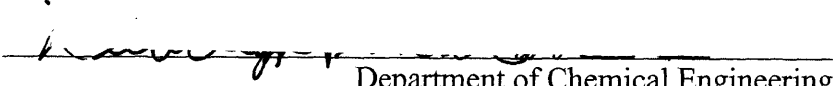
[February, 2006]


December, 2005

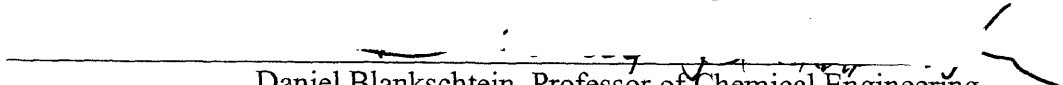
ARCHIVES

© 2005 Massachusetts Institute of Technology

All rights reserved

Signature of the Author: 
Department of Chemical Engineering

Certified by: 
Linda G. Griffith, Professor of Biological and Mechanical Engineering
Director of Biotechnology Process Engineering Center

Accepted by: 
Daniel Blankschtein, Professor of Chemical Engineering
Chairman, Committee for Graduate Students

EGF Receptor-mediated Fibroblast Signaling and Motility: Role Of Nanoscale Spatial Ligand Organization

by
Llewellyn B. Richardson III

Submitted to the Department of Chemical Engineering on December 7, 2005
in partial fulfillment of the requirements for the degree of
Doctor of Philosophy in Chemical Engineering

Abstract

Cell motility is often governed by growth factor receptor and integrin adhesion receptor interactions with the extracellular environment followed by collaborative intracellular signaling. While integrin ligands are necessarily bound within the extracellular matrix to permit force transduction by the cell, the canonical view of growth factors is of soluble molecules freely diffusible and internalizable by the cell. Recent evidence suggests that in some cases growth factor receptor ligands may be embedded in the extracellular matrix and may signal primarily from the cell surface. By altering the trafficking of receptor and ligand, the potential exists to change the spatiotemporal distribution of signaling within the cell. These changes in the magnitude, duration, and spatial localization of specific signals influence the biophysical regulation of cell migration, which is a multi-step process directed by a number of timely and spatially coordinated signaling events.

In this work, we develop a polymer incorporating both growth factors and adhesion molecules with nanoscale spatial ligand control to model matrix-embedded ligand presentation. The polymer is a poly(methyl methacrylate)-poly(ethylene oxide) (PMMA-g-PEO) comb copolymer that displays the ligands via 2-3 nm molecular tethers. Two forms of the polymer are employed, one in which epidermal growth factor (EGF) is tethered amidst an adhesive background of adsorbed fibronectin (FN) and a second in which EGF and a FN-like PHSRN-RGD peptide (SynKRGD) are simultaneously tethered. The surface densities of each ligand are independently controlled during their incorporation into the polymer. Thus, variation in substrate adhesiveness is achieved by adsorbing different densities of FN or by covalently tethering different densities of SynKRGD.

With these substrates, we use a model cell line of NR6 fibroblasts expressing the wild-type human EGF receptor (EGFR) to observe the effects of surface-tethered EGF on signaling, adhesion, and migration compared to the traditional soluble EGF presentation. Using the EGF-FN substrates, we determine that tethered EGF signals EGFR primarily at the cell-substrate interface. Tethered EGF, like soluble EGF, elicits enhanced migration speed with a biphasic dependence on FN density. However, the peak cell speed for tethered EGF is achieved at an order of magnitude greater FN density. Quantification of cell spread area suggests that tethered EGF reduces cell-substrate adhesion strength relative to soluble EGF. Although we are unable to conclusively attribute the biphasic curve shift on EGF-FN substrates to a specific signaling mechanism, we do observe a dependence of focal adhesion kinase (FAK) signal strength on substrate adhesiveness. Further investigation of EGFR phosphorylations and downstream motility-relevant

signals using the EGF-SynKRGD substrates reveals characteristics of tethered EGF signal transduction that are quantitatively distinct from soluble EGF and concomitantly influenced by integrin-mediated adhesion. These results underscore the complex synergy between EGFR and integrins while demonstrating the significance of spatial ligand presentation in regulating cell behavior.

Thesis Supervisor: Linda G. Griffith
Title: Professor of Biological and Mechanical Engineering,
Director of Biotechnology Process Engineering Center

*This work is dedicated to the Jones and Richardson families,
for whom obtaining knowledge through education
has always been a priority.*

Acknowledgements

Knowledge through education – it cannot be obtained without teachers who share with us and motivators who inspire us. I have been blessed with both during my six years at MIT. Looking back, I cannot believe how many people have touched my life. I only hope that I've been able to do the same for someone else.

I must first acknowledge my advisor, Linda Griffith, who gave me the freedom to learn. Sometimes it happened at the expense of failure, a learning experience in itself, but she was always there to pick me up and urge me onward. My thesis committee of Doug Lauffenburger, Anne Mayes, and Alan Wells provided invaluable advice and knowledge along the way from years of experience and very different perspectives. I offer a special thanks to Alan Wells, who although he resided the farthest away in Pittsburgh, seemed to be at my side with rapid email responses and warmly opened his lab to me for further learning.

Then there are those with whom you share almost every waking hour during the course of a Ph.D. program. From late nights in the lab to early mornings in the office, they teach you not just about science but about life. They exemplified to me why life is worth living. From Adam Capitano, I learned that perseverance pays off and that it's okay to embrace our nerdiness. I still have the dollar bill, and it pays me more and more each day. Lily Koo was an inspiration spiritually and always brought me back to the big picture. God has a plan for all of us, even if it requires being the senior student for longer than we desire. Maria Ufret showed me the value of listening to music in another language. If you sing loud enough, you can only hear yourself anyway. Thank you for kindly doing many things for me I could not bring myself to do but should have done. Eileen Dimalanta, thank you for your neverending encouragement and for the knowledge that you had been where I was. I enjoyed our "breaks", and I encourage you to never stop laughing; it makes everyone else feel so much better. Bart Hendriks, from many days in 56-389b to many nights spent with Bessie, you are an intelligent man who receives less credit than he deserves. One day I'll learn how to make a 10 point landing over the handlebars and dodge dollar bets like you. I'll miss the sun going down in Wampatuck, although the keys to my Jeep would be nice to have. Csani Varga, all I can say is with friends like you, who needs enemies? ☺ But I know you do it all out of love. "Moo" cows and scary gay guys with top hats – I know you didn't drop the dollars, but somehow I still think you were responsible. That leads me to Crash Langrill, the honorable "It's So Easy" Doctor of Biological Engineering. I only hope a scary gay guy with a top hat is in your future. For your livelihood and mine, I'm glad you found your people in California. Short visits are good enough for me. Neil Kumar, the DJ of the late night lab, I give you mad props as a superstar-to-be. When you're rolling in your Benz on Wall Street, don't forget the little guys who danced a lab jig in the wee hours and shared the 3am IHOP experience with you. Without Vivian Fan, I never would have graduated. Thanks for the contribution to my project, but thanks even more for camaraderie while doing it. And thank you, Kevin Janes, for sharing Vivian with me until the very end. I was able to commiserate during the thesis writing period with Ada Au, who is a promising scientist

but an even more promising musical talent. Keep following your dream, Ada. It inspires me.

I also had a long list of undergraduates and Masters students who worked on my project. When looking at the list, it's a wonder I did any of this work myself. I cannot thank my slew of REUs and UROPs enough, not only for the hours of lab work, but also for making it a fun experience and for returning me to my youth. David Yin and Mandy Hess, who completed Masters degrees alongside me, thank you as well. David always brought a smile to my face. Mandy, perpetrator of the infamous biphasic curve, I'm not sure if your biphasic curve got me out of here or kept me here longer than necessary. I would still like to go to that State dinner in Richmond.

A special thanks also goes to Lisa Joslin, Catherine Cresson, Maria Ufret, and Eileen Dimalanta for opening your couches to me when I had nowhere else to sleep. You saved me six months of rent and several otherwise sleepless nights.

Finally, I must thank my family for their support and encouragement along the way. My wonderful parents raised me to value education, to always do my best, and to persist through tough times, all of which were necessary for me to complete this long and difficult task. My beautiful, talented, and compassionate wife, Christy, I cannot thank you enough for helping me through the bad times and celebrating with me during the good ones. I am blessed to share my life with you. You are my rock, and without you this document never would have come to be.

Thanks Be to God...

Table of Contents

ABSTRACT	3
ACKNOWLEDGEMENTS	6
TABLE OF CONTENTS	8
1. INTRODUCTION	10
1.1 TETHERED GROWTH FACTORS IN PHYSIOLOGY AND TISSUE ENGINEERING	10
1.2 SPATIOTEMPORAL ASPECTS OF EGF RECEPTOR-MEDIATED SIGNALING	12
1.2.1 <i>EGFR Signaling Overview</i>	12
1.2.2 <i>EGFR Trafficking</i>	16
1.2.3 <i>Temporal Regulation of EGFR Signaling</i>	17
1.2.4 <i>Spatial Localization of EGFR Signaling</i>	18
1.3 EGFR AND INTEGRIN SYNERGY IN ADHESION AND MOTILITY	21
1.3.1 <i>Cell Adhesion in EGF-induced Motility</i>	21
1.3.2 <i>Integration of EGFR and Integrin Signaling</i>	22
1.4 MODEL SYSTEMS FOR SPATIAL CONTROL OF LIGAND PRESENTATION	26
1.5 SCOPE OF THESIS AND OBJECTIVES.....	28
1.6 REFERENCES	30
2. SURFACE TETHERED ADHESION LIGANDS AND GROWTH FACTORS	35
2.1 INTRODUCTION	35
2.2 EXPERIMENTAL METHODS	37
2.2.1 <i>Reagents</i>	37
2.2.2 <i>Cell Culture</i>	37
2.2.3 <i>PMMA-g-PEO Comb Polymer Synthesis</i>	38
2.2.4 <i>Activation of Comb 1 and Comb 2 to React with Primary Amines</i>	40
2.2.5 <i>Activation of Comb 2 to React with Sulfhydryls</i>	42
2.2.6 <i>Polymer Thin Film Preparation</i>	42
2.2.7 <i>EGF-FN Substrate Preparation</i>	43
2.2.8 <i>EGF-Peptide Substrate Preparation</i>	44
2.2.9 <i>Quantification of Protein and Peptide Densities</i>	46
2.2.10 <i>Cell Adhesion Assays</i>	47
2.3 RESULTS AND DISCUSSION.....	49
2.3.1 <i>Controlling Cell Adhesion to PMMA-g-PEO Comb Polymers</i>	49
2.3.2 <i>Tethered PHSRN-RGD Peptide Engenders $\alpha_5\beta_1$ and $\alpha_v\beta_3$ Integrin-mediated Adhesion</i>	53
2.3.3 <i>Optimization of Tethered EGF Density on EGF-FN Substrates</i>	59
2.3.4 <i>Nanoscale Control of Co-tethered Ligand Densities</i>	62
2.3.5 <i>Analysis of Tethered Ligand EGFR Homodimerization and Integrin Clustering</i>	65
2.3.6 <i>Tethering Other Growth Factors: Tenascin C EGF-Like Fragment 14</i>	71
2.4 REFERENCES	74
APPENDIX: ESTIMATION OF RECEPTOR OCCUPANCY ON TETHERED EGF SUBSTRATES	76
3. TETHERED AND SOLUBLE EGF DIFFERENTIALLY AFFECT FIBROBLAST MIGRATION AND ADHESION	77
3.1 INTRODUCTION	77
3.2 EXPERIMENTAL METHODS	80
3.2.1 <i>Reagents</i>	80
3.2.2 <i>Cell Culture</i>	80
3.2.3 <i>Cell Migration and Adhesion Assay</i>	80
3.2.4 <i>Migration Speed and Spread Area Data Analysis</i>	81
3.3 RESULTS AND DISCUSSION.....	83

3.3.1	<i>Tethered EGF Requires Increased Substrate Adhesiveness to Induce Maximal Migration Speed</i>	83
3.3.2	<i>Tethered EGF Reduces Cell-Substrate Adhesion Strength Relative to Soluble EGF</i>	86
3.4	REFERENCES	88
4.	SPATIOTEMPORAL SIGNAL REGULATION BY TETHERED EGF	89
4.1	INTRODUCTION	89
4.2.1	<i>Reagents</i>	91
4.2.2	<i>Cell Culture</i>	91
4.2.3	<i>Phospho-EGFR Immunostaining</i>	92
4.2.4	<i>Western Blot</i>	93
4.2.5	<i>Densitometry</i>	94
4.2.6	<i>Tethered EGF Release Assay</i>	94
4.2.7	<i>BOC Assay for Calpain Activity</i>	94
4.3.1	<i>Tethered EGF Spatially Restricts EGFR Activation to Cell Surface</i>	96
4.3.2	<i>Variation in EGFR Activation by Tethered EGF Surface Density</i>	97
4.3.3	<i>Tethered EGF Reduces EGFR Degradation</i>	101
4.3.4	<i>ErbB2 is Activated by Tethered EGF</i>	105
4.3.5	<i>Tethered EGF Activates ERK and Enhances Akt and FAK Signaling</i>	107
4.3.6	<i>ERK Phosphorylation Depends on Adhesion and EGF Presentation</i>	109
4.3.7	<i>Tethered EGF Elicits Calpain Activity</i>	114
4.3.8	<i>FAK Phosphorylation Depends on Adhesion Ligand Density and EGF Presentation</i>	115
4.3.9	<i>Variation in FAK and ERK Phosphorylation on EGF-FN Substrates</i>	120
4.4	DISCUSSION	125
4.4.1	<i>Matrikine Growth Factors: Avidity Signaling Via Spatially Restricted EGFR</i>	125
4.4.2	<i>Spatiotemporal Governance of Specific Signals</i>	126
4.4.3	<i>Signal Regulation By Adhesion and EGF Presentation</i>	128
4.5	REFERENCES	133
5	CONCLUSION AND FUTURE DIRECTION	136
5.1	CONCLUSION	136
5.2	FUTURE DIRECTION	138
5.3	REFERENCES	139

1. Introduction

1.1 *Tethered Growth Factors in Physiology and Tissue Engineering*

A fundamental goal of tissue engineering is to repair or replace damaged tissues or organs by fabricating living tissue substitutes. This may be accomplished through *in situ* directed tissue development or by *ex vivo* tissue growth and transplantation. Regardless of the approach, tissue engineers must create environments conducive to cell survival, organization, and function. This requires synthetic or native-derived materials capable of providing chemical and mechanical signals to promote tissue development. The current generation of tissue engineering biomaterials incorporates signaling peptides to mimic biochemical aspects of the extracellular matrix (ECM) that are responsible for controlling cell adhesion, proliferation, migration, and differentiation. In addition, tethering peptides or growth factors to biomaterial scaffolds permits their localization at sites of tissue organization over the necessary timescales of hours and days. Ongoing pursuits to develop tethered growth factor and adhesion peptide scaffolds to direct adhesion, proliferation, and differentiation of connective tissue progenitor cells into bone exemplify this principle.

Much of our knowledge of the role of growth factors in physiological processes comes from *in vitro* biochemical and cell response studies using the soluble forms of ligands. However, *in vivo* many signaling moieties may be physically restrained to signal at the cell surface. Molecules that are embedded in or strongly bound to ECM include EGF-like repeats in tenascin C and laminin 5 (Schenk et al. 2003; Swindle et al. 2001) as well as heparin-binding EGF-like growth factor (HB-EGF) and amphiregulin which bind to heparin and heparan sulfate proteoglycans (Piepkorn et al. 1998; Raab and Klagsbrun 1997). Several

EGFR ligands, including transforming growth factor- α (TGF α), HB-EGF, and amphiregulin, are synthesized as transmembrane forms that may be cleaved by metalloproteinases and released as soluble factors (Iwamoto et al. 1999; Ono et al. 1994; Piepkorn et al. 1998; Yang et al. 2000). However, it has also been suggested that these ECM-tethered or cell surface-tethered moieties act in a matrikine or juxtacrine fashion, signaling cells in their substrate-bound forms (Dong et al. 2005; Harris et al. 2003a; Piepkorn et al. 1998; Tran et al. 2004).

Spatiotemporal differences in signaling and trafficking arising from surface-restricted signaling may regulate cell responses. This impacts our ability to mimic and manipulate physiology in engineering tissues via growth factor-delivering biomaterials. Therefore, we seek to understand how tethering a growth factor to an extracellular substrate alters the cue-signal-response relationship as it is typically viewed in the case of a soluble factor. To do so, we consider the spatiotemporal aspects of signaling and trafficking as well as the integration of integrin and growth factor receptor regulation in the context of a well characterized ligand-receptor model, epidermal growth factor (EGF) and its receptor (EGFR).

1.2 Spatiotemporal Aspects of EGF Receptor-mediated Signaling

1.2.1 EGFR Signaling Overview

EGFR is a 170 kDa transmembrane receptor with intrinsic tyrosine kinase activity. It was the first such receptor tyrosine kinase discovered and is one of four homologous members of the receptor family bearing its name. EGFR is arguably the most frequently studied and best characterized growth factor receptor. It is responsible for regulating many cell responses, including proliferation, migration, and differentiation and is found in most primary cells *in vivo*. In addition, it is expressed at various levels in most cell lines (Wells 1999). EGFR knockout mice generally die during gestation or shortly after birth with severe defects in skin, lungs, gastrointestinal tract, brain, and liver (Jorissen et al. 2003). Seven known EGFR ligands with different binding affinities and trafficking properties exist. The list of ligands consists of EGF, TGF α , HB-EGF, amphiregulin, betacellulin, epiregulin, and epigen (Harris et al. 2003b). Studies of physiological changes in neonatal mice reveal precocious eyelid opening and tooth eruption in response to TGF- α and EGF (Smith et al. 1985; Topham et al. 1987).

Multiple signaling pathways following EGFR activation have been mapped. Figure 1.1 illustrates the diverse signaling network downstream of different pairs of EGFR family members.

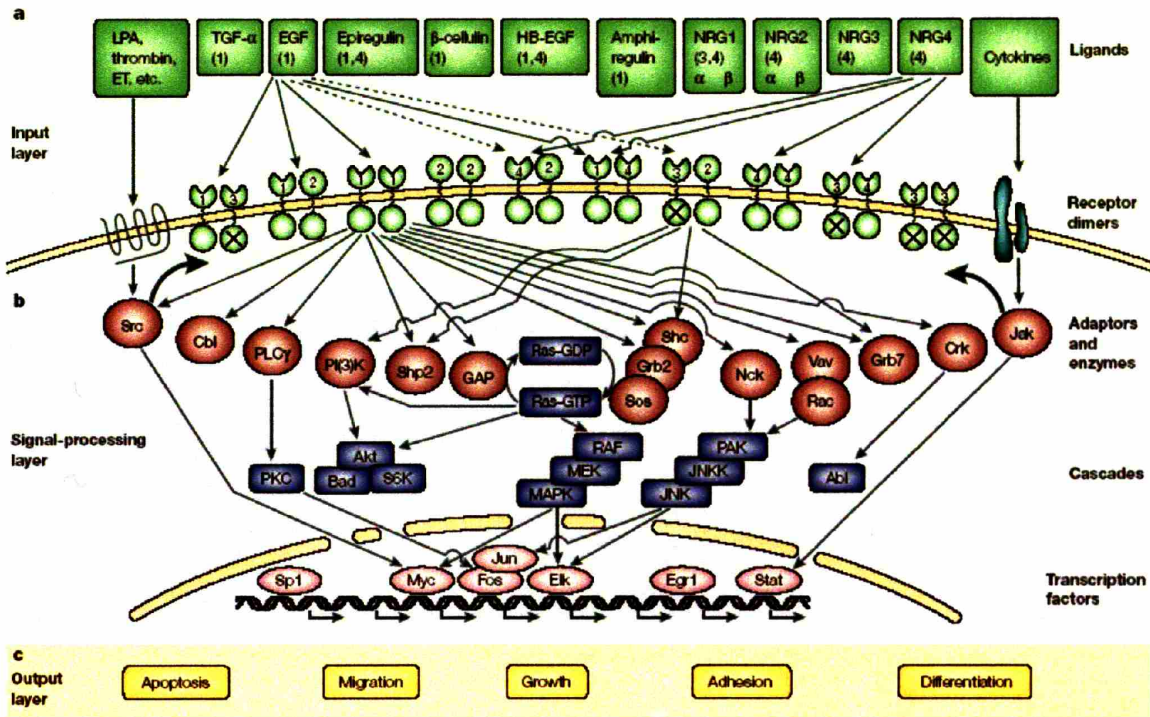


Figure 1.1 – Signaling pathways downstream of EGFR family of receptors.

A large network of signaling pathways downstream of the EGFR family of receptors has been determined. Some may be specific to ligand or receptor dimers, while others display redundancy by being activated by multiple inputs. *Figure taken from (Yarden and Sliwkowski 2001).*

The majority of signaling pathways have been determined by EGFR homodimers, although some, including Akt and ERK/MAP kinase, may be activated by multiple combinations of EGFR family members (Yarden and Sliwkowski 2001). Some of the signaling pathways induce transcription factors while others have been linked to specific biophysical mechanisms governing aspects of cell proliferation and motility. Figure 1.2 illustrates three such biophysical regulators, phospholipase C- γ (PLC γ), extracellular signal-regulated kinase (ERK), and focal adhesion kinase (FAK), whose functions are particularly relevant to this thesis. With all the knowledge about its activation mechanisms, signaling, and cell responses, EGFR provides an excellent model receptor system for studying tethered growth factor physiology.

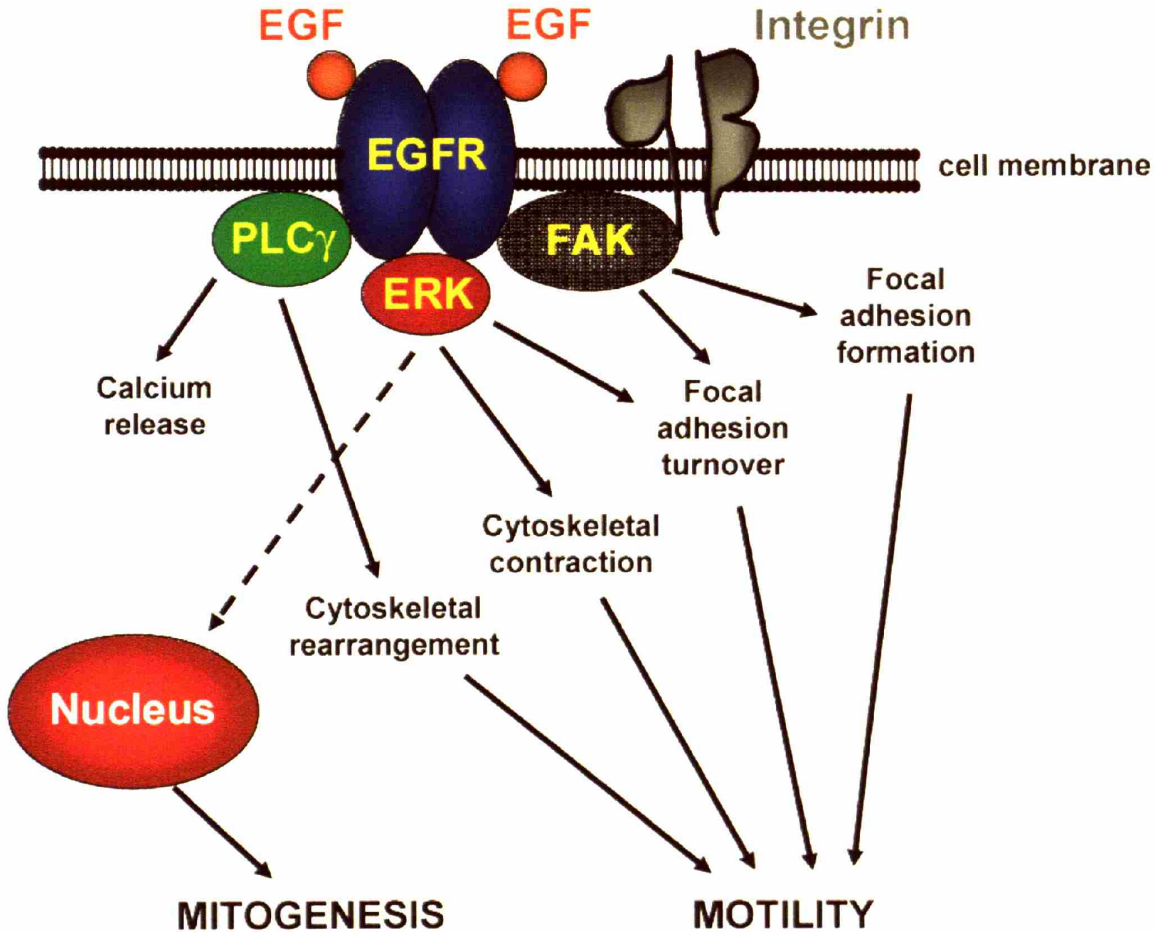


Figure 1.2 – Biophysical mechanisms of EGFR signaling.

Phospholipase C- γ (PLC γ), extracellular signal-regulated kinase (ERK), and focal adhesion kinase (FAK) have been linked to regulation of several biophysical mechanisms important in cell motility and proliferation.

EGFR-mediated signaling requires the binding of ligand to the receptor followed either by homodimerization with another EGFR or heterodimerization with another EGFR family member. Dimerization permits receptor activation, which is characterized by the phosphorylation of various tyrosine residues in the EGFR tail by intrinsic kinase activity (Schlessinger 2002). Activated EGFRs then bind downstream signaling targets such as adaptor molecules, docking proteins, and kinases. Several important tyrosine residues in the

EGFR tail are shown in Figure 1.3 along with reported downstream targets. The bound effector molecules are themselves activated via tyrosine, serine, or threonine phosphorylations and act on other molecules as part of intracellular signaling cascades (Jorissen et al. 2003). These numerous signaling pathways may be shared by multiple receptor types, are often compartmentalized, and occur over a broad range of timescales, providing for versatile regulation of cell function.

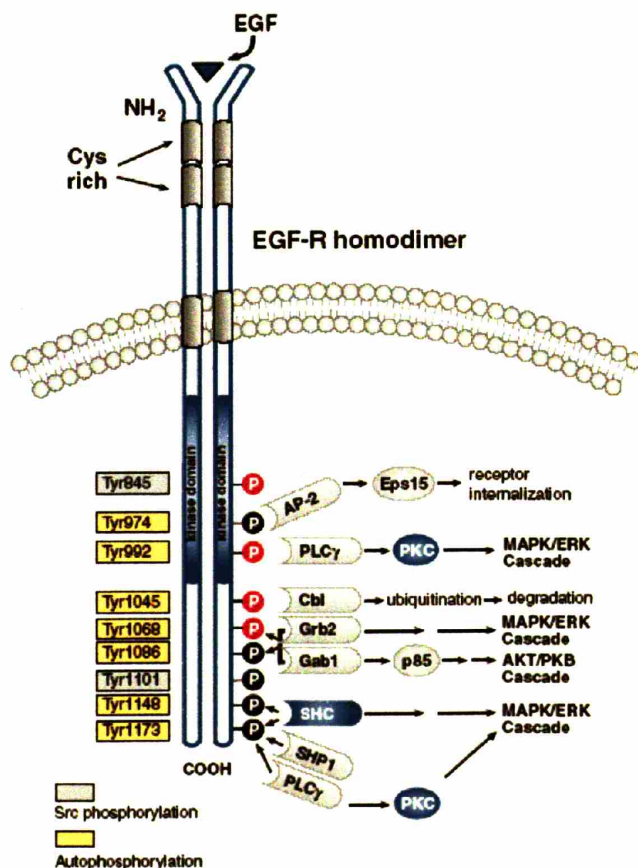


Figure 1.3 – Tyrosines phosphorylated in the cytoplasmic EGFR tail during activation.

A number of tyrosines located within the cytoplasmic tail of EGFR are phosphorylated during receptor activation. Specific tyrosine residues may be responsible for activation of particular downstream effector molecules, although some tyrosines bind multiple downstream targets and several targets are themselves activated by more than one phosphorylated tyrosine. *Figure taken from product datasheet for Cell Signaling EGFR antibodies; <http://www.cellsignal.com/pdf/2232.pdf>.*

1.2.2 EGFR Trafficking

A significant event following EGFR activation is the internalization of ligand-receptor complexes by clathrin-mediated endocytosis as depicted in Figure 1.4. Endosomes of the internalized receptors and ligands are sorted such that their occupants are either degraded or recycled back to the cell surface. While the exact mechanism of sorting is not precisely known, the binding of c-Cbl to Y1045 on EGFR promotes ubiquitination of the receptor, which may target EGFR to lysosomes for degradation (Levkowitz et al. 1999; Levkowitz et al. 1998).

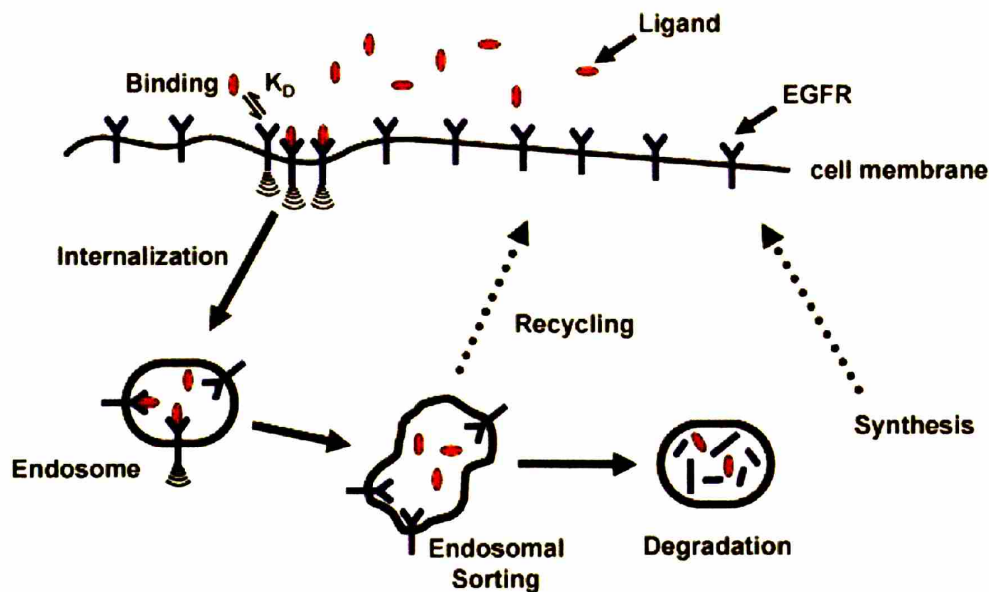


Figure 1.4 – EGFR-mediated binding and trafficking.

The EGFR-mediated process is characterized by binding of ligand to EGFR at the cell surface, dimerization of bound receptors, and internalization of the ligand-receptor complex into endosomes. The ligand-EGFR complex is sorted in the late endosome either to be recycled to the cell surface or degraded in lysosomes.

An important determining factor in endosomal sorting to degradation or recycling is how long the ligand remains bound to the internalized receptor (Wiley and Burke 2001). This is specific to the binding affinity of the ligand at acidic endosomal pH. Whereas EGF remains bound to EGFR in the endosome resulting in lysosomal degradation of the receptor and ligand, TGF α is released from the receptor at endosomal pH, and the receptor is preferentially recycled to the cell surface (French et al. 1995). As discussed in the next two sections, internalization and ligand-specific sorting of activated EGFR's provide a means of spatiotemporal regulation of signaling.

1.2.3 Temporal Regulation of EGFR Signaling

The timescale over which intracellular signaling occurs is important in regulating biophysical processes and determining cell response. The canonical example of different growth factors, EGF and nerve growth factor (NGF), producing distinct responses in PC12 cells is attributed to the transient versus sustained timescales of extracellular signal-regulated kinase (ERK) elicited by each (Traverse et al. 1992). Thus, we must consider the mechanisms regulating signal duration to understand the influence that a tethered growth factor might have on them.

The degradation of ligand and receptor following internalization is a major mechanism for signal attenuation. By depleting receptors and ligand from the cell membrane and ECM, respectively, cells effectively desensitize themselves by reducing the extracellular stimulus and the surface-sampling receptor (French et al. 1995; Wiley 2003). It has been postulated that recycling or deficient internalization may permit a more sustained signal (Reddy et al. 1994; Wiley 2003). A direct correlation of trafficking phenomena with the proliferative response in fibroblasts has been demonstrated. At low ligand concentrations,

EGF is a more potent mitogen than TGF α because TGF α -bound receptors are preferentially recycled to the cell surface resulting in greater ligand depletion. In receptor-limited situations, the converse is true due to faster surface receptor depletion by EGF. (Reddy et al. 1996; Reddy et al. 1998).

Distinct from signal attenuation by internalization and degradation, phosphatase activity also modulates the timescale of EGFR signaling. Intact EGFRs and their downstream substrates are frequently inactivated by phosphatase dephosphorylation of various amino acid residues. For example, the phosphatase SHP1 binds and dephosphorylates EGFR tyrosine 1173 (Keilhack et al. 1998), while Grb2 is targeted by the phosphatase RPTP α (den Hertog et al. 1994). Phosphatases have also been reported to increase signal duration by competing with other regulators for specific sites on EGFR. SHP2 dephosphorylation of EGFR tyrosine 992 permits prolonged ERK signaling by blocking the activation of Ras GTPase-activating protein (RasGAP), a negative effector of the Ras/MEK/ERK pathway (Agazie and Hayman 2003). Since phosphatases appear to be specific to certain sites on the receptor tail or particular downstream molecules, they may negatively or positively regulate the duration of specific EGFR-mediated signals (Haugh et al. 2004).

Thus, the cell has both global and pathway specific mechanisms to temporally regulate signaling. Unfortunately, the particular biophysical roles of signal duration are not completely understood. They are typically specific to cell type and signaling pathway, adding to the complexity of the cue-signal-response relationship.

1.2.4 Spatial Localization of EGFR Signaling

Another facet of EGFR-mediated signaling that governs biophysical processes is its spatial distribution. A cell consists of many organelles and dynamic internal structures that

inhibit the free diffusion of signaling molecules. Molecules are recruited and bound specifically to structures like the cell membrane, cytoskeleton, or internalized vesicles as well as to precise groups of complementary molecules via scaffold proteins (Morrison and Davis 2003; Sorkin and Von Zastrow 2002). This creates a set of compartments whereby signal effectors are spatially localized to perform particular functions.

It has been demonstrated that internalized ligand-receptor complexes may remain activated within the cell, prolonging EGFR-mediated signals and facilitating their transport to cytoplasmic and perinuclear regions (Burke et al. 2001). Some pathways are activated specifically at the cell membrane; others act in the vicinity of endosomal compartments. The phospholipase C- γ (PLC- γ) pathway is functional only at the cell membrane due to a lack of available phosphoinositide substrates in the endosomal membrane (Haugh and Meyer 2002; Haugh et al. 1999b). Eps8, a molecule involved in EGFR signaling and trafficking, and c-Cbl, a regulator of EGFR degradation, associate primarily with internalized EGFR (Burke et al. 2001). The availability of different subsets of EGFR substrates located in spatial compartments expands the functionality of the receptor while providing spatially localized control.

In contrast, some signaling pathways operate ubiquitously. Ras is phosphorylated both at the cell surface and within endosomes, resulting in ERK activity throughout the cell (Haugh et al. 1999a; Kempiak et al. 2003). However, spatial distinctions may remain even within the ubiquitous ERK cascade. Two adaptor proteins having overlapping functions in the ERK pathway, Grb2 and Shc, display different spatial distributions. Grb2 preferentially associates with cell surface EGFR while Shc binds equally to surface and internalized EGFR (Burke et al. 2001). This may permit an altered balance of membrane-proximal versus

cytoplasmic signaling as well as localize diverse pools of ERK having distinct functional responsibilities. For example, focal adhesion disassembly by m-calpain activity occurs at the cell membrane and is attributed to a membrane-proximal pool of ERK (Glading et al. 2004; Glading et al. 2001), while cytoplasmic ERK is likely to play a regulatory role in other biophysical mechanisms.

The spatial localization of specific EGFR-mediated signals provides control of multiple biophysical processes in different cellular compartments by the receptor. As a result, it may also permit the cell to distinguish between different EGFR ligands by their affinity or presentation. This may be a key factor in coordinating a multi-step response like migration or even dictate a distinct cell response.

1.3 *EGFR and Integrin Synergy in Adhesion and Motility*

1.3.1 Cell Adhesion in EGF-induced Motility

EGF is well known to induce cell motility in fibroblasts via EGFR activation. The migration response involves a sequence of coordinated steps in which the cell extends its membrane, forms a stable frontal adhesion polarizing the cell, exerts contractile forces across its cytoskeleton, and preferentially releases rear adhesions to permit the cell to move forward (Lauffenburger and Horwitz 1996). Thus, as one of multiple processes contributing to motility, cell adhesion in a migrating cell is quite dynamic. It relies upon the timely and spatially controlled formation and disassembly of focal adhesions, which must be coordinated with membrane extension, cytoskeletal reorganization, and contractile force generation. While these other processes seem to be mediated primarily by biochemical events downstream of EGFR, a significant body of literature exists demonstrating a synergistic governance of cell adhesion by EGFR and integrins.

On the characteristic response level, EGFR-mediated migration requires that proper strength be present in cell-substratum adhesions. If adhesion between the cell and substrate is too weak, the cell cannot create the stable adhesions necessary for locomotion following membrane extension. If adhesion is too great, the cell cannot detach its rear in response to contractile forces. The proper adhesion strength should be in balance with contraction forces generated in the cell. Thus, a biphasic relationship between migration speed and adhesion strength is predicted (DiMilla et al. 1991). This has been validated experimentally for EGF-induced fibroblast migration on varying densities of fibronectin (Maheshwari et al. 1999).

To explain how integrin-mediated adhesion strength is physically modulated, these experiments were also conducted on substrates displaying varying global and local cluster

densities of the integrin ligand, RGD. It was determined that the nanoscale ligand cluster density is a primary factor in modulating integrin-mediated adhesion strength to allow cell migration (Maheshwari et al. 2000). Integrin clustering not only serves as a physical mechanism for increasing adhesion strength. It also recruits cytoskeletal and signaling molecules to focal complexes on which both integrins and EGFR act to induce and regulate cell motility (Comoglio et al. 2003; Miyamoto et al. 1995b).

1.3.2 Integration of EGFR and Integrin Signaling

EGFR and integrins are known to collaborate as regulators of cell adhesion and motility through a variety of mechanisms. Certain signals involving both receptors may contribute to the formation or stabilization of focal adhesions while others are responsible for their turnover. Exactly how the myriad mechanisms are integrated to govern biophysically is not completely understood, but several revealing observations have been made.

EGFR and integrins have been shown to cluster on the cell membrane in supramolecular complexes that include shared effector molecules (Moro et al. 2002). Thus, it is not surprising that they modulate each other's activity via indirect and direct methods of inside-out signaling and transactivation. In some instances, activated EGFR's prime integrins for matrix attachment by increasing their affinity for ligand (Pichard et al. 2001); other times, they may signal an increase in integrin expression levels (Narita et al. 1996). Interestingly, EGFR can act as a positive *or* negative regulator of integrin-mediated adhesion dependent upon its own expression level (Genersch et al. 1996). Integrins conversely modulate EGFR activity. In fact, integrin-mediated adhesion is necessary for complete ligand activation of the receptor and potentiation of its downstream signals (Bill et al. 2004; Miyamoto et al. 1996). Unligated EGFRs become phosphorylated as well by clustered integrins. However, the

magnitude, timescale, and phosphorylation pattern are uniquely different from EGF-induced receptor activation (Moro et al. 2002). This may provide the cell with the ability to distinguish between adhesion and growth factor-mediated signals through the same receptor. Thus, the synergistic relationship between EGFR and integrins is one of mutual signal initiation and regulation.

Interestingly, the downstream pathways that EGFR and integrins influence overlap, illustrating further integration of these receptors' roles within the cell. EGFR and integrin crosstalk is exemplified by their collaborative signaling through ERK and focal adhesion kinase (FAK). EGF-bound EGFR mediates robust ERK phosphorylation, but integrins elicit transient low-level ERK phosphorylation by activating unligated EGFR during the early phases of cell adhesion (Bill et al. 2004; Miyamoto et al. 1996; Moro et al. 1998). This is most likely related to the different pattern of integrin-mediated EGFR phosphorylation (Moro et al. 2002). Meanwhile, FAK localizes to focal adhesions where it forms complexes with EGFR and the β_1 cytoplasmic integrin tail (Crowe and Ohannessian 2004; Sieg et al. 2000). It is subsequently autophosphorylated on tyrosine 397 which is responsible for the kinase activity that leads to other phosphorylations within the molecule. Other signaling and structural molecules like Src, paxillin, talin, and Grb2 are recruited to the multiple FAK phosphorylation sites as depicted in Figure 1.5. Thus, FAK localizes a number of proteins with varying roles in adhesion and growth factor signaling to focal adhesions (Schlaepfer and Mitra 2004).

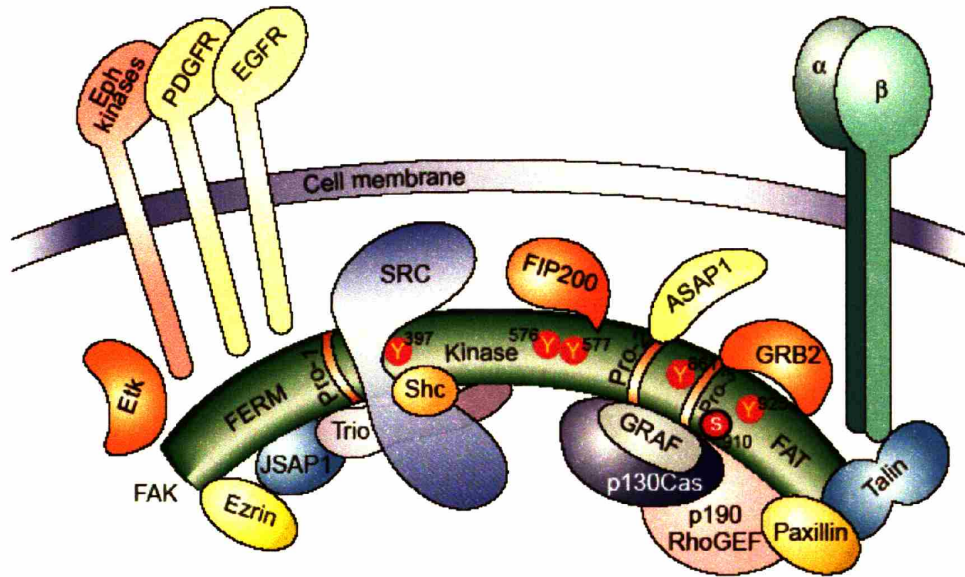


Figure 1.5 – FAK interaction with growth factor receptors, integrins, and signaling proteins. FAK complexes with EGFR and integrins and recruits structural and signaling proteins to focal adhesions. *Figure taken from (Schlaepfer and Mitra 2004).*

ERK and FAK are particularly important in contributing to the dynamics of cell adhesion during motility. ERK-mediated m-calpain activity is required for de-adhesion in EGF-induced cell migration (Dourdin et al. 2001; Glading et al. 2000). It operates by cleaving talin in focal adhesions, which permits the disassembly of other focal adhesion components such as zyxin (Franco et al. 2004). FAK also promotes focal adhesion turnover and is required for EGFR-mediated motility (Sieg et al. 2000). It apparently acts as an adaptor protein and recruits a complex including ERK and m-calpain to focal adhesions as illustrated in Figure 1.6. By localizing the calpain protease and its upstream activator to membrane sites of cell-substratum adhesion, FAK maximizes its proteolytic activity leading to the disassembly of focal adhesions (Carragher et al. 2003; Cuevas et al. 2003). Thus, the ERK pathway and FAK both are co-regulated by EGFR and integrins, eventually converging to modulate the same biophysical de-adhesion mechanism within cell motility.

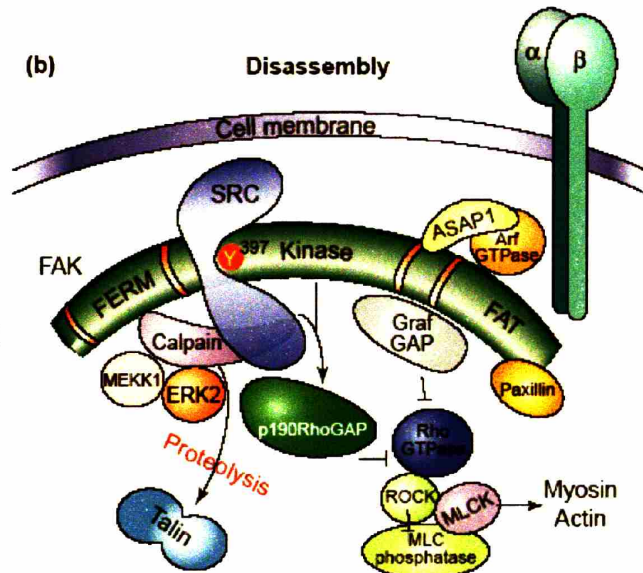


Figure 1.6 – Cooperative FAK and ERK-mediated calpain activity in focal adhesion disassembly. FAK localizes ERK and m-calpain to focal adhesions to promote their proteolytic disassembly. *Figure taken from (Schlaepfer and Mitra 2004).*

1.4 Model Systems for Spatial Control of Ligand Presentation

Polymeric systems are often used to present biologically active ligands to cells to observe cell-substrate interactions within a controlled environment. They offer the ability to resist non-specific protein adsorption, thereby reducing the confounding effects of numerous serum ligands that often adsorb to material surfaces at high densities. This is typically accomplished by incorporating poly(ethylene oxide) (PEO) segments (Jeon and Andrade 1991). Polymeric systems also allow for the presentation of biological ligands with control of ligand density and release rate. As such, they provide good models to study specific ligand-receptor interactions.

We are interested in observing the spatiotemporal effects of ligand presentation on downstream signaling and cell responses for EGFR and integrins. In previous work, polymer models have frequently displayed the integrin-binding RGD sequence found in several extracellular matrix molecules. A number of cell types and responses have been investigated (Hersel et al. 2003). Kao et al. studied the adhesion and foreign body reaction of macrophages to peptide-grafted interpenetrating polymer networks (Kao and Hubbell 1998; Kao et al. 2001). Others have studied osteoblast and fibroblast adhesion to RGD-modified PEO-based and hyaluronic acid (HA)-based hydrogels (Burdick and Anseth 2002; Park et al. 2003). In addition, RGD-modified star PEO polymers and PMMA-PEO comb polymers were developed to parse particular aspects of integrin-mediated adhesion and motility in fibroblasts. (Irvine et al. 2001; Koo et al. 2002; Maheshwari et al. 2000)

Growth factors like EGF have also been incorporated into naturally derived and synthetic polymers. These systems are more complex, requiring the presence of both the growth factor and an adhesion moiety to sustain cell attachment and function. The multiple

ligand requirement complicates the functionalization schemes needed to create growth factor-presenting substrates (Hubbell 2003). Sakiyama-Elbert et al. demonstrated covalent attachment of VEGF as well as heparin binding of bFGF and NGF to innately adhesive fibrin matrices (Sakiyama-Elbert and Hubbell 2000a; Sakiyama-Elbert and Hubbell 2000b; Zisch et al. 2001). Kuhl and Griffith covalently tethered EGF to two-dimensional star PEO polymer substrates. They engendered hepatocyte adhesion by adsorbing type I collagen in the star polymer interstices (Kuhl and Griffith-Cima 1996). Others have incorporated TGF- β , EGF, and bFGF into RGD-modified PEO-based hydrogel scaffolds (DeLong et al. 2005; Gobin and West 2003; Mann et al. 2001). Positive effects on mitogenesis, neurite extension, migration, and matrix production have been observed in these various substrate-bound growth factor systems.

A complete understanding of EGFR and integrin interactions with their ligands necessitates variation in the ligand concentrations presented to cells. As noted earlier, effective integrin-mediated adhesion requires nanoscale integrin aggregation (Miyamoto et al. 1995a), and ligated EGFR activation occurs via receptor dimerization (Schlessinger 2002). Since signaling and phenotypic responses depend on global and nanoscale local ligand densities, model substrates are particularly beneficial if they provide control of each. In this regard, the star PEO polymer (Kuhl and Griffith-Cima 1996; Maheshwari et al. 2000) and the PMMA-PEO comb polymer (Koo et al. 2002) have been used successfully to characterize the nanoscale integrin clustering in EGF-induced motility as well as in force-induced adhesion. As such, they are good candidate polymer platforms to present multiple ligands for the study of EGFR-integrin synergy.

1.5 Scope of Thesis and Objectives

This thesis focuses on the nanoscale spatial control of growth factor receptor and integrin-mediated signaling in cell adhesion and motility. The integration of growth factor receptor and integrin signaling is receiving much attention in cell biology. We approach the subject from a tissue engineering perspective by using an ECM-like biomaterial that mimics matrix-embedded growth factors and integrin ligands to study how surface-restricted ligands alter the regulation of adhesion and motility by EGFR and integrins. While an overall goal of tissue engineering is to create materials that interact with cells and tissues to promote macroscale organized growth and repair, it is imperative that we understand specific regulatory mechanisms that contribute to the process on the molecular and cellular levels, which is the purpose of this dissertation. In particular, the work has three specific aims:

1. Develop and characterize surfaces that simultaneously present tethered EGF and integrin ligands to cells with control of nanoscale spatial ligand organization and cell adhesion properties.
2. Observe enhanced fibroblast motility in response to tethered EGF compared to soluble EGF, specifically measuring migration speed as a function of cell-substrate adhesion.
3. Evaluate and understand the spatiotemporal aspects of EGFR activation by tethered versus soluble EGF as well as their impact on the synergistic properties of motility-regulating signaling pathways downstream of both EGFR and integrins.

While the scientific goal of my work is to achieve a greater understanding of spatial regulation of EGFR and integrin-mediated cell signaling and motility, my hope is that during

the course of this dissertation I reveal new insights into important parameters whose control may aid in the development of successful tissue engineering therapies.

1.6 References

- Agazie YM, Hayman MJ. 2003. Molecular mechanism for a role of SHP2 in epidermal growth factor receptor signaling. *Mol Cell Biol* 23(21):7875-86.
- Bill HM, Knudsen B, Moores SL, Muthuswamy SK, Rao VR, Brugge JS, Miranti CK. 2004. Epidermal growth factor receptor-dependent regulation of integrin-mediated signaling and cell cycle entry in epithelial cells. *Mol Cell Biol* 24(19):8586-99.
- Burdick JA, Anseth KS. 2002. Photoencapsulation of osteoblasts in injectable RGD-modified PEG hydrogels for bone tissue engineering. *Biomaterials* 23(22):4315-23.
- Burke P, Schooler K, Wiley HS. 2001. Regulation of epidermal growth factor receptor signaling by endocytosis and intracellular trafficking. *Mol Biol Cell* 12(6):1897-910.
- Carragher NO, Westhoff MA, Fincham VJ, Schaller MD, Frame MC. 2003. A novel role for FAK as a protease-targeting adaptor protein: regulation by p42 ERK and Src. *Curr Biol* 13(16):1442-50.
- Comoglio PM, Boccaccio C, Trusolino L. 2003. Interactions between growth factor receptors and adhesion molecules: breaking the rules. *Curr Opin Cell Biol* 15(5):565-71.
- Crowe DL, Ohannessian A. 2004. Recruitment of focal adhesion kinase and paxillin to beta1 integrin promotes cancer cell migration via mitogen activated protein kinase activation. *BMC Cancer* 4(1):18.
- Cuevas BD, Abell AN, Witowsky JA, Yujiri T, Johnson NL, Kesavan K, Ware M, Jones PL, Weed SA, DeBiasi RL and others. 2003. MEKK1 regulates calpain-dependent proteolysis of focal adhesion proteins for rear-end detachment of migrating fibroblasts. *Embo J* 22(13):3346-55.
- DeLong SA, Moon JJ, West JL. 2005. Covalently immobilized gradients of bFGF on hydrogel scaffolds for directed cell migration. *Biomaterials* 26(16):3227-34.
- den Hertog J, Tracy S, Hunter T. 1994. Phosphorylation of receptor protein-tyrosine phosphatase alpha on Tyr789, a binding site for the SH3-SH2-SH3 adaptor protein GRB-2 in vivo. *Embo J* 13(13):3020-32.
- DiMilla PA, Barbee K, Lauffenburger DA. 1991. Mathematical model for the effects of adhesion and mechanics on cell migration speed. *Biophys J* 60(1):15-37.
- Dong J, Opresko LK, Chrisler W, Orr G, Quesenberry RD, Lauffenburger DA, Wiley HS. 2005. The membrane-anchoring domain of epidermal growth factor receptor ligands dictates their ability to operate in juxtacrine mode. *Mol Biol Cell* 16(6):2984-98.
- Dourdin N, Bhatt AK, Dutt P, Greer PA, Arthur JS, Elce JS, Huttenlocher A. 2001. Reduced cell migration and disruption of the actin cytoskeleton in calpain-deficient embryonic fibroblasts. *J Biol Chem* 276(51):48382-8.

- Franco SJ, Rodgers MA, Perrin BJ, Han J, Bennin DA, Critchley DR, Huttenlocher A. 2004. Calpain-mediated proteolysis of talin regulates adhesion dynamics. *Nat Cell Biol* 6(10):977-83.
- French AR, Tadaki DK, Niyogi SK, Lauffenburger DA. 1995. Intracellular trafficking of epidermal growth factor family ligands is directly influenced by the pH sensitivity of the receptor/ligand interaction. *J Biol Chem* 270(9):4334-40.
- Genersch E, Schuppan D, Lichtner RB. 1996. Signaling by epidermal growth factor differentially affects integrin-mediated adhesion of tumor cells to extracellular matrix proteins. *J Mol Med* 74(10):609-16.
- Glading A, Bodnar RJ, Reynolds IJ, Shiraha H, Satish L, Potter DA, Blair HC, Wells A. 2004. Epidermal growth factor activates m-calpain (calpain II), at least in part, by extracellular signal-regulated kinase-mediated phosphorylation. *Mol Cell Biol* 24(6):2499-512.
- Glading A, Chang P, Lauffenburger DA, Wells A. 2000. Epidermal growth factor receptor activation of calpain is required for fibroblast motility and occurs via an ERK/MAP kinase signaling pathway. *J Biol Chem* 275(4):2390-8.
- Glading A, Uberall F, Keyse SM, Lauffenburger DA, Wells A. 2001. Membrane proximal ERK signaling is required for M-calpain activation downstream of epidermal growth factor receptor signaling. *J Biol Chem* 276(26):23341-8.
- Gobin AS, West JL. 2003. Effects of epidermal growth factor on fibroblast migration through biomimetic hydrogels. *Biotechnol Prog* 19(6):1781-5.
- Harris RC, Chung E, Coffey RJ. 2003a. EGF receptor ligands. *Exp Cell Res* 284(1):2-13.
- Harris RC, Chung E, Coffey RJ. 2003b. EGF receptor ligands. *Experimental Cell Research* 284(1):2-13.
- Haugh JM, Huang AC, Wiley HS, Wells A, Lauffenburger DA. 1999a. Internalized epidermal growth factor receptors participate in the activation of p21(ras) in fibroblasts. *J Biol Chem* 274(48):34350-60.
- Haugh JM, Meyer T. 2002. Active EGF receptors have limited access to PtdIns(4,5)P(2) in endosomes: implications for phospholipase C and PI 3-kinase signaling. *J Cell Sci* 115(Pt 2):303-10.
- Haugh JM, Schneider IC, Lewis JM. 2004. On the cross-regulation of protein tyrosine phosphatases and receptor tyrosine kinases in intracellular signaling. *J Theor Biol* 230(1):119-32.
- Haugh JM, Schooler K, Wells A, Wiley HS, Lauffenburger DA. 1999b. Effect of epidermal growth factor receptor internalization on regulation of the phospholipase C-gamma1 signaling pathway. *J Biol Chem* 274(13):8958-65.
- Hersel U, Dahmen C, Kessler H. 2003. RGD modified polymers: biomaterials for stimulated cell adhesion and beyond. *Biomaterials* 24(24):4385-415.
- Hubbell JA. 2003. Materials as morphogenetic guides in tissue engineering. *Curr Opin Biotechnol* 14(5):551-8.
- Irvine DJ, Mayes AM, Griffith LG. 2001. Nanoscale clustering of RGD peptides at surfaces using Comb polymers. 1. Synthesis and characterization of Comb thin films. *Biomacromolecules* 2(1):85-94.
- Iwamoto R, Handa K, Mekada E. 1999. Contact-dependent growth inhibition and apoptosis of epidermal growth factor (EGF) receptor-expressing cells by the

- membrane-anchored form of heparin-binding EGF-like growth factor. *J Biol Chem* 274(36):25906-12.
- Jeon SI, Andrade JD. 1991. Protein--surface interactions in the presence of polyethylene oxide : II. Effect of protein size. *Journal of Colloid and Interface Science* 142(1):159-166.
- Jorissen RN, Walker F, Pouliot N, Garrett TP, Ward CW, Burgess AW. 2003. Epidermal growth factor receptor: mechanisms of activation and signalling. *Exp Cell Res* 284(1):31-53.
- Kao WJ, Hubbell JA. 1998. Murine macrophage behavior on peptide-grafted polyethyleneglycol-containing networks. *Biotechnol Bioeng* 59(1):2-9.
- Kao WJ, Lee D, Schense JC, Hubbell JA. 2001. Fibronectin modulates macrophage adhesion and FBGC formation: the role of RGD, PHSRN, and PRRARV domains. *J Biomed Mater Res* 55(1):79-88.
- Keilhack H, Tenev T, Nyakatura E, Godovac-Zimmermann J, Nielsen L, Seedorf K, Bohmer FD. 1998. Phosphotyrosine 1173 mediates binding of the protein-tyrosine phosphatase SHP-1 to the epidermal growth factor receptor and attenuation of receptor signaling. *J Biol Chem* 273(38):24839-46.
- Kempiak SJ, Yip SC, Backer JM, Segall JE. 2003. Local signaling by the EGF receptor. *J Cell Biol* 162(5):781-7.
- Koo LY, Irvine DJ, Mayes AM, Lauffenburger DA, Griffith LG. 2002. Co-regulation of cell adhesion by nanoscale RGD organization and mechanical stimulus. *J Cell Sci* 115(Pt 7):1423-33.
- Kuhl PR, Griffith-Cima LG. 1996. Tethered epidermal growth factor as a paradigm for growth factor-induced stimulation from the solid phase. *Nat Med* 2(9):1022-7.
- Lauffenburger DA, Horwitz AF. 1996. Cell migration: a physically integrated molecular process. *Cell* 84(3):359-69.
- Levkowitz G, Waterman H, Ettenberg SA, Katz M, Tsygankov AY, Alroy I, Lavi S, Iwai K, Reiss Y, Ciechanover A and others. 1999. Ubiquitin ligase activity and tyrosine phosphorylation underlie suppression of growth factor signaling by c-Cbl/Sli-1. *Mol Cell* 4(6):1029-40.
- Levkowitz G, Waterman H, Zamir E, Kam Z, Oved S, Langdon WY, Beguinot L, Geiger B, Yarden Y. 1998. c-Cbl/Sli-1 regulates endocytic sorting and ubiquitination of the epidermal growth factor receptor. *Genes Dev* 12(23):3663-74.
- Maheshwari G, Brown G, Lauffenburger DA, Wells A, Griffith LG. 2000. Cell adhesion and motility depend on nanoscale RGD clustering. *J Cell Sci* 113 (Pt 10):1677-86.
- Maheshwari G, Wells A, Griffith LG, Lauffenburger DA. 1999. Biophysical integration of effects of epidermal growth factor and fibronectin on fibroblast migration. *Biophys J* 76(5):2814-23.
- Mann BK, Schmedlen RH, West JL. 2001. Tethered-TGF-beta increases extracellular matrix production of vascular smooth muscle cells. *Biomaterials* 22(5):439-44.
- Miyamoto S, Akiyama SK, Yamada KM. 1995a. Synergistic roles for receptor occupancy and aggregation in integrin transmembrane function. *Science* 267(5199):883-5.
- Miyamoto S, Teramoto H, Coso OA, Gutkind JS, Burbelo PD, Akiyama SK, Yamada KM. 1995b. Integrin function: molecular hierarchies of cytoskeletal and signaling molecules. *J Cell Biol* 131(3):791-805.

- Miyamoto S, Teramoto H, Gutkind JS, Yamada KM. 1996. Integrins can collaborate with growth factors for phosphorylation of receptor tyrosine kinases and MAP kinase activation: roles of integrin aggregation and occupancy of receptors. *J Cell Biol* 135(6 Pt 1):1633-42.
- Moro L, Dolce L, Cabodi S, Bergatto E, Erba EB, Smeriglio M, Turco E, Retta SF, Giuffrida MG, Venturino M and others. 2002. Integrin-induced epidermal growth factor (EGF) receptor activation requires c-Src and p130Cas and leads to phosphorylation of specific EGF receptor tyrosines. *J Biol Chem* 277(11):9405-14.
- Moro L, Venturino M, Bozzo C, Silengo L, Altruda F, Beguinot L, Tarone G, Defilippi P. 1998. Integrins induce activation of EGF receptor: role in MAP kinase induction and adhesion-dependent cell survival. *Embo J* 17(22):6622-32.
- Morrison DK, Davis RJ. 2003. Regulation of MAP kinase signaling modules by scaffold proteins in mammals. *Annu Rev Cell Dev Biol* 19:91-118.
- Narita T, Kawakami-Kimura N, Sato M, Matsuura N, Higashiyama S, Taniguchi N, Kannagi R. 1996. Alteration of integrins by heparin-binding EGF-like growth factor in human breast cancer cells. *Oncology* 53(5):374-81.
- Ono M, Raab G, Lau K, Abraham JA, Klagsbrun M. 1994. Purification and characterization of transmembrane forms of heparin-binding EGF-like growth factor. *J Biol Chem* 269(49):31315-21.
- Park YD, Tirelli N, Hubbell JA. 2003. Photopolymerized hyaluronic acid-based hydrogels and interpenetrating networks. *Biomaterials* 24(6):893-900.
- Pichard V, Honore S, Kovacic H, Li C, Prevot C, Briand C, Rognoni JB. 2001. Adhesion, actin cytoskeleton organisation and the spreading of colon adenocarcinoma cells induced by EGF are mediated by alpha2beta1 integrin low clustering through focal adhesion kinase. *Histochem Cell Biol* 116(4):337-48.
- Piepkorn M, Pittelkow MR, Cook PW. 1998. Autocrine regulation of keratinocytes: the emerging role of heparin-binding, epidermal growth factor-related growth factors. *J Invest Dermatol* 111(5):715-21.
- Raab G, Klagsbrun M. 1997. Heparin-binding EGF-like growth factor. *Biochimica et Biophysica Acta (BBA) - Reviews on Cancer* 1333(3):F179-F199.
- Reddy CC, Wells A, Lauffenburger DA. 1994. Proliferative response of fibroblasts expressing internalization-deficient epidermal growth factor (EGF) receptors is altered via differential EGF depletion effect. *Biotechnol Prog* 10(4):377-84.
- Reddy CC, Wells A, Lauffenburger DA. 1996. Receptor-mediated effects on ligand availability influence relative mitogenic potencies of epidermal growth factor and transforming growth factor alpha. *J Cell Physiol* 166(3):512-22.
- Reddy CC, Wells A, Lauffenburger DA. 1998. Comparative mitogenic potencies of EGF and TGF alpha and their dependence on receptor-limitation versus ligand-limitation. *Med Biol Eng Comput* 36(4):499-507.
- Sakiyama-Elbert SE, Hubbell JA. 2000a. Controlled release of nerve growth factor from a heparin-containing fibrin-based cell ingrowth matrix. *J Control Release* 69(1):149-58.
- Sakiyama-Elbert SE, Hubbell JA. 2000b. Development of fibrin derivatives for controlled release of heparin-binding growth factors. *J Control Release* 65(3):389-402.

- Schenk S, Hintermann E, Bilban M, Koshikawa N, Hojilla C, Khokha R, Quaranta V. 2003. Binding to EGF receptor of a laminin-5 EGF-like fragment liberated during MMP-dependent mammary gland involution. *J Cell Biol* 161(1):197-209.
- Schlaepfer DD, Mitra SK. 2004. Multiple connections link FAK to cell motility and invasion. *Curr Opin Genet Dev* 14(1):92-101.
- Schlessinger J. 2002. Ligand-induced, receptor-mediated dimerization and activation of EGF receptor. *Cell* 110(6):669-72.
- Sieg DJ, Hauck CR, Ilic D, Klingbeil CK, Schaefer E, Damsky CH, Schlaepfer DD. 2000. FAK integrates growth-factor and integrin signals to promote cell migration. *Nat Cell Biol* 2(5):249-56.
- Smith JM, Sporn MB, Roberts AB, Derynck R, Winkler ME, Gregory H. 1985. Human transforming growth factor-alpha causes precocious eyelid opening in newborn mice. *Nature* 315(6019):515-6.
- Sorkin A, Von Zastrow M. 2002. Signal transduction and endocytosis: close encounters of many kinds. *Nat Rev Mol Cell Biol* 3(8):600-14.
- Swindle CS, Tran KT, Johnson TD, Banerjee P, Mayes AM, Griffith L, Wells A. 2001. Epidermal growth factor (EGF)-like repeats of human tenascin-C as ligands for EGF receptor. *J Cell Biol* 154(2):459-68.
- Topham RT, Chiego DJ, Jr., Gattone VH, 2nd, Hinton DA, Klein RM. 1987. The effect of epidermal growth factor on neonatal incisor differentiation in the mouse. *Dev Biol* 124(2):532-43.
- Tran KT, Griffith L, Wells A. 2004. Extracellular matrix signaling through growth factor receptors during wound healing. *Wound Repair Regen* 12(3):262-8.
- Traverse S, Gomez N, Paterson H, Marshall C, Cohen P. 1992. Sustained activation of the mitogen-activated protein (MAP) kinase cascade may be required for differentiation of PC12 cells. Comparison of the effects of nerve growth factor and epidermal growth factor. *Biochem J* 288 (Pt 2):351-5.
- Wells A. 1999. EGF receptor. *Int J Biochem Cell Biol* 31(6):637-43.
- Wiley HS. 2003. Trafficking of the ErbB receptors and its influence on signaling. *Experimental Cell Research* 284(1):78-88.
- Wiley HS, Burke PM. 2001. Regulation of receptor tyrosine kinase signaling by endocytic trafficking. *Traffic* 2(1):12-8.
- Yang H, Jiang D, Li W, Liang J, Gentry LE, Brattain MG. 2000. Defective cleavage of membrane bound TGFalpha leads to enhanced activation of the EGF receptor in malignant cells. *Oncogene* 19(15):1901-14.
- Yarden Y, Sliwkowski MX. 2001. Untangling the ErbB signalling network. *Nat Rev Mol Cell Biol* 2(2):127-37.
- Zisch AH, Schenk U, Schense JC, Sakiyama-Elbert SE, Hubbell JA. 2001. Covalently conjugated VEGF--fibrin matrices for endothelialization. *J Control Release* 72(1-3):101-13.

2. Surface Tethered Adhesion Ligands and Growth Factors

2.1 Introduction

We are designing a synthetic substrate to present adhesion ligands and growth factors to cells in a spatially controlled way. The material must present ligands in a biologically active conformation. This may be accomplished via adsorption or covalent linkage to the substrate, although adsorption may alter molecular conformations and change or hinder ligand activity (Baugh and Vogel 2004; Kuhl and Griffith-Cima 1996). A significant surface density of functionalizable groups is required to covalently tether proteins or peptides to a substrate material. Further, these groups must be accessible to both the molecules to be tethered and ultimately the cell's surface receptors. Finally, the global and local ligand densities must be readily modulated within an efficacious range that permits nanoscale ligand aggregation for the clustering of integrins and dimerization of growth factor receptors.

We are utilizing a poly(methyl methacrylate)-g-poly(ethylene oxide) (PMMA-g-PEO) comb polymer that consists of a hydrophobic backbone and many hydrophilic PEO side chains creating a PEO brush at the material interface with water. Variation in the PEO brush density offers tailored resistance to protein adsorption, and thus, it may prevent or permit varying levels of cell adhesion. The PEO side chains are hydroxyl-terminated and can be functionalized by several chemistries to tether proteins or peptides. In addition, individual polymer chains containing multiple PEO side chains allow a degree of local nanoscale ligand clustering and the potential to present different ligands, i.e. adhesion peptides and growth factors, on the same substrate (Irvine et al. 2001).

The goal of Chapter 2 is to introduce the methods for preparing the PMMA-g-PEO comb polymer as a thin film substrate that controls cell adhesion and presents biologically active tethered growth factors to cells. Two formulations of the polymer are synthesized. One engenders cell adhesion by permitting the adsorption of adhesion proteins like fibronectin (FN) while presenting epidermal growth factor (EGF) via functionalized PEO side chains. The other employs the covalent linkage of both EGF and adhesion peptide sequences to the PEO side chains. Systematic variation of cell adhesion is accomplished by displaying different surface densities of adsorbed FN or tethered adhesion peptides. We conclude Chapter 2 by estimating the global and local ligand densities achieved on PMMA-g-PEO comb polymer surfaces in the context of promoting integrin clustering and EGFR homodimerization.

2.2 Experimental Methods

2.2.1 Reagents

The following chemicals were obtained from VWR Scientific and used as received unless otherwise noted: tetrahydrofuran (THF), benzene, methyl ethyl ketone, anhydrous dimethyl sulfoxide (DMSO), anhydrous methanol, petroleum ether, triethylamine, dichloromethane, diethyl ether, and ethanol. Molecular sieves (3 A) were also obtained from VWR Scientific. Methyl methacrylate (MMA), hydroxy-polyoxyethylene methacrylate (HPOEM, $M_n \sim 360$ g/mol or 526 g/mol), azo(bis)isobutyronitrile (AIBN), 1-methylphenol, 2,2,2-trifluoroethanesulfonyl chloride (tresyl chloride), 4-nitrophenyl chloroformate (NPC), tris(2-carboxyethyl)phosphine hydrochloride (TCEP), and human plasma fibronectin (FN) were purchased from Sigma-Aldrich. Methacryloxypropyltrimethoxysilane (MPTS) was acquired from Gelest, Inc. Murine epidermal growth factor (EGF) was obtained from Peprotech. N-(p-maleimidophenyl)isocyanate (PMPI) was purchased from Pierce. Branched FN-like PHSRN-RGD peptide ($M \sim 2000$ g/mol) and other small peptides used were synthesized in lab under the direction of Dr. Maria Ufret. Tenascin C EGF-like repeat 14 was provided by Alan Wells' lab at the University of Pittsburgh Medical Center. Phosphate buffered saline (PBS) and cell culture reagents were acquired from Invitrogen.

2.2.2 Cell Culture

Wild-type (WT) NR6 fibroblast cells, a murine 3T3-derived cell line that lacks endogenous EGF and EGFR synthesis and has been stably transfected with wild-type human EGFR (Chen et al. 1994), were cultured in minimum essential medium- α (MEM- α) supplemented with 7.5% fetal bovine serum (FBS), 350 μ g/ml G418, 1 mM sodium

pyruvate, 2 mM L-glutamine, 1 mM non-essential amino acids, 100 i.u./ml penicillin, and 200 µg/ml streptomycin. For certain cell adhesion assays, 7.5% FBS in the medium was replaced by 0.1% or 0.5% dialyzed FBS (10,000 molecular weight cut-off), 1 mg/ml bovine serum albumin (BSA), and MEM- α . In the spread area adhesion experiments that included air incubation, 25 mM HEPES replaced sodium bicarbonate as the buffer.

2.2.3 PMMA-g-PEO Comb Polymer Synthesis

Poly(methyl methacrylate)-g-poly(ethylene oxide) (PMMA-g-PEO) comb polymers were synthesized similarly to those previously described as depicted in Figure 2.1 (Irvine et al. 2001). Two comb copolymers with different PEO side chain lengths and densities, Comb 1 and Comb 2, were synthesized via free radical polymerization for use in this work. Because free radical synthesis leads to product variability between batches, a large batch (several grams) of each polymer was produced to provide consistency throughout the studies. Comb 1, which incorporated 22 wt.% hydroxy poly(oxyethylene methacrylate) (HPOEM), was polymerized by research technician Helice Schramm. Comb 2, which included 33 wt.% HPOEM, was synthesized by summer student Dan Pregibon. The free radical polymerizations took place in THF using MMA and HPOEM monomers. AIBN was used as an initiator. The monomer solution in THF was degassed 20 minutes with nitrogen and refluxed 18 hours at 70°C. The reaction was terminated by addition of 1-methylphenol. The resulting copolymers were precipitated twice in petroleum ether with 10% (v/v) methanol and dried under vacuum at room temperature 24 to 48 hours.

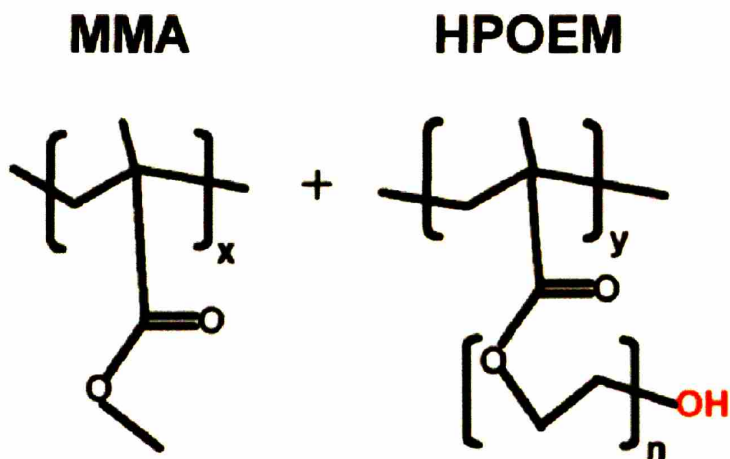


Figure 2.1 – Monomer Chemical Structures for PMMA-g-PEO Comb Polymer. Methyl methacrylate (MMA) and hydroxy poly(oxyethylene) methacrylate (HPOEM) are used to synthesize PMMA-g-PEO comb polymers. Different PMMA and PEO fractions are obtained by varying the fractions, x and y, in the polymerization. PEO chain length is determined by the number of PEO repeat units, n.

The properties of Comb 1 and Comb 2 are shown in Table 2.1. The number-average molecular weights (M_n) and polydispersity indices (PDI) were determined by gel permeation chromatography with inline light scattering based on polystyrene standards. The ratios by weight of co-monomers (MMA:HPOEM) incorporated in each polymer were determined by $^1\text{H-NMR}$ using 1% solutions of polymer in deuterated chloroform.

Table 2.1 – PMMA-g-PEO Comb Polymer Properties

Description	M_n	M_w	PDI	MMA: HPOEM (wt. %)	PEO/ chain	PEO length
Comb 1	25,000	45,000	1.8	78:22	15	n = 6.5
Comb 2	30,000	96,000	3.2	67:33	19	n = 10

2.2.4 Activation of Comb 1 and Comb 2 to React with Primary Amines

The hydroxyl termini of PEO side chains on Comb 1 (22% PEO) were activated with tresyl chloride, which provides a leaving group that reacts with primary amines, using a protocol developed for PEO (Sperinde et al. 1999) as illustrated in Figure 2.2.

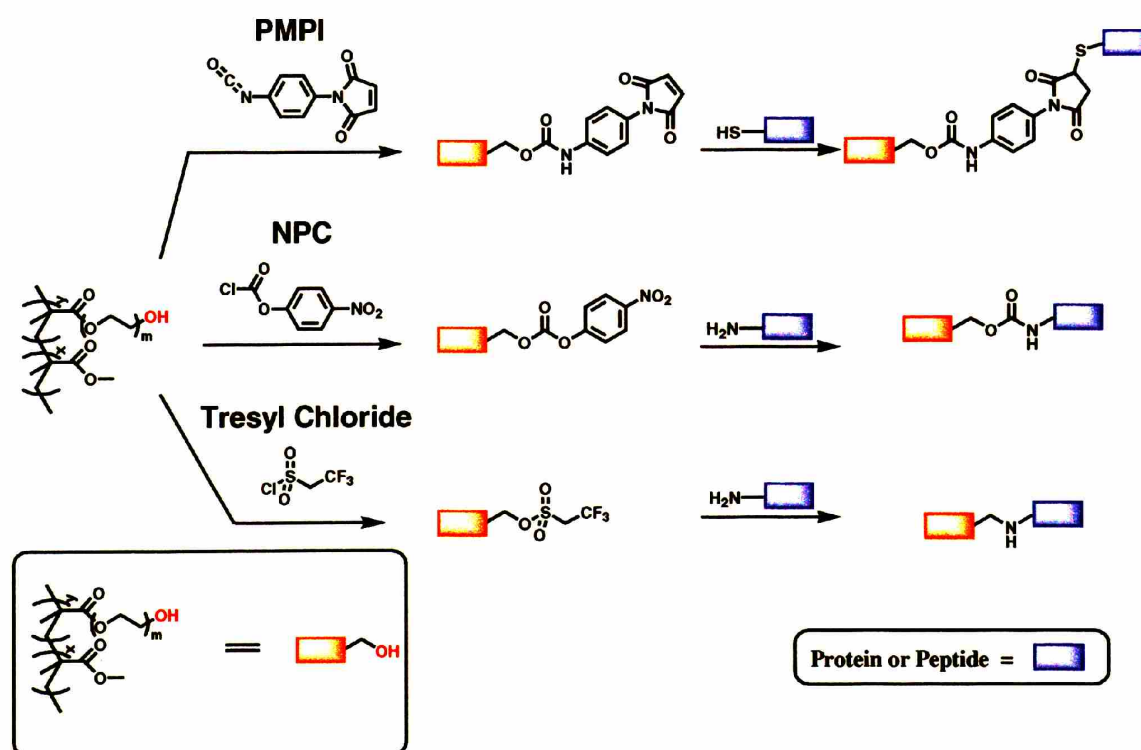


Figure 2.2 – Polymer-tethered Protein Activation and Coupling Methods.

PMPI is a bi-functional cross-linker that rapidly targets sulfhydryls at pH 6.5-7.5. It is not vulnerable to hydrolysis once linked to the polymer side chain. NPC is a relatively slow primary amine-reactive functional group that reacts at alkaline pH. Tresyl chloride is an extremely labile functional group that targets primary amines most efficiently at alkaline pH and 4°C as it is susceptible to rapid hydrolysis.

Typically, 500 mg of Comb 1 polymer was activated as follows: The polymer was freeze-dried from benzene and dissolved in 75 ml of 3A molecular sieve-dried methyl ethyl ketone

in a round bottom flask. The solution was cooled under nitrogen to 4°C followed by addition of 1 g of tresyl chloride and 600 µl of triethylamine. The stirred reaction proceeded at 4°C for three hours. The activated polymer solution was decanted and centrifuged 10 minutes at 3000xg, and the supernatant was 0.2 µm filtered to remove precipitated salts. The activated polymer was precipitated in 2% anhydrous methanol in petroleum ether at 4°C and dried 24 hours under vacuum before being harvested and stored desiccated under nitrogen at -70°C until film preparation. ¹H-NMR confirmed the functional group addition with typical yields of ~65%. The stored product was stable for at least 6 months and was reported to remain active over a year (Martin Schwartz, personal communication).

Comb 2 (33% PEO) polymer was activated to react with primary amines by an alternative scheme employing 4-nitrophenyl chloroformate (NPC) (Figure 2.2). The NPC coupling reaction is slower than tresyl chloride amine substitution and less vulnerable to hydrolysis. This permitted its use in sequential aqueous coupling schemes for covalently linking multiple ligands to the same substrate.

Comb 2 was NPC-activated in 3g batches. The polymer was freeze-dried from benzene and dissolved in dichloromethane under nitrogen in a round bottom flask. Triethylamine in 4.5 molar excess based on the number of PEO chain ends was added and the flask cooled for 30 minutes on ice. NPC in 2.5 molar excess was dissolved in dichloromethane and added to the reaction mixture. The reaction proceeded 2 hours on ice and overnight at room temperature. The activated polymer was precipitated three times in diethyl ether with redissolving steps conducted in methyl ethyl ketone. The final activated polymer solution in methyl ethyl ketone was aliquotted ~30 mg per vial, rotovaporized, and placed under vacuum overnight. The vials were then weighed and stored desiccated under

nitrogen at -20°C until thin film preparation. ¹H-NMR confirmed the functional group addition with typical yields of 60-70%. The polymer was stable at least one year.

2.2.5 Activation of Comb 2 to React with Sulfhydryls

PMPI, a sulfhydryl-targeting bi-functional cross-linker, was employed to couple cysteine-containing peptides to Comb 2 polymer side chains. Figure 2.2 depicts the PMPI coupling reaction, which occurs rapidly at neutral pH with high yield.

Comb 2 polymer was activated with PMPI in 200 mg batches. The polymer was freeze-dried from benzene and dissolved in anhydrous DMSO in a round bottom flask under nitrogen at room temperature. PMPI in 2.5 molar excess was dissolved in anhydrous DMSO and added to the reaction vessel. The reaction proceeded 2 hours at room temperature during which the color of the mixture turned from light to dark yellow. The activated polymer was precipitated three times in diethyl ether with redissolving steps conducted in methyl ethyl ketone. The final activated polymer solution in methyl ethyl ketone was aliquotted ~15 mg per vial, rotovaporized, and placed under vacuum overnight. The vials were then weighed and stored dessicated at room temperature until thin film preparation. ¹H-NMR confirmed the functional group addition with yields ranging from 25% to nearly 100%. The polymer was stable indefinitely as the PMPI functional group was not vulnerable to hydrolysis.

2.2.6 Polymer Thin Film Preparation

Polymer thin films were prepared on round glass coverslips of varying sizes (10mm, 12mm, 18mm, or 22mm diameter). The glass coverslips were sonicated for 30 minutes in ethanol. 50 mL of a 4% solution of methacryloxypropyltrimethoxysilane (MPTS) in a solvent of 95% ethanol / 5% water (pH 4.5) was prepared and allowed to hydrolyze for 5 minutes.

Glass coverslips were silanized in the MPTS solution in a small crystallization dish for 5 minutes under agitation. This produced a hydrophobic methacryl-coated surface to which polymer thin films would adhere. The treated coverslips were washed three times in ethanol to remove excess silane. They were air dried and cured at room temperature for 24 hours prior to use.

Polymer was dissolved at 20 mg/ml in 3A molecular sieve-dried methyl ethyl ketone. Using a Headway PWM32 spinner, varying volumes of the polymer solution dependent upon coverslip diameter (10 mm ~ 8 ul, 12 mm ~ 10 ul, 18 mm ~ 50 ul, 22 mm ~ 80 ul) were spin coated onto glass coverslips with 30 seconds of spinning. Rotational speeds ranged from 1000 RPM for 10-mm and 12-mm coverslips to 1400 RPM for 18-mm and 22-mm coverslips. Thin film glass substrates were dried overnight under vacuum and stored under vacuum at room temperature until use. Thin films were typically used within 2 weeks of preparation.

2.2.7 EGF-FN Substrate Preparation

Using Comb 1 activated with tresyl chloride, EGF-FN substrates were prepared that presented covalently tethered EGF amidst an adsorbed layer of FN. Murine EGF was diluted in 100 mM phosphate buffer at pH 7.0 or 9.0 to 0.5 ug/ml or 5 ug/ml. The EGF solution (75 ul for 10-mm coverslips; 120 ul for 12-mm; 250 ul for 18-mm; or 350 ul for 22-mm) was pipetted onto tresyl-activated Comb 1 thin film substrates on parafilm and reacted at 4°C in a humid box for 3 hours. The tethered EGF thin films were washed four times by aspirating and pipetting PBS onto them to remove uncoupled EGF. To block unreacted tresyl groups, 100 mM tris buffer at pH 9.0 was added to the substrates for 1 hour at room temperature in a

humid box. Surfaces were then washed four times with PBS and stored under PBS at 4°C until use. Tethered EGF substrates were used within two weeks of preparation.

Mock activated substrates were produced following the same reaction steps but without EGF in the phosphate buffer coupling step. These surfaces were used in experimental conditions requiring no EGF or soluble EGF. In addition, EGF was adsorbed to mock activated substrates for 3 hours at 4°C to quantify the level of non-specifically adsorbed EGF present on tethered EGF surfaces.

FN was adsorbed to tethered EGF or mock activated Comb 1 surfaces to engender different levels of cell adhesion. Immediately prior to cell seeding, FN solutions in PBS were pipetted onto the substrates on parafilm for 24 hours at 4°C. FN coating concentrations ranged from 0.1 ug/ml to 30 ug/ml, creating surfaces with varying densities of adsorbed FN. EGF-FN substrates were washed 3 times with PBS prior to cell seeding.

2.2.8 EGF-Peptide Substrate Preparation

Comb 2 polymers activated with PMPI and with NPC were combined to produce protein resistant substrates that would covalently bind two ligands. The PMPI-activated polymer linked cysteine-containing adhesion peptides to the surface, while the NPC-activated polymer tethered amine-terminated EGF. Cysteine-terminated branched FN-like PHSRN-RGD peptides (SynKRGD) synthesized by Dr. Maria Ufret and illustrated in Figure 2.5 served as the adhesion peptide in the majority of experiments.

Spincoast thin films of PMPI and NPC activated polymer were prepared by blending desired fractions of PMPI-activated, NPC-activated, and unactivated Comb 2 polymers in the spin coating solution. As depicted in Figure 2.3, micromolar concentrations of adhesion

peptides (range of 2 μM to 200 μM) in 100 mM phosphate buffer at pH 7.5 were reacted with substrates for 2 hours at room temperature in the presence of 1 mM TCEP, a reducing agent.

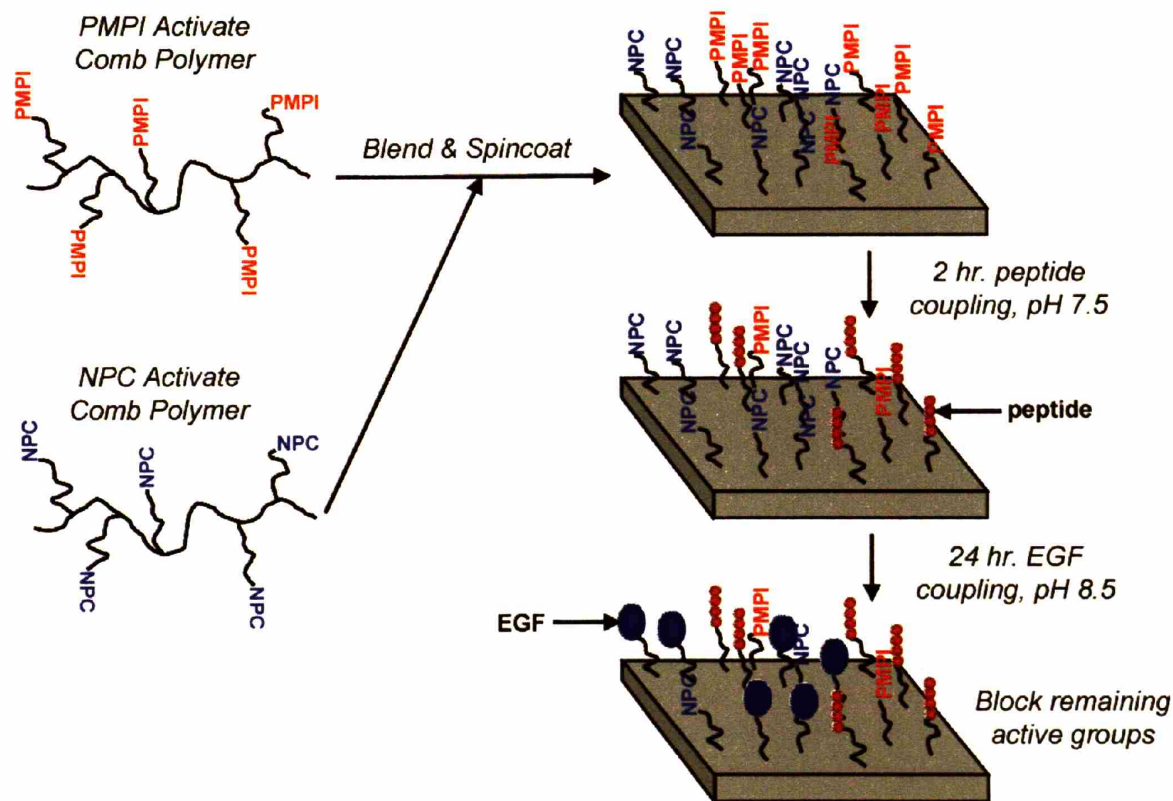


Figure 2.3 – Co-tethered EGF and Adhesion Peptide.

PMPI-activated and NPC-activated Comb 2 polymers are blended and spincoated as thin films. Cysteine-terminated adhesion peptides are initially coupled to the surface via PMPI cross-linkers. EGF is subsequently tethered via amine-reactive NPC groups. Surface densities of each ligand are determined by the fractions of activated polymers in the blend.

To accomplish this, beads of the coupling solution were placed on parafilm (30 μl for 10-mm or 100 μl for 18-mm coverslips), and the coverslips were placed polymer-side down onto the beads. The peptide-coupled surfaces were turned up and washed twice with PBS. Murine EGF at 5 $\mu\text{g/ml}$ or 25 $\mu\text{g/ml}$ in 100 mM sodium bicarbonate buffer at pH 8.5 was then reacted with the peptide-coupled surfaces for 4 or 24 hours at room temperature. The EGF and PBS wash solutions were added on top of the polymer-side up coverslips in volumes of 75 μl for

10-mm or 250 ul for 18-mm coverslips. After coupling, substrates were washed 4 times with PBS followed by a two-hour blocking step with 100 mM tris buffer at pH 8.5. Surfaces were washed 4 times with PBS and stored under PBS at 4°C until use. The co-tethered EGF-peptide substrates were used within one week of preparation.

2.2.9 Quantification of Protein and Peptide Densities

Surface densities of whole proteins (EGF, FN, and Ten14) and adhesion peptides (RGD and SynKRGD) were determined by radiolabeled iodine-125 experiments. Tyrosine residues present in the whole proteins and incorporated in the synthesized peptides were labeled with Na¹²⁵I by iodobead. Labeled whole proteins were separated from free iodine-125 by size exclusion chromatography (Sephadex G-10 column), while labeled peptides were purified using Sep-Pak reversed phase filter cartridges with a methanol / water gradient in 1% trifluoroacetic acid (TFA). Concentrations of the eluted whole protein fractions were determined by precipitation of pre-column and post-column samples with phosphotungstic acid (PTA) and a mass balance around the column. Small peptides did not precipitate with PTA so radiolabeled peptide was added to an excess of unlabeled peptide at a known concentration.

10-mm diameter activated polymer thin films were coupled to radiolabeled proteins or peptides under the same concentration, temperature, and pH conditions used to prepare EGF-FN or EGF-peptide substrates. Tethered and adsorbed ¹²⁵I-protein surface densities were measured by one of two methods. In the first method, radiolabeled substrates were exposed to a phosphor screen along with 10-mm glass substrate standards having a known density of adsorbed radiolabeled protein. The phosphor screen was read on a Perkin Elmer Cyclone phosphor imager and substrate intensities measured against a standard curve for

density determination. The second method entailed loading the coupled thin film substrates into gamma tubes and counting the samples on a gamma counter against standards of known radiolabeled protein amounts.

2.2.10 Cell Adhesion Assays

Multiple measurements of cell adhesion were used to characterize PMMA-g-PEO comb polymer substrates. Qualitative tests for resistance to cell adhesion involved seeding fibroblasts onto thin film polymer substrates in 7.5% FBS containing medium for 4 to 12 hours. Surfaces were observed for the presence of attached and spread cells. Serum proteins adsorbed to non-protein resistant Comb 1 surfaces, permitting cell attachment and spreading. Protein resistant Comb 2 substrates did not allow cells to attach or spread. Tissue culture polystyrene was the standard reference for cell adhesive surfaces.

Qualitative tests for integrin-specific cell adhesion to peptide-presenting substrates were performed in a similar manner. Fibroblasts were seeded onto thin film polymer substrates up to 12 hours but in the presence of 0.1% dialyzed FBS-containing medium. The substantial reduction in serum proteins did not permit cells to fully spread unless additional adhesion molecules were present on the surface. Phase contrast images were generally acquired for comparison of substrate adhesion. In some instances, calcein AM, a live cell dye that stains the entire cell, was added 15 minutes at 2 ul/ml medium to permit fluorescence imaging for greater contrast.

Cell spread area was used as a surrogate measure of relative cell adhesion. Fibroblasts were seeded on polymer substrates under desired conditions. Differential interference contrast (DIC) images using a calibrated 10X objective were acquired every 10 minutes during the six-hour period 8 to 14 hours post-seeding so that cells had reached spreading

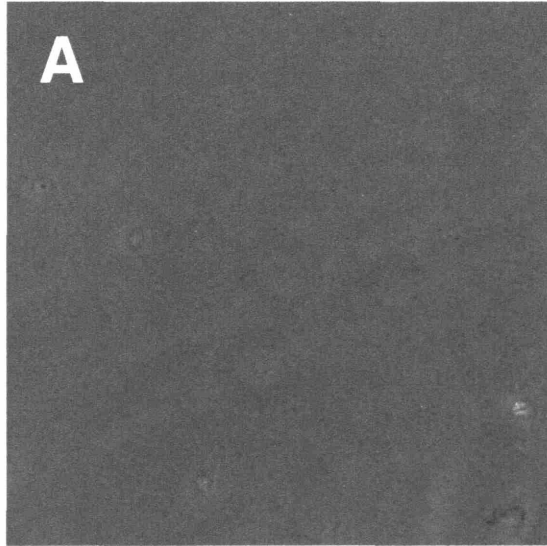
equilibrium. Images were analyzed using DIAS cell-tracing software. The images were contrast enhanced using the “best guess” feature, and cell outlines were traced using the auto-trace feature. Because auto-tracing mistakes occurred on the jagged edges and thin lamellipodial projections of NR6 cells, the traces were corrected by hand with a mouse using a feature that allowed portions of the outlines to be redrawn. Cell spread areas were then calculated by the software using a 0.658 pixel/um factor from the 10X objective calibration.

2.3 Results and Discussion

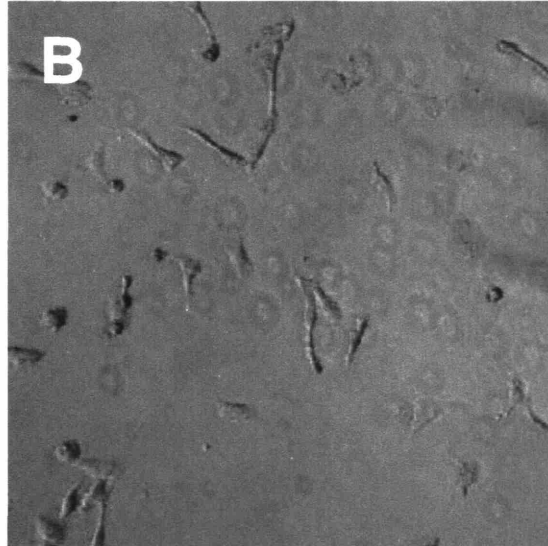
2.3.1 Controlling Cell Adhesion to PMMA-g-PEO Comb Polymers

The well-characterized PMMA-g-PEO comb polymer platform allows systematic modulation of the cell adhesion environment. Previous work with PMMA-g-PEO comb polymers demonstrated that polymers incorporating at least 30 wt.% PEO monomer resisted cell adhesion in serum-containing medium (Irvine et al. 2001). This offered two means of engendering variable levels of cell adhesion on polymer substrates in the context of tethered EGF: 1) synthesize an innately adhesive polymer with less than 30 wt.% PEO, and adsorb different levels of FN to the backbone or 2) synthesize a cell-resistant polymer containing at least 30 wt.% PEO, and tether different densities of adhesion peptides to the functionalized side chains. The first method that modulated adhesion via adsorbed FN allowed comparison to the existing literature on FN (Maheshwari et al. 1999), which provided a benchmark for our EGF-induced migration studies. The latter method using the PHSRN-RGD peptide against a non-adhesive background provided more specific interaction with $\alpha_5\beta_1$ and $\alpha_v\beta_3$ integrins since the peptide binds both integrins, specifically $\alpha_5\beta_1$ with high affinity (Aota et al. 1994; Garcia et al. 2002; Ufret unpublished data)

The previously observed effect of PEO chain density on cell resistance was tested for the newly synthesized polymers via a qualitative fibroblast adhesion assay conducted with high levels of serum in the medium. As expected, Comb 2 completely resisted cell adhesion while Comb 1 permitted cell attachment (Figure 2.4). Adhesion to Comb 1, mediated by adsorbed serum proteins, was not as robust as adhesion to tissue culture polystyrene; cells were less spread, and fewer cells were attached.



Comb 2 (33 wt% PEO)



Comb 1 (22 wt% PEO)

Figure 2.4 – PEO Chain Density Determines Cell Adhesion Resistance.

PMMA-g-PEO comb polymers incorporating at least 30 wt% HPOEM monomer resist non-specific protein adsorption and cell adhesion. 10,000 WTNR6 fibroblasts / cm² were seeded on thin films for 4 hours in 7.5% FBS growth medium and observed for cell attachment and spreading. (A) Comb 2 polymer (33% PEO) completely resisted cell adhesion. (B) Comb 1 polymer (22% PEO) adsorbed sufficient serum proteins to support cell adhesion.

Poor adhesion to Comb 1 provided the opportunity to modulate fibroblast adhesion on these substrates by adsorbing different densities of FN to the polymer. This would allow comparison of cell migration at different adhesion states on EGF-FN substrates to previous results for the same cell line on FN in the presence of soluble EGF (Maheshwari et al. 1999). The addition of FN to Comb 1 substrates noticeably increased cell adhesion, as indicated by the increased cell spreading in Figure 2.5. Adhesion was systematically varied from low to high by adsorbing FN concentrations ranging from 0.1 ug/ml to 30 ug/ml. Cell spread areas measured on mock-activated substrates at the intermediate coating concentrations of 1 ug/ml and 10 ug/ml demonstrated that fibroblast adhesion was indeed altered between the surface

densities. The respective average fibroblast spread areas (\pm SEM) of $2438 \pm 162 \text{ um}^2$ for 59 cells and $2874 \pm 134 \text{ um}^2$ for 65 cells were significantly different by one-tailed t test with $p < 0.02$, indicating that cell adhesion was modulated within our working range of adsorbed FN densities.

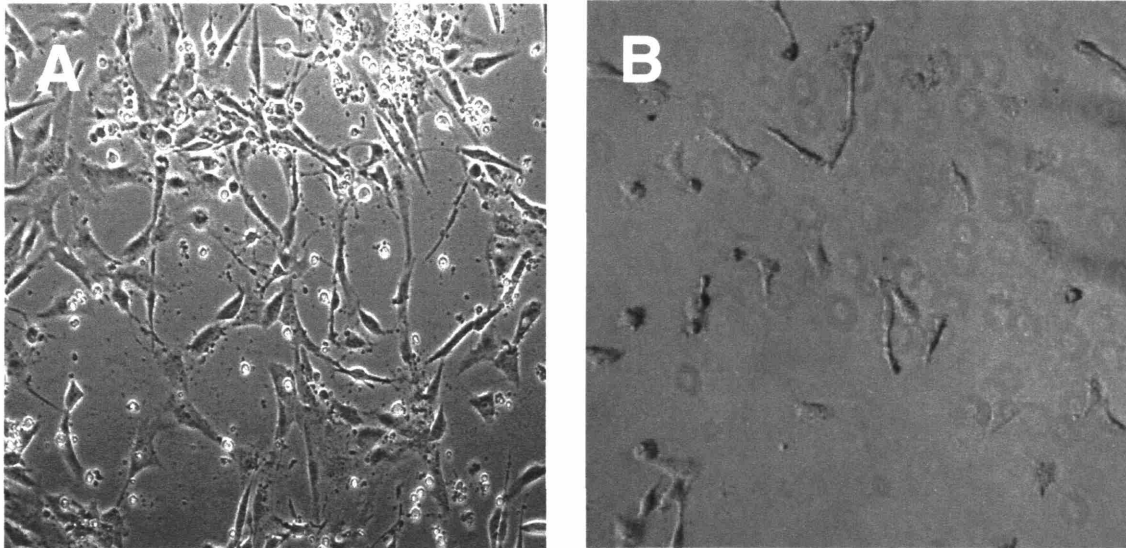


Figure 2.5 – Adsorbed FN Increases Fibroblast Adhesion to Comb 1 Polymer.

Comb 1 polymer thin films (A) with 1 $\mu\text{g/ml}$ adsorbed FN or (B) without FN were seeded with WTNR6 fibroblasts in different experiments but are observed here for morphological distinctions. Seeding conditions prior to imaging were: (A) 15,000 cells/ cm^2 seeded in 0.1% dFBS-containing medium for 12 hours, and (B) 10,000 cells/ cm^2 seeded in 7.5% FBS growth medium. Although serum conditions and timing were not the same, the long term cell morphologies are distinct as adsorbed FN with low serum promotes better attachment and spreading than high serum levels without adsorbed FN.

To differentiate FN-specific effects from EGF effects in our experiments, it was important to determine if tethering EGF had a significant effect on substrate adhesiveness. Namely, were equivalent densities of FN present on surfaces with and without tethered EGF that were coated with a given FN concentration? If not, we would need to adjust the FN coating concentrations to achieve equivalent densities for a given adhesion state. Thus, we measured the adsorbed FN densities on mock-activated, i.e. tris blocked, and tethered EGF

surfaces coated with FN for comparison at the two intermediate concentrations, 1 ug/ml and 10 ug/ml. No significant difference in adsorbed FN levels was observed between mock-activated and tethered EGF surfaces at either FN coating concentration, which correlated to ~1000 FN molecules/um² for 1 ug/ml and ~6000 FN molecules/um² for 10 ug/ml (Figure 2.6). This confirmed that statistically similar densities of FN, i.e. equivalent “adhesiveness”, were presented to cells on substrates with or without tethered EGF. Therefore, experimentally observed differences in cell signaling and motility among surfaces with a given FN coating were attributable to tethered EGF-induced factors.

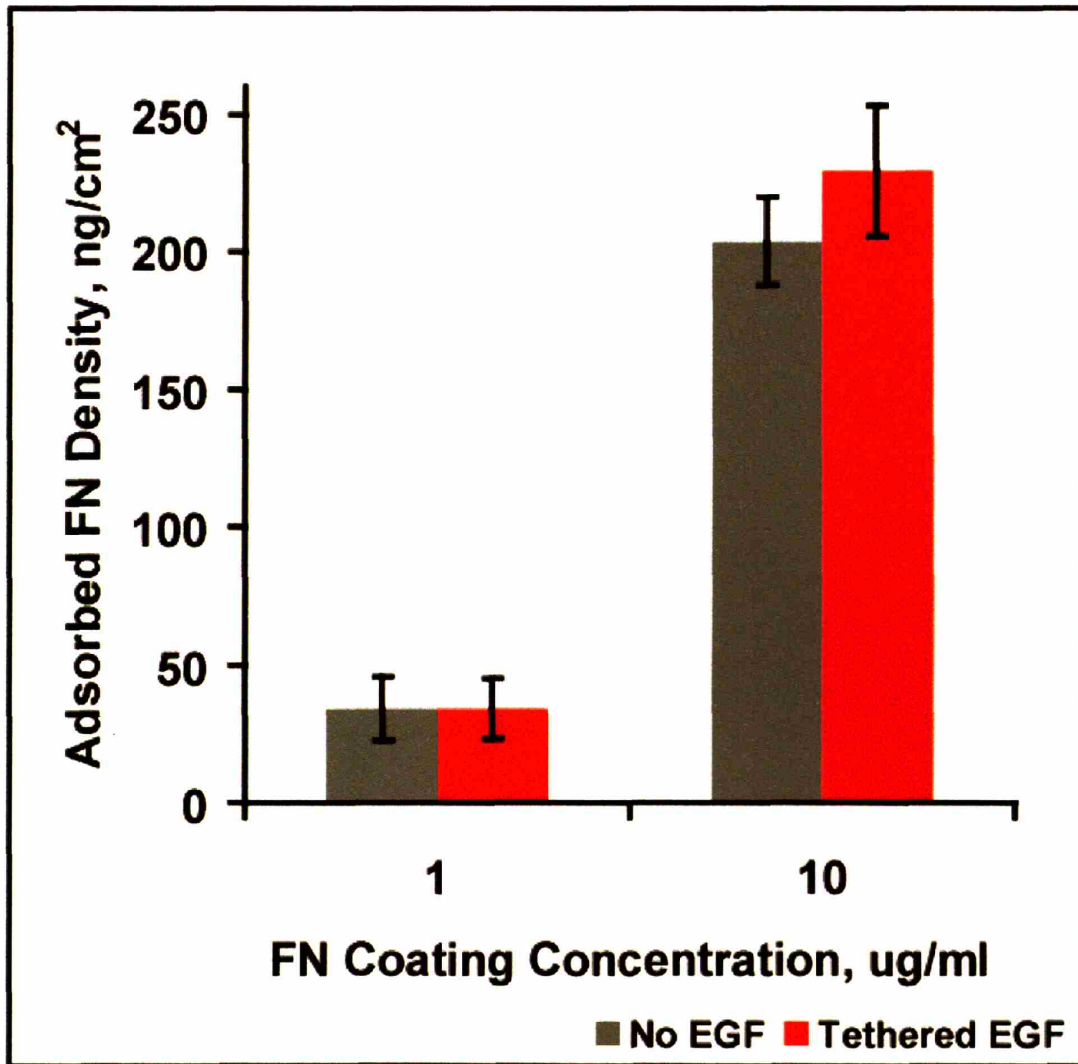


Figure 2.6 – Equivalent FN Densities for Mock-Activated vs. Tethered EGF Substrates. 1 ug/ml and 10 ug/ml ¹²⁵I-FN coating solutions were adsorbed to mock-activated (gray bars) and tethered EGF (red bars) substrates for 24 hours at 4°C. FN densities were a function of coating solution concentration but were independent of the presence of tethered EGF on the surface.

2.3.2 Tethered PHSRN-RGD Peptide Engenders $\alpha_5\beta_1$ and $\alpha_v\beta_3$ Integrin-mediated Adhesion

A branched FN-like PHSRN-RGD peptide (SynKRGD) illustrated in Figure 2.7 was covalently attached to Comb 2 via PMPI activation and coupling to engender cell adhesion. The peptide was synthesized by Dr. Maria Ufret and was chosen over the traditional RGD

domain because of its promise in promoting stronger FN-like adhesion in cells expressing $\alpha_5\beta_1$ integrins. Previous work has demonstrated that PHSRN acts as a synergy site with RGD to promote higher affinity binding to $\alpha_5\beta_1$ integrins over RGD alone (Aota et al. 1994; Garcia et al. 2002).

SynKRGD: Branched FN-like Peptide

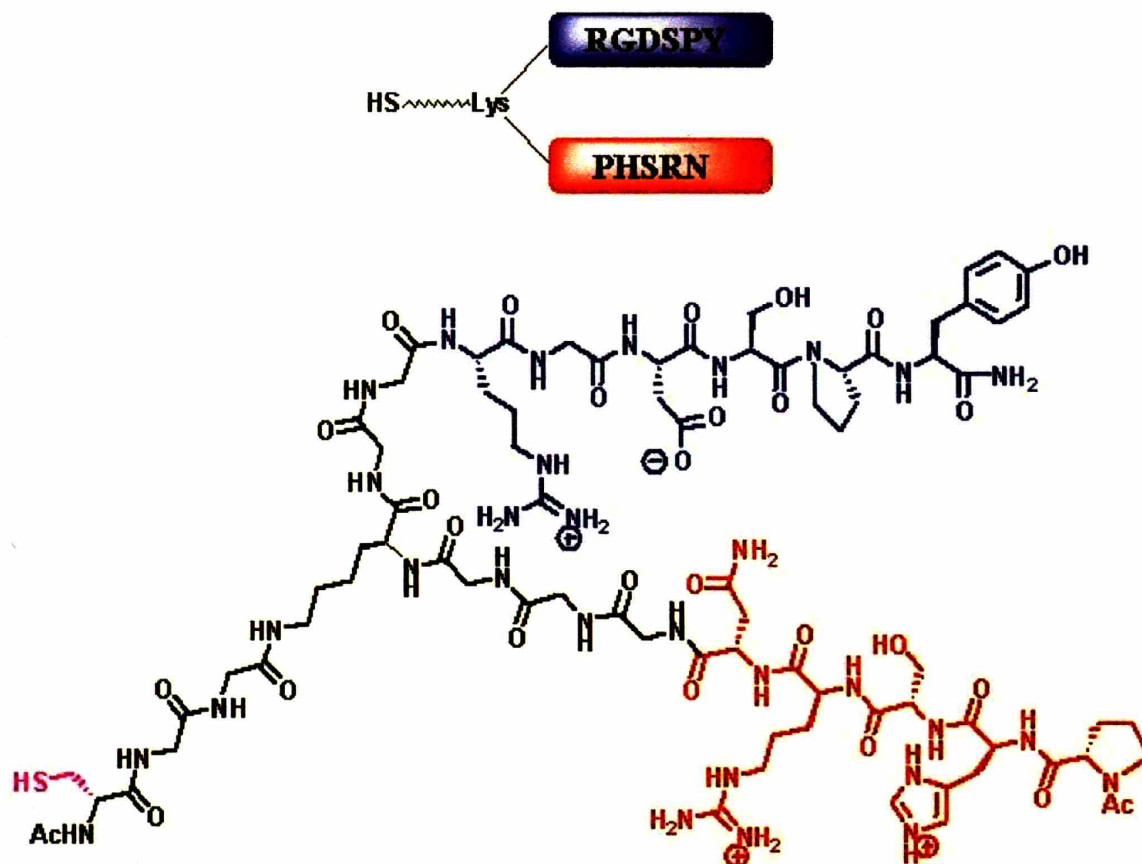


Figure 2.7 – Branched FN-like Peptide (SynKRGD).

SynKRGD incorporates the RGD adhesive domain from FN and its PHSRN synergy site. Five glycines and a lysine are used as a spacer to mimic the distance between RGD and PHSRN in native FN. These two domains together have been shown to target $\alpha_5\beta_1$ integrins with higher affinity than RGD alone (Garcia et al. 2002; Kao et al. 2001).

Figure 2.8 shows that Comb 2 polymer-tethered SynKRGD supports $\alpha_5\beta_1$ and $\alpha_v\beta_3$ integrin-mediated fibroblast adhesion as WTNR6 cells primarily express these two integrins. The cells did not adhere to Comb 2 polymer without SynKRGD (Figure 2.8A) or with adsorbed SynKRGD (Figure 2.8B), but attached and spread well on substrates presenting high density tethered SynKRGD (Figure 2.8C). Figure 2.8D illustrates that the fibroblasts required the integrin ligand for adhesion in lieu of serum proteins as they did not adhere well to tissue culture polystyrene under the low serum conditions. Tethered SynKRGD densities ranging from ~ 4000 to $300,000$ peptides/ μm^2 were demonstrated on 80% NPC / 20% PMPI Comb 2 polymer surfaces to permit adhesion modulation during subsequent experiments.

Qualitative observation suggests that fibroblast adhesion to the branched FN-like peptide resembles adhesion to whole FN. Comb 2 polymer surfaces presenting $\sim 10,000$ SynKRGD/ μm^2 were compared to Comb 1 substrates with a similar FN density (~ 6000 adsorbed FN/ μm^2). Figure 2.9 shows that while the rate of spreading on SynKRGD was approximately half that on adsorbed FN (2 hours versus 1 hour), cells on both ultimately achieved a well-spread morphology indicative of well-developed adhesion. The slower spreading rate is advantageous in allowing us to examine over a greater timescale the dynamics of early adhesion and its contribution to the EGFR-integrin signaling synergy, which we investigate in Chapter 4.

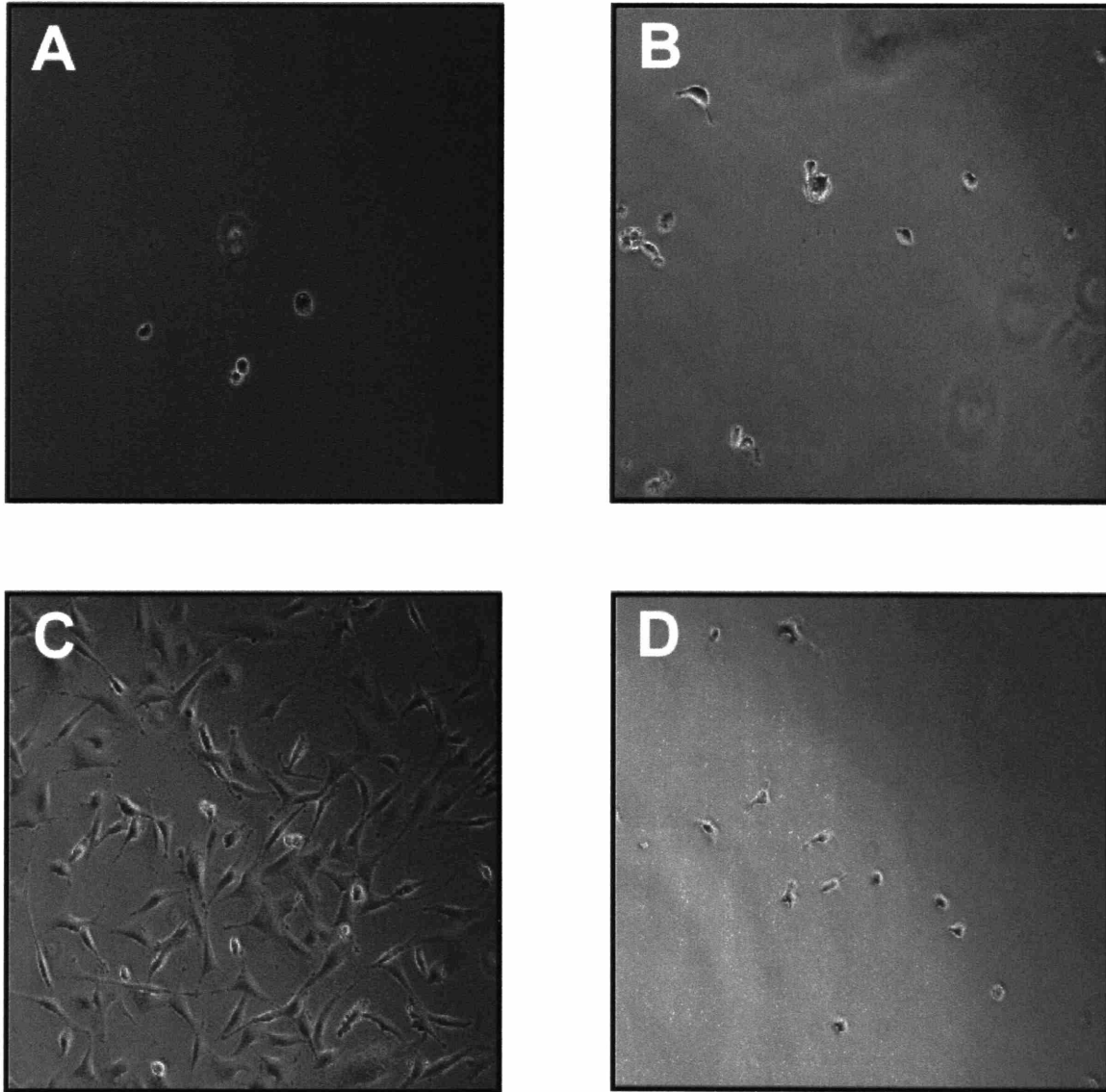


Figure 2.8 – Tethered SynKRGD engenders integrin-mediated cell adhesion. 15,000 WTNR6 fibroblasts/cm² expressing $\alpha_5\beta_1$ and $\alpha_v\beta_3$ integrins were seeded onto thin polymer films with various surface treatments in 0.1% dFBS-containing medium for 12 hours and observed for cell adhesion. Comb 2 polymer (A) untreated and (B) with adsorbed SynKRGD resisted fibroblast adhesion. Cells adhered to (C) Comb 2 polymer with 1,610,000 \pm 57,000 tethered SynKRGD/ μm^2 but did not adhere well to (D) tissue culture polystyrene, demonstrating their requirement of integrin ligands on the surface.

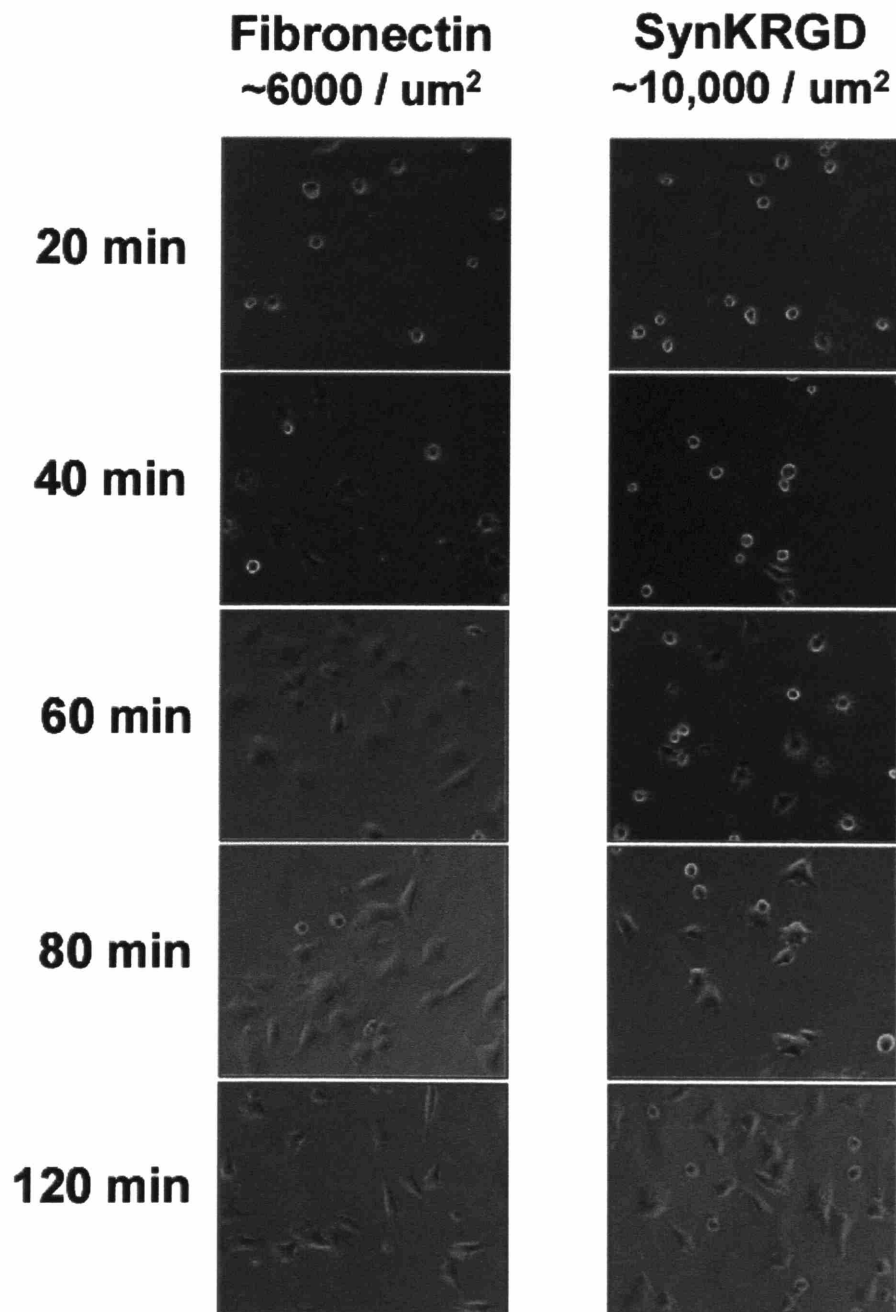


Figure 2.9 – Fibroblast spreading rate on SynKRGD is half the rate on similar FN density.

7500 WTNR6 fibroblasts/ cm^2 were seeded on polymer thin films in 0.1% dFBS-containing medium. Samples were either Comb 1 polymer presenting ~6000 adsorbed FN/ μm^2 (left) or Comb 2 polymer presenting ~10,000 tethered SynKRGD/ μm^2 (right). Images were taken every 20 minutes for 2 hours to observe the course of cell attachment and spreading. Fibroblasts on adsorbed FN were fully spread within 1 hour. Cells on tethered SynKRGD required 2 hours to spread completely but achieved comparable morphologies to FN.

As expected, adhesion to SynKRGD is an improvement over RGD alone. Fibroblasts on an equivalent density of RGD did not attach as well nor did they exhibit the same well-spread morphology as those on SynKRGD, even after 4.5 hours on the surface (Figure 2.10).

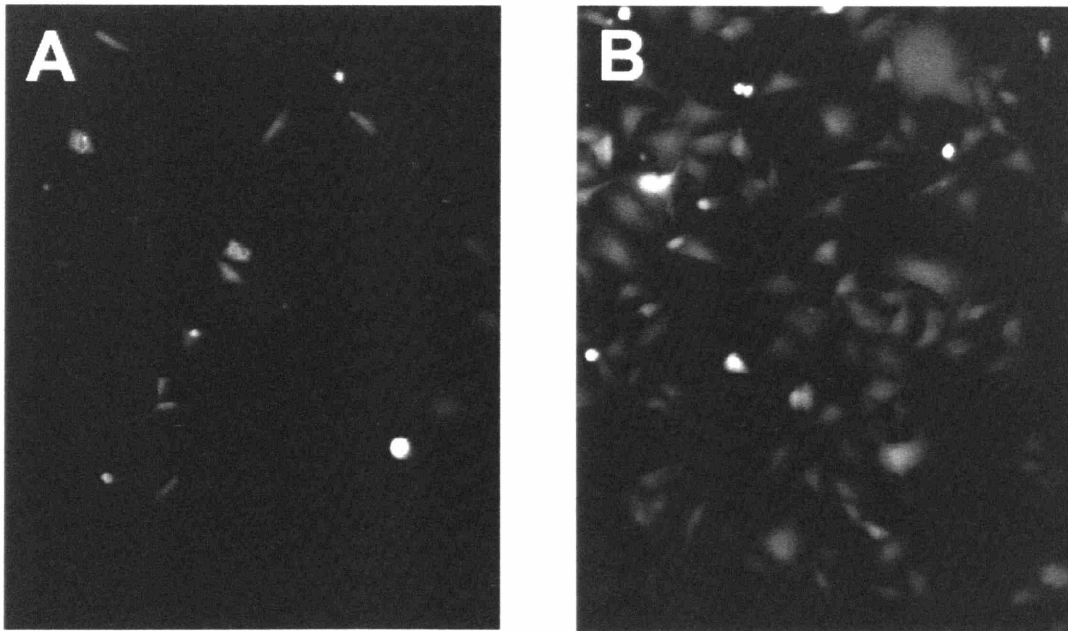


Figure 2.10 – SynKRGD enhances fibroblast attachment and spreading over RGD alone. 6400 WTNR6 fibroblasts were seeded in 0.1% dFBS medium onto Comb 2 polymer substrates presenting either (A) KRGD or (B) SynKRGD peptides at $\sim 40,000$ peptides/ μm^2 . Calcein AM at 2 $\mu\text{l/ml}$ medium was added 15 minutes prior to acquiring fluorescent images. Cells on KRGD were imaged 4.5 hours post seeding and showed sparse attachment with minimal spreading. Cells on SynKRGD were imaged 2 hours post seeding and already were well spread after attaching in significantly greater numbers than KRGD.

Previous comparisons of 3T3 fibroblast spreading on substrates modified with FN versus RGD demonstrated that spread areas on RGD were 25% to 35% less than those on FN for a broad range of concentrations. The largest areas attained by cells on RGD approximated the smallest spread areas on FN in the study, and the absolute forces generated were 3 to 5 times less (Rajagopalan et al. 2004). Our observation of increased spreading by fibroblasts on

SynKRGD compared to RGD supports the hypothesis that SynKRGD is a more ideal integrin-binding peptide. The fact that cells on SynKRGD exhibit a well-spread morphology at long times similar to FN suggests that SynKRGD provides a more physiologically relevant integrin-mediated adhesion environment than RGD, an important substrate characteristic for our study of the contribution of integrin-mediated adhesion and signaling to cell motility.

2.3.3 Optimization of Tethered EGF Density on EGF-FN Substrates

EGF-FN substrates were prepared by tethering EGF to Comb 1 polymer via a tresyl chloride primary amine coupling reaction followed by adsorption of FN. Previously, Sperinde et al. characterized tresyl chloride coupling of amino acids to poly(ethylene glycol) and showed a dependence upon temperature, pH, and steric factors (Sperinde et al. 1999). These findings were adapted to optimize the tethered EGF density when coupling the growth factor to Comb 1 polymer.

EGF coupling reactions were conducted at 4°C to maximize the amine reaction rate relative to hydrolysis. A reaction time of 3 hours was chosen as longer reaction times improved yield neither in the Sperinde work nor in our own observations. However, the EGF coupling solution pH and concentration did impact yield and were varied to optimize the surface-tethered EGF density. The molecule was coupled to tresyl-activated substrates and adsorbed to mock activated surfaces at two pH's and two concentrations to compare levels of tethered and non-specifically adsorbed EGF as functions of pH and concentration. As depicted in Figure 2.11, the density of adsorbed EGF remained unchanged at $\sim 10 \text{ ng/cm}^2$ despite a two-unit pH increase, but the tethered EGF surface density rose more than six-fold with the increase in pH, yielding $\sim 65 \text{ ng/cm}^2$ after adsorbed EGF subtraction. The reaction's sensitivity to pH was attributed to the deprotonation of primary amines as the coupling

solution approached their pKa, which rendered them more reactive. Figure 2.12 illustrates the importance of concentration to the coupling reaction where an order of magnitude increase in coupling concentration resulted in a nine-fold yield improvement.

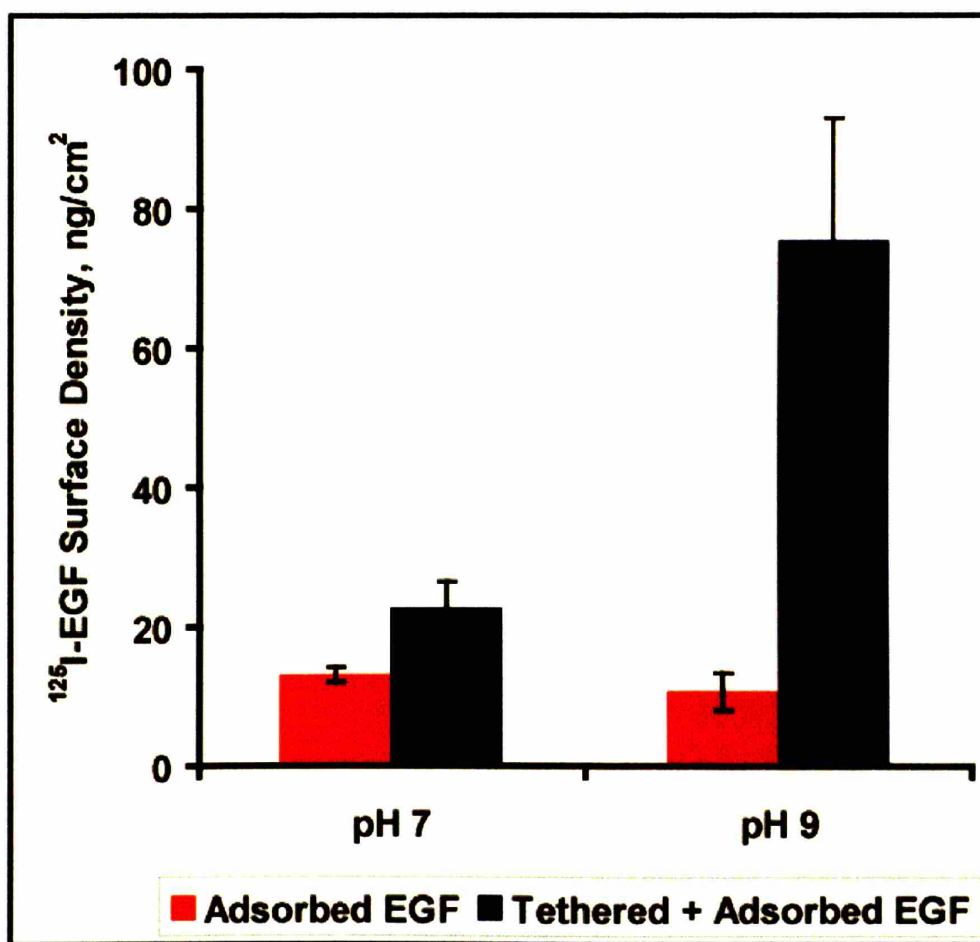


Figure 2.11 – Comb 1 Tethered EGF Density is a Function of Coupling Solution pH. Tressyl chloride-activated (blue bars) and mock-activated (red bars) Comb 1 polymer thin films were exposed to 5 ug/ml ¹²⁵I-EGF solutions at pH 7.0 and pH 9.0 for 3 hours at 4°C. Quantification of surface-associated EGF revealed a 6.5-fold improvement in tethered EGF with the pH increase while adsorbed EGF remained unchanged (~10,000 EGF/um²).

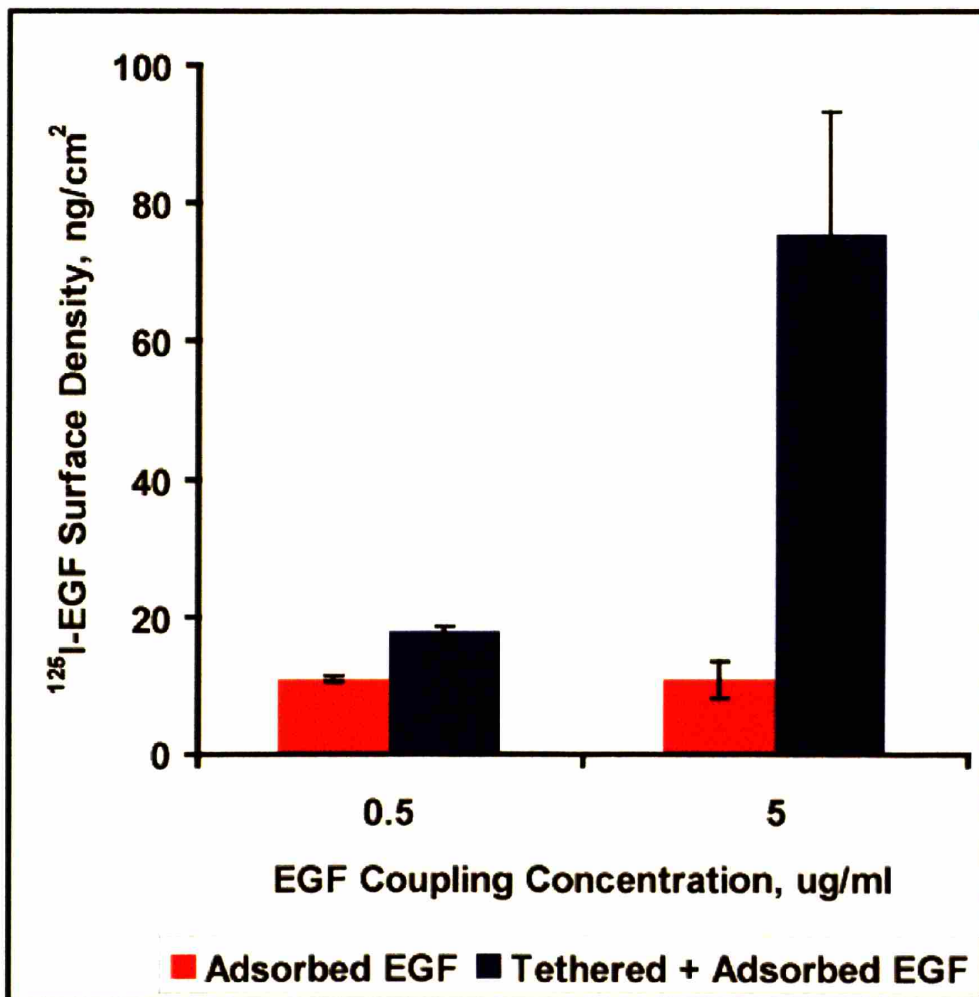


Figure 2.12 – Comb 1 Tethered EGF Density is a Function of Coupling Solution Concentration. Tresyl chloride-activated (blue bars) and mock-activated (red bars) Comb 1 polymer thin films were exposed to 0.5 ug/ml or 5 ug/ml ¹²⁵I-EGF solutions at pH 9.0 for 3 hours at 4°C. Quantification of surface-associated EGF revealed a 9-fold improvement in tethered EGF over the 10X concentration increase while adsorbed EGF remained unchanged (~10,000 EGF/um²).

From this work, the three-hour coupling conditions of 5 ug/ml EGF at pH 9 and 4°C were chosen to produce substrates with a tethered EGF density of ~65 ng/cm² for use in the motility studies of Chapter 3. It was calculated from ligand-receptor kinetics and receptor expression levels that 65 ng tethered EGF/cm², or approximately 65,000 EGF/um², would theoretically saturate cell surface EGFR's assuming receptor availability in the cell

membrane contacting the material surface and their ability to bind the tethered ligand. These calculations are described in detail in this chapter's Appendix.

2.3.4 Nanoscale Control of Co-tethered Ligand Densities

The Comb 2 polymer permits covalent attachment of two ligands to the same substrate. Blends of PMPI-activated and NPC-activated Comb 2 polymers were prepared to attach cysteine-terminated adhesion peptides to PMPI-activated polymer and amine-terminated EGF to NPC-activated polymer as illustrated in Figures 2.1 and 2.3. Individual Comb 2 polymer chains display 19 functionalizable PEO side chains on average. Blends of polymer chains activated with either PMPI or NPC make nanoscale control of individual ligand densities possible with local areas enriched in either adhesion peptide or EGF. This increases the likelihood of integrin clustering and EGFR homodimerization on tethered ligand surfaces.

The PMPI peptide coupling reaction occurs rapidly at pH 7.5 without primary amines present so it was conducted first for two hours without significant hydrolysis of NPC-activated side chains. The slower NPC EGF coupling reaction was initiated subsequently for longer times at a higher pH 8.5 to deprotonate primary amines and drive the reaction forward. The fractions of PMPI-activated and NPC-activated polymers were independently varied by addition of a third unactivated polymer component to the blend. We quantitatively demonstrated that by changing the activated polymer fractions we could alter the tethered peptide and EGF densities. Figure 2.13 depicts a range of PMPI-activated polymer fractions coupled at the same concentration for two hours. Tethered SynKRGD densities from ~100,000 to 300,000 peptides/ μm^2 were achieved with PMPI fractions between 0.10 and 0.25. EGF displayed similar trends of increasing tethered protein density with greater NPC-

activated polymer fraction. Tethered EGF densities on the order of 100 and 1000 molecules/ μm^2 were obtained by changing NPC polymer fraction (Figure 2.14A).

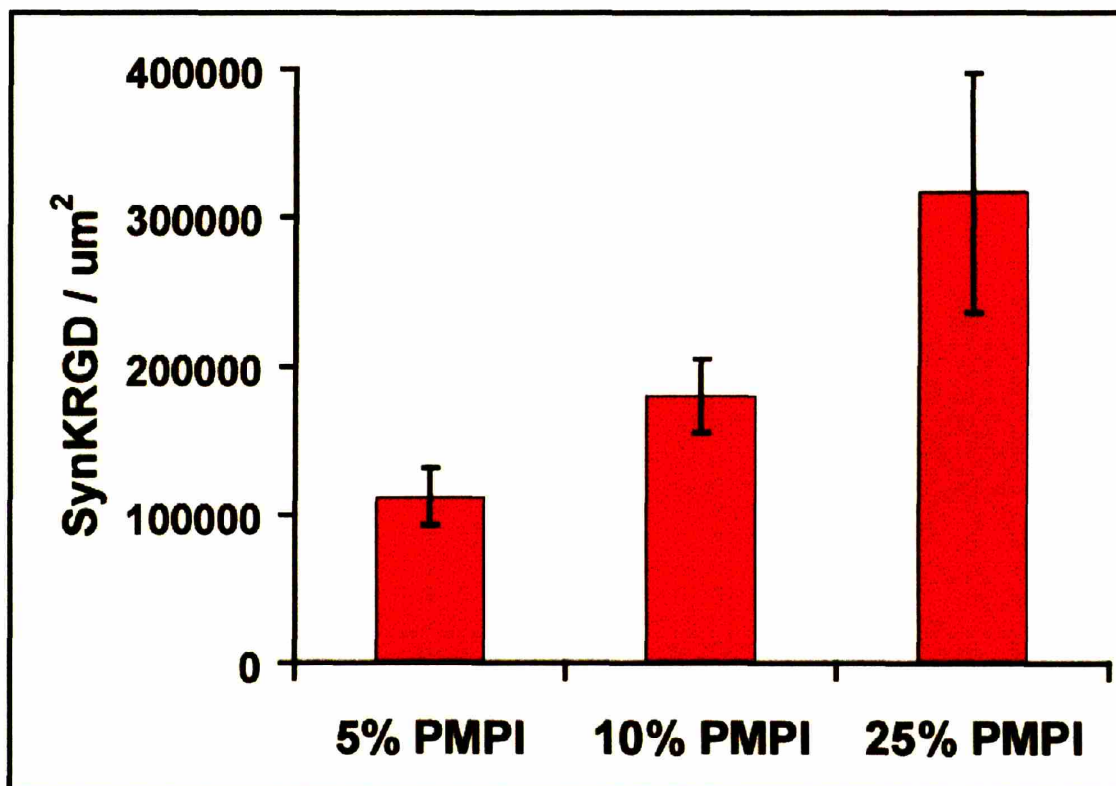


Figure 2.13 – Comb 2 Tethered Adhesion Peptide Varies with PMPI Fraction. 125 μM ^{125}I -SynKRGD was reacted for 2 hours at room temperature with Comb 2 polymer thin films containing different fractions of PMPI-activated polymer. Tethered SynKRGD densities increased with increasing PMPI fraction.

Reaction time also regulated the slowly proceeding NPC EGF coupling. An order of magnitude greater density, ~ 5000 to 7000 EGF/ μm^2 vs. ~ 100 to 700 EGF/ μm^2 , was achieved by increasing the EGF coupling time from 4 to 24 hours (Figure 2.14B). EGF-SynKRGD surfaces used in the biological studies of Chapter 4 presented 5000 to 7000 EGF/ μm^2 following 24-hour coupling times.

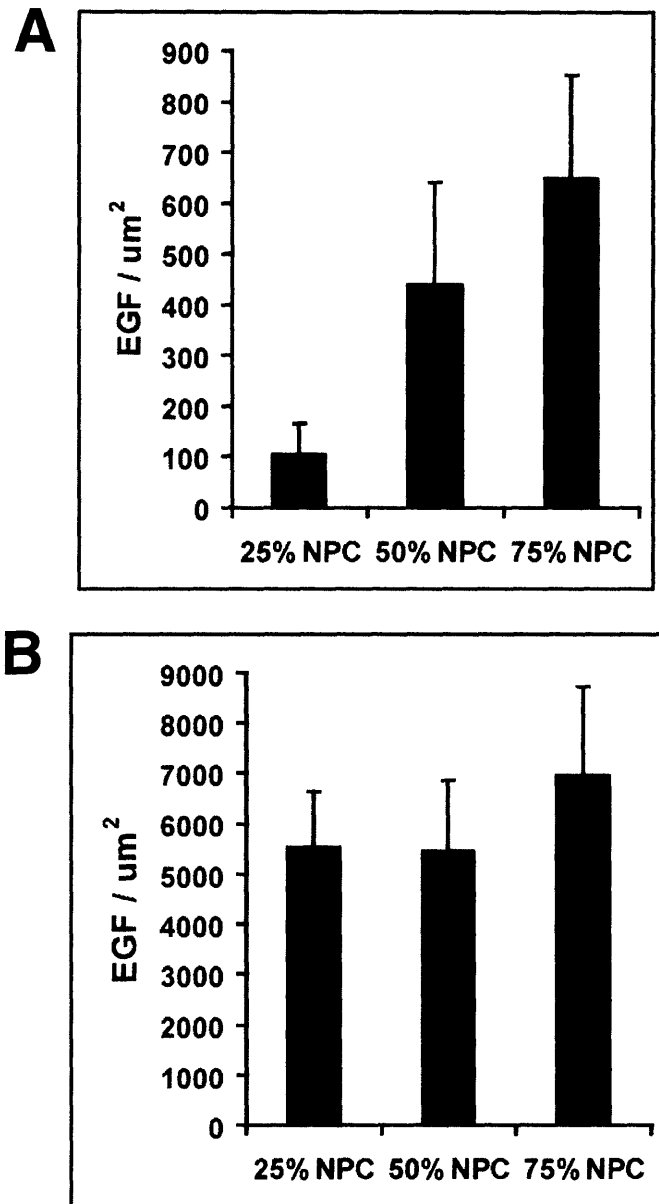


Figure 2.14 – Comb 2 Tethered EGF Varies with NPC Fraction and Coupling Time. 25 $\mu\text{g}/\text{ml}$ ^{125}I -EGF was reacted for (A) 4 hours or (B) 24 hours at room temperature with Comb 2 polymer thin films containing different fractions of NPC-activated polymer. Tethered EGF densities varied with NPC fraction and displayed an order of magnitude increase when coupled 24 hours versus 4 hours. Values represent tethered EGF after subtraction of adsorbed EGF, which was typically ~ 100 EGF/ μm^2 .

Coupling solution concentration effectively modulated the density of tethered SynKRGD. Varying SynKRGD concentration in the high nanomolar and micromolar range

produced a broad spectrum of densities from ~4000 to more than 300,000 peptides/ μm^2 on 20% PMPI-activated substrates. Dr. Maria Ufret reported an even wider range under different blend and time conditions (Maria Ufret, unpublished data). Since a broad range of peptide densities was attainable by varying relatively low peptide concentrations, concentration was used to modulate the tethered SynKRGD density in studies where variations in cell adhesion were desired. Due to the relatively high and expensive EGF concentration required for appreciable reaction with NPC (5 $\mu\text{g}/\text{ml}$ was insufficient), similar concentration-varying experiments with EGF and NPC were not conducted once a threshold value (25 $\mu\text{g}/\text{ml}$) for suitably dense tethered EGF was found.

2.3.5 Analysis of Tethered Ligand EGFR Homodimerization and Integrin Clustering

Bound EGFR requires homodimerization with another ligated EGFR or heterodimerization with another member of the ErbB receptor family for effective downstream signaling (Schlessinger 2000). Similarly, effective adhesion necessitates the clustering of multiple ligand-bound integrins to create focal complexes or focal adhesions large enough to transduce intracellular forces to the extracellular environment (Koo et al. 2002; Yauch et al. 1997). Thus, we made order-of-magnitude physical estimates of the tethered ligand densities necessary for EGFR homodimerization and integrin clustering on PMMA-g-PEO comb polymer substrates.

Estimates assuming an immobile tether as well as a flexible tether were considered. The immobile tether model was considered the most conservative case, while the flexible tether model was thought to more closely recapitulate the PMMA-g-PEO polymer substrates due to the flexibility of PEO chains. However, these order-of-magnitude estimates were best

case scenarios in which all tethered ligands could bind receptors. In reality, receptor binding by tethered EGF and adhesion molecules is likely hindered by steric factors and restricted ligand orientation due to the molecular tethers. As such, we expect a fraction of the available surface-bound ligands to successfully bind cell surface growth factor and adhesion receptors.

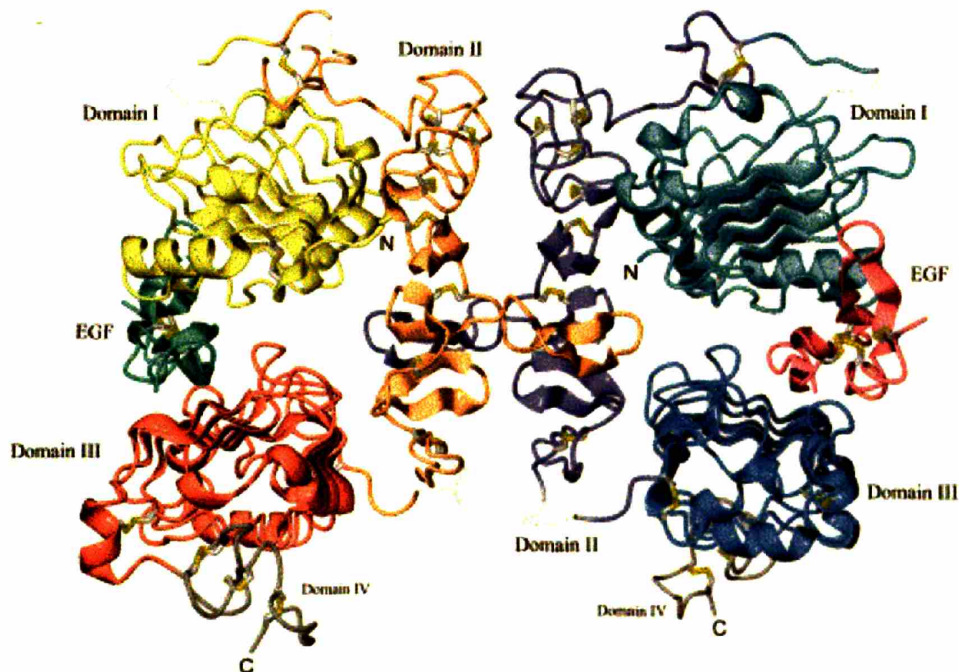


Figure 2.15 – Extracellular domain of an EGF-bound EGFR homodimer.

Domains I, II, and III of the extracellular portion of EGFR form a C shape in which EGF binds between domains I and III. In the homodimer, direct interaction occurs between domains II of each receptor. The distance between EGF molecules is 7.9 nm. This crystal structure was taken from (Ogiso et al. 2002).

Ogiso et al. resolved the crystal structure of the extracellular domain of an EGF-bound EGFR homodimer. As shown in Figure 2.15, it revealed two outwardly facing C shapes formed by domains I, II, and III of the receptors in which an EGF molecule was bound to both EGFR's between domains I and III. Dimerization occurred by direct interaction between domain II of each receptor. Based on the crystal structure, the distance

between EGF that permitted homodimerization was 7.9 nm (Ogiso et al. 2002). This translated to one EGF molecule every 62 nm² or ~16,000 EGF/um² with an immobile tether. Assuming a flexible 2 nm PEO tether, the maximum distance between EGF increased to 11.9 nm. This distance required one EGF molecule every 142 nm² or a density of ~7000 EGF/um². Because all polymer chains were equally activated in Comb 1 polymer thin films and only EGF was tethered, a uniform density of tethered EGF on these surfaces was assumed. The experimentally determined tethered EGF density on Comb 1 substrates was 64,000 ± 18,000 EGF/um², an order-of-magnitude greater than the density requirements for homodimerization suggested by either tether model (Table 2.2).

Table 2.2 –Estimate of Comb 1 Polymer-tethered EGF Uniform Density for EGFR Homodimerization

<i>Theoretical Required Density for EGFR Homodimerization</i>		
Immobile Tether Model	Flexible Tether Model[†]	Experimental Density
16,000 EGF / um ²	7000 EGF / um ²	64,000 ± 18,000 EGF / um ²

[†] Assumes 2 nm PEO tether.

In contrast to Comb 1 polymer, the global tethered EGF density experimentally achieved on the NPC-activated Comb 2 polymer surfaces was an order-of-magnitude lower at 7000 ± 1700 EGF/um². However, these thin films were prepared from 80% NPC / 20%

PMPI blends so that the local densities of each tethered ligand were actually greater. They also displayed longer 10-mer side chains compared to the 6.5-mer PEO chains of Comb 1. This reduced the required local EGF density in the flexible tether model. To achieve the local density of 16,000 EGF/ μm^2 (immobile tether model) or 5200 EGF/ μm^2 (flexible tether model with 3 nm PEO tethers) required for EGFR homodimerization, the experimentally measured global density on substrates having 80% EGF coverage needed to be only 12,800 EGF/ μm^2 or 4200 EGF/ μm^2 (Table 2.3). Thus, the flexible tether estimate suggested that the Comb 2 tethered EGF density obtained experimentally would be sufficient for EGFR homodimerization and subsequent signaling.

Table 2.3 - Estimate of Comb 2 Polymer-tethered EGF Clustered Density for EGFR Homodimerization

<i>Theoretical Required Density* for EGFR Homodimerization</i>		
Immobile Tether Model	Flexible Tether Model[†]	Experimental Density
12,800 EGF / μm^2	4200 EGF / μm^2	7000 \pm 1700 EGF / μm^2

* Global density assuming 80% NPC (EGF) / 20% PMPI (peptide) clustered substrates.

[†] Assumes 3 nm PEO tether.

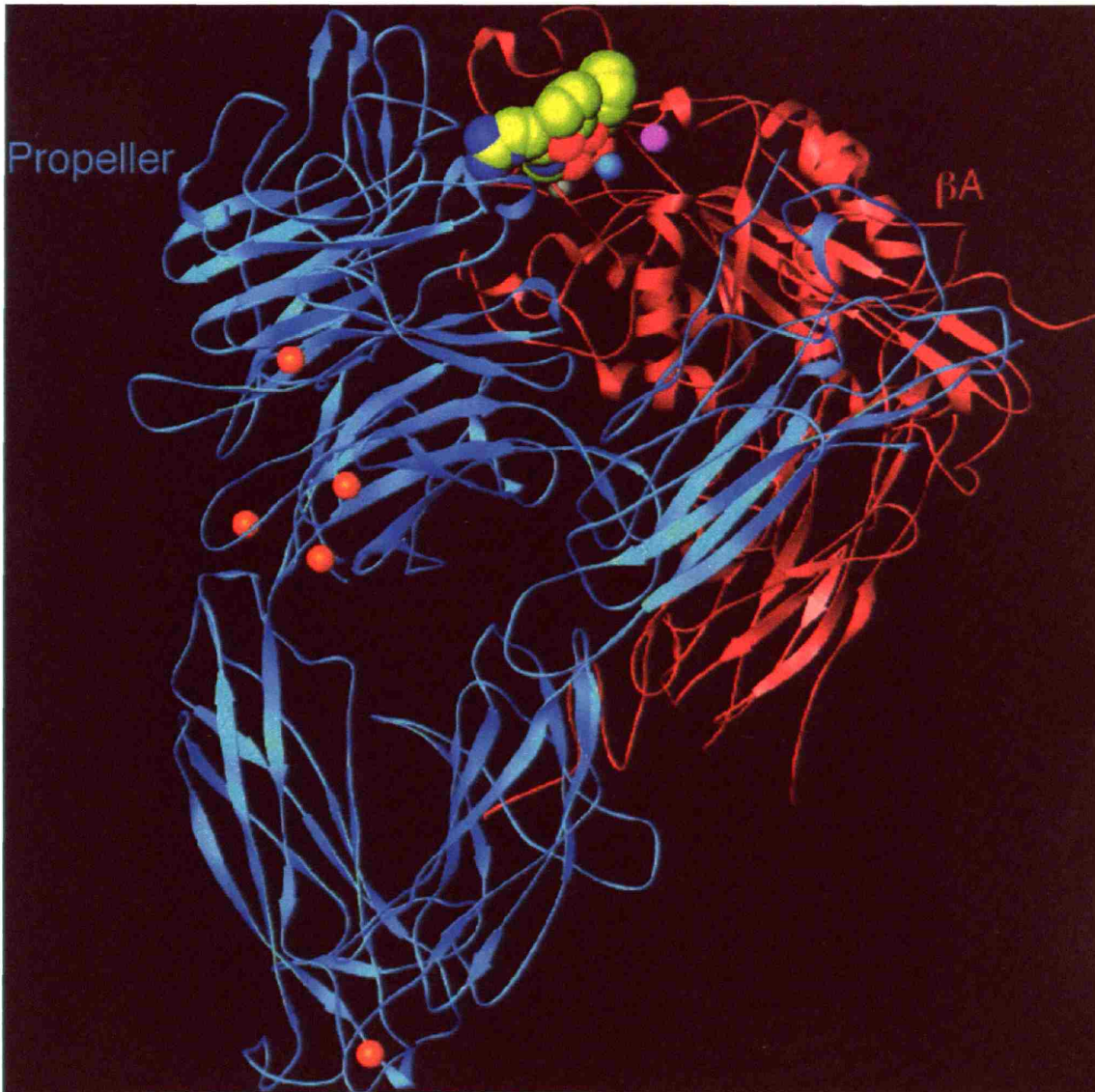


Figure 2.16 – Integrin $\alpha_v\beta_3$ in complex with cyclic RGD.

The $\alpha_v\beta_3$ integrin consists of the α_v (blue) and β_3 (red) subunits. The extracellular domain shown by ribbon structure here measures 9 nm in length and is 6 nm x 4.5 nm at the integrin head where ligand binding occurs. The carbon, nitrogen, and oxygen atoms of the bound cyclic RGD peptide are denoted as yellow, blue, and red balls, respectively, at the interface between subunits. This crystal structure was taken from (Xiong et al. 2002).

The same immobile and flexible tether models also were used as order-of-magnitude estimates to predict integrin clustering on the co-tethered EGF and adhesion peptide surfaces.

From the crystal structure of a ligated $\alpha_v\beta_3$ integrin shown in Figure 2.16 (Xiong et al. 2001;

Xiong et al. 2002), the maximum distance between peptides to allow integrin clustering was determined to be 6 nm. This meant that one peptide was required every 36 nm² for a local density of 28,000 peptides/um² by the immobile tether model. The maximum peptide-peptide distance increased to 12 nm in the flexible tether model, suggesting that a peptide be present every 144 nm². This was accomplished by a 7000 peptides/um² local density. As noted in Table 2.4, the local peptide densities required by the immobile and flexible tether models translated to global densities of 5600 and 1400 peptides/um², respectively, on 20% peptide-covered substrates. Significantly higher densities were experimentally demonstrated and used to promote excellent cell adhesion in subsequent cell studies.

Table 2.4 –Estimate of Comb 2 Polymer-tethered Adhesion Peptide Clustered Density for Integrin Clustering

<i>Theoretical Required Density* for Integrin Clustering</i>		
Immobile Tether Model	Flexible Tether Model†	Experimental Density
5600 peptides / um ²	1400 peptides / um ²	Range of ~4000 to 300,000 SynKRGD / um ²

* Global density assuming 80% NPC (EGF) / 20% PMPI (peptide) clustered substrates.

† Assumes 3 nm PEO tether.

2.3.6 Tethering Other Growth Factors: Tenascin C EGF-Like Fragment 14

To demonstrate the ability to tether other relevant growth factors to PMMA-g-PEO comb polymer surfaces, the 14th EGF-like repeat found in tenascin C (Ten14) was co-tethered with SynKRGD to the Comb 2 polymer. Tenascin C is a large extracellular matrix protein containing 14 EGF-like repeats, some of which have been shown to bind EGFR with low affinity in a soluble form (Swindle et al. 2001). It has been proposed that low affinity EGF-like fragments embedded in larger matrix molecules might signal cells from the matrix in a spatially restricted form, called matrikine signaling (Schenk et al. 2003; Swindle et al. 2001; Tran et al. 2004). Ten14 (M ~ 7900 g/mol) had a similar size to EGF. Having been shown previously to bind to EGFR with low affinity (Swindle et al. 2001) and to promote cell migration (Alan Wells, unpublished work), it was a physiologically relevant candidate to study matrikine EGFR-mediated signaling and response by tethering it to a polymer substrate.

When covalently linking whole proteins such as EGF or Ten14 growth factors to a material surface, the size of the molecule dictates how densely it can be tethered. Proteins may be diffusion-limited, requiring longer reaction times than smaller peptides. Competing reactions like hydrolysis can reduce the attainable yield under such conditions. As a result, coupling conditions like time, temperature, and concentration must be optimized for each protein being tethered. Steric factors also play a role as the packing of large molecules on a surface limits their density. The accessibility of reactive groups for linkage also governs the tethering reaction for proteins. A coupling reaction that targets a growth factor's N-terminal amine may never occur if the N-terminus is buried within the folded protein.

We cannot assume a growth factor will be biologically active following substrate linkage. If reaction conditions such as high pH or extended exposure to room temperature are too harsh, the protein may no longer assume an active conformation. Its spatial presentation on the surface may also render it inactive. For example, if the site where the growth factor is linked to the surface is also part of its receptor binding domain or if the receptor binding domain is hidden as it is presented to the cell, the growth factor's ability to bind the receptor may be compromised.

Ten14, our second candidate protein, was reacted with Comb 2 substrates under similar conditions to previous EGF couplings. As illustrated in Figure 2.17, only 610 ± 63 Ten14/ μm^2 were covalently linked to the surface, almost a 12-fold decrease compared to EGF. Unfortunately, these substrates did not elicit observable EGFR activation in WTNR6 fibroblasts when measured by Western blot (data not shown). This may have been due to insufficient density to promote EGFR homodimerization as suggested by the order-of-magnitude estimates of EGFR homodimerization by tethered EGF. Optimizing coupling conditions might increase the attainable tethered Ten14 density. However, the lack of activity also could have been the result of inactive spatial presentation as a tethered molecule or development of an inactive conformation as an artifact of the surface coupling.

Despite the inactivity of Ten14-SynKRGD substrates, we demonstrated that we could successfully bind other small growth factors to the PMMA-g-PEO comb polymer. Addition of new ligands to the comb polymer platform is an iterative process in optimization, one that is quite feasible considering the techniques for controlling multiple ligand densities and nanoscale spatial organizations presented in this work.

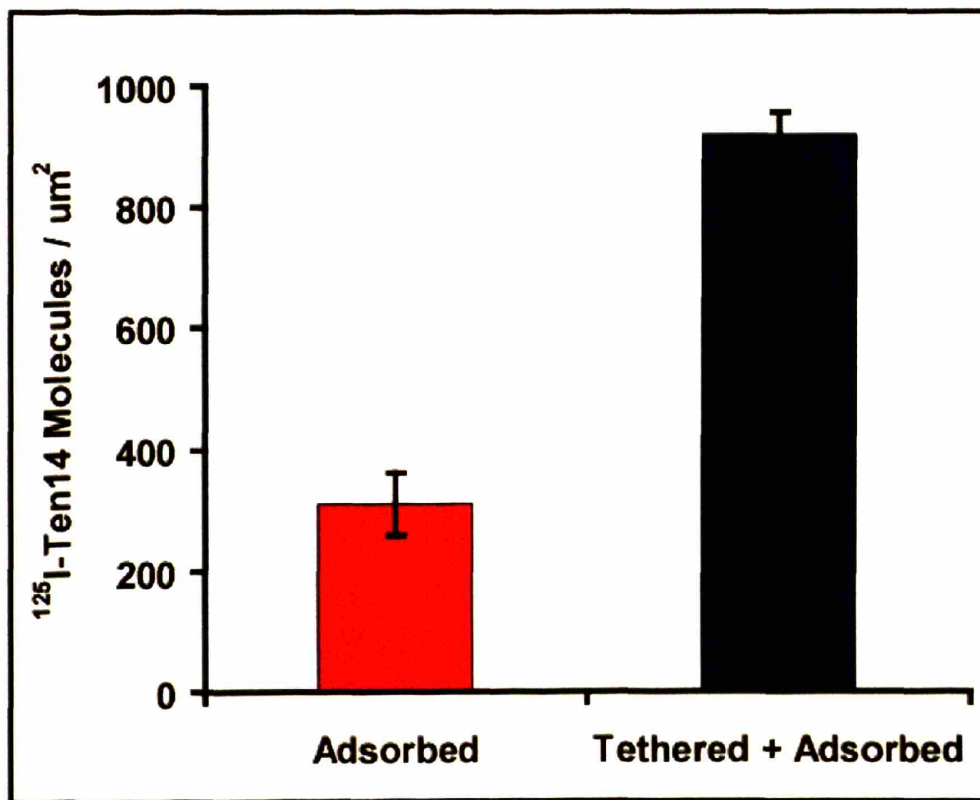


Figure 2.17 – Quantification of Tethered Tenascin C EGF-like Repeat 14.

Following a two-hour coupling of 2 μM SynKRGD that yielded ~ 4000 SynKRGD/ μm^2 , 32 $\mu\text{g/ml}$ $^{125}\text{I-Ten14}$ (same molarity as EGF coupling concentration) was reacted for 24 hours at room temperature with Comb 2 polymer containing 80% NPC-activated and 20% PMPI-activated polymer. Ten14 was successfully tethered at low density, demonstrating the application of co-tethered polymer substrates to other growth factor systems.

2.4 References

- Aota S, Nomizu M, Yamada KM. 1994. The short amino acid sequence Pro-His-Ser-Arg-Asn in human fibronectin enhances cell-adhesive function. *J Biol Chem* 269(40):24756-61.
- Baugh L, Vogel V. 2004. Structural changes of fibronectin adsorbed to model surfaces probed by fluorescence resonance energy transfer. *J Biomed Mater Res A* 69(3):525-34.
- Chen P, Gupta K, Wells A. 1994. Cell movement elicited by epidermal growth factor receptor requires kinase and autophosphorylation but is separable from mitogenesis. *J Cell Biol* 124(4):547-55.
- Garcia AJ, Schwarzbauer JE, Boettiger D. 2002. Distinct activation states of alpha5beta1 integrin show differential binding to RGD and synergy domains of fibronectin. *Biochemistry* 41(29):9063-9.
- Irvine DJ, Mayes AM, Griffith LG. 2001. Nanoscale clustering of RGD peptides at surfaces using Comb polymers. 1. Synthesis and characterization of Comb thin films. *Biomacromolecules* 2(1):85-94.
- Kao WJ, Lee D, Schense JC, Hubbell JA. 2001. Fibronectin modulates macrophage adhesion and FBGC formation: the role of RGD, PHSRN, and PRRARV domains. *J Biomed Mater Res* 55(1):79-88.
- Koo LY, Irvine DJ, Mayes AM, Lauffenburger DA, Griffith LG. 2002. Co-regulation of cell adhesion by nanoscale RGD organization and mechanical stimulus. *J Cell Sci* 115(Pt 7):1423-33.
- Kuhl PR, Griffith-Cima LG. 1996. Tethered epidermal growth factor as a paradigm for growth factor-induced stimulation from the solid phase. *Nat Med* 2(9):1022-7.
- Maheshwari G, Wells A, Griffith LG, Lauffenburger DA. 1999. Biophysical integration of effects of epidermal growth factor and fibronectin on fibroblast migration. *Biophys J* 76(5):2814-23.
- Ogiso H, Ishitani R, Nureki O, Fukai S, Yamanaka M, Kim JH, Saito K, Sakamoto A, Inoue M, Shirouzu M and others. 2002. Crystal structure of the complex of human epidermal growth factor and receptor extracellular domains. *Cell* 110(6):775-87.
- Rajagopalan P, Marganski WA, Brown XQ, Wong JY. 2004. Direct comparison of the spread area, contractility, and migration of balb/c 3T3 fibroblasts adhered to fibronectin- and RGD-modified substrata. *Biophys J* 87(4):2818-27.
- Schenk S, Hintermann E, Bilban M, Koshikawa N, Hojilla C, Khokha R, Quaranta V. 2003. Binding to EGF receptor of a laminin-5 EGF-like fragment liberated during MMP-dependent mammary gland involution. *J Cell Biol* 161(1):197-209.
- Schlessinger J. 2000. Cell signaling by receptor tyrosine kinases. *Cell* 103(2):211-25.
- Sperinde JJ, Martens BD, Griffith LG. 1999. Tresyl-mediated synthesis: kinetics of competing coupling and hydrolysis reactions as a function of pH, temperature, and steric factors. *Bioconjug Chem* 10(2):213-20.
- Swindle CS, Tran KT, Johnson TD, Banerjee P, Mayes AM, Griffith L, Wells A. 2001. Epidermal growth factor (EGF)-like repeats of human tenascin-C as ligands for EGF receptor. *J Cell Biol* 154(2):459-68.

- Tran KT, Griffith L, Wells A. 2004. Extracellular matrix signaling through growth factor receptors during wound healing. *Wound Repair Regen* 12(3):262-8.
- Ufret M. unpublished data.
- Xiong JP, Stehle T, Diefenbach B, Zhang R, Dunker R, Scott DL, Joachimiak A, Goodman SL, Arnaout MA. 2001. Crystal structure of the extracellular segment of integrin alpha Vbeta3. *Science* 294(5541):339-45.
- Xiong JP, Stehle T, Zhang R, Joachimiak A, Frech M, Goodman SL, Arnaout MA. 2002. Crystal structure of the extracellular segment of integrin alpha Vbeta3 in complex with an Arg-Gly-Asp ligand. *Science* 296(5565):151-5.
- Yauch RL, Felsenfeld DP, Kraeft SK, Chen LB, Sheetz MP, Hemler ME. 1997. Mutational evidence for control of cell adhesion through integrin diffusion/clustering, independent of ligand binding. *J Exp Med* 186(8):1347-55.

Appendix: Estimation of Receptor Occupancy on Tethered EGF Substrates

$$C_{eq} = \frac{R_T L_0}{K_D + L_0}$$

C_{eq} ~ equilibrium ligand-receptor complexes

R_T ~ total receptors

L_0 ~ ligand concentration

K_D ~ ligand affinity (k_{off} / k_{on})

(90% Occupancy if $L_0 = 10 K_D$)

- $K_D \sim 1$ nM for EGF-EGFR
- $L_0 \sim 10$ mM for tethered EGF
 - Tethered EGF Surface Density $\sim 65,000$ EGF/ μm^2
 - Distance between surface and cell membrane ~ 8 nm
(2 nm PEO tether + 3 nm EGF + 3 nm EGFR head)

$$\frac{65,000 \text{ EGF} / \mu m^2}{8e(-3) \mu m} \times 1e(15) \mu m^3 / L \times N_A \approx 10mM$$

$L_0 \gg K_D$ so $C_{eq} \sim R_T \rightarrow$ *Receptors saturated*

3. Tethered and Soluble EGF Differentially Affect Fibroblast Migration and Adhesion

3.1 Introduction

Cell migration is an important process in physiological development, tissue regeneration, and cancer. It is a repeated cycle of membrane protrusion, stable frontal adhesion formation, cytoskeletal reorganization, contraction, and rear de-adhesion that moves the cell from one location to another (Figure 3.1).

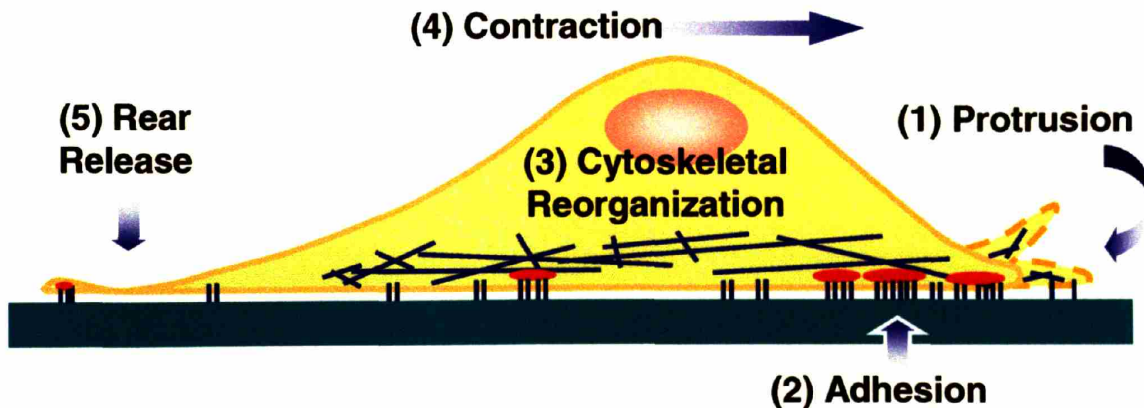


Figure 3.1 – Coordinated mechanics of cell migration.

A migrating cell (1) protrudes its membrane and may do so in several directions before (2) forming a stable adhesion. (3) The cytoskeleton is rearranged polarizing the cell and forming front-to-rear stress fibers across which (4) contraction occurs. Under the contractile forces, (5) the cell rear is preferentially released as the cell moves forward, and the cycle is repeated.

Cell migration speed is predicted to be dependent upon the cell-substrate adhesion strength and contractile forces generated within the cell where a balance between the two is necessary. If adhesion between the cell and substrate is too weak, the cell cannot create the stable adhesions necessary for locomotion following membrane extension. If adhesion is too great, the cell cannot detach its rear in response to contractile forces.

Thus, a biphasic relationship between migration speed and adhesion strength is predicted (DiMilla, Barbee et al. 1991) and has been demonstrated in smooth muscle cells (DiMilla, Stone et al. 1993).

EGF is known to increase migration speed in fibroblasts expressing EGFR as EGFR signaling elicits cytoskeletal reorganization and contraction and also governs aspects of integrin-mediated cell adhesion (Cheresh, Leng et al. 1999; Wells, Ware et al. 1999; Glading, Lauffenburger et al. 2002). This was experimentally validated in WTNR6 fibroblasts on surfaces coated with varied FN densities. The addition of EGF was found to decrease the cell-substrate adhesion strength at all conditions of substrate adhesiveness. It also was shown to increase membrane protrusion and retraction at moderate adhesion states where increased migration speed was observed (Maheshwari, Wells et al. 1999). Therefore, the proper levels of cell-substrate adhesion strength, cytoskeletal reorganization, and contraction force are indeed required for EGF-enhanced cell migration.

In vivo, EGFR ligands are known to be bound or embedded in the ECM and presumably act by signaling from the cell surface. Association with matrix may permit stimulation of cells by a ligand gradient that directs migration over longer time and length scales than soluble EGFR ligands. Here, such a matrix association is modeled using tethered EGF. Because EGFR activates multiple signaling pathways, each with different intracellular spatial distributions, signaling by tethered EGF may affect the balance of signaling that regulates cell motility by preferentially activating signaling pathways that are surface-localized.

In Chapter 3, we measure migration speed when presenting tethered EGF in the context of the previously studied soluble EGF at different levels of FN-modulated substrate adhesiveness. We conclude by correlating a distinct biophysical effect that tethered EGF has on cell-substrate adhesion to our observations of cell migration speed.

3.2 Experimental Methods

3.2.1 Reagents

General cell culture reagents including minimum essential medium- α (MEM- α), fetal bovine serum (FBS), Geneticin G418, sodium pyruvate, L-glutamine, non-essential amino acids, penicillin-streptomycin, trypsin-EDTA, and Versene (EDTA) were purchased from Invitrogen. HEPES and bovine serum albumin (BSA) were obtained from Sigma-Aldrich. PD153035 EGFR tyrosine kinase inhibitor was purchased from Calbiochem.

3.2.2 Cell Culture

Wild-type (WT) NR6 fibroblast cells, a murine 3T3-derived cell line that lacks endogenous EGF and EGFR synthesis and has been stably transfected with wild-type human EGFR (Chen, Gupta et al. 1994), were cultured in MEM- α supplemented with 7.5% FBS, 350 $\mu\text{g/ml}$ G418, 1 mM sodium pyruvate, 2 mM L-glutamine, 1 mM non-essential amino acids, 100 i.u./ml penicillin, and 200 $\mu\text{g/ml}$ streptomycin. For cell migration and adhesion assays, 7.5% FBS in the medium was replaced by 0.5% dialyzed FBS (dFBS) (10,000 molecular weight cut-off), 1 mg/ml BSA, and MEM- α . During air incubation steps, 25 mM HEPES replaced sodium bicarbonate as the buffer.

3.2.3 Cell Migration and Adhesion Assay

WTNR6 fibroblasts were quiesced 24 hours in 0.5% dFBS medium and non-enzymatically suspended with Versene prior to being seeded onto 22-mm diameter prepared substrates mounted in Delta T dishes (Biopetechs, Inc.). The quiescent cells were

seeded at 8000 cells/cm² in 0.5% dFBS medium ± 25 nM soluble EGF with 1 μM PD 153035 EGFR tyrosine kinase inhibitor. Cell attachment was permitted for 2 hours followed by a medium change to 0.5% dFBS medium with 25 mM HEPES ± 25 nM soluble EGF without inhibitor. Dishes were incubated at 37°C in air for 8 hours before cell tracking was initiated as previous work determined WTNR6 cells challenged with EGF require 6 to 8 hours to reach maximal migration speed (Maheshwari, Wells et al. 1999). Dishes were mounted on the motorized temperature-controlled stage of a Zeiss Axiovert 35 inverted microscope running Openlab and DIAS software. Images of multiple fields per experiment were acquired in Openlab every 10 minutes for 6 hours using a 10X objective and differential interference contrast optics. They were analyzed as described below to determine mean migration speed and mean cell spread area as an indicator of cell-substrate adhesion strength.

3.2.4 Migration Speed and Spread Area Data Analysis

Images were auto contrast enhanced in Openlab and cell outlines traced in DIAS using its auto-trace function. Because auto-tracing was not perfect on some of the jagged edges and thin lamellipodial projections of NR6 cells, the traces were corrected manually with a mouse using a feature that allowed portions of the outlines to be redrawn. Using a 0.658 pixel/μm factor from the 10X objective calibration, DIAS calculated the spread area of each cell at each time point. Spread areas were averaged over 6 hours for each cell and used as a surrogate measure of cell-substrate adhesion. DIAS also calculated area-based centroids for each cell and time point and compiled individual cell paths over the 6-hour period. These paths determined the mean cell migration speed. Individual cells were discounted if they underwent cell division, collided with other cells, or touched the

image periphery. Based on these interruption criteria valid cell paths required a three-hour minimum of uninterrupted cell movement. 40 – 70 cells were tracked per EGF/FN condition.

3.3 Results and Discussion

3.3.1 Tethered EGF Requires Increased Substrate Adhesiveness to Induce Maximal Migration Speed

We hypothesized that tethered EGF would alter WTNR6 fibroblast motility compared to soluble EGF, as tethered ligands may restrict signaling to the cell membrane, potentially changing the signal magnitude, timescale, and specificity. As a result, we measured WTNR6 cell migration in the presence of either soluble or tethered EGF. The adhesivity of Comb 1 polymer surfaces was modulated by varying the amount of FN as described in Chapter 2.

Time lapse images and cell paths (Figure 3.2) illustrate increased motility on the comb polymer substrates for fibroblasts exposed to soluble or tethered EGF compared to unstimulated cells, specifically at adhesion conditions where maximal speed was observed, which were different for soluble and tethered EGF. The morphology of motile cells on tethered EGF and in the presence of soluble EGF was distinct from non-motile cells on the polymer substrate alone. Non-motile cells tended to be flat and more evenly spread with fewer protrusions while motile cells exhibited a spindly morphology with more protrusions. This has been described previously in the context of EGF-stimulated migrating fibroblasts (Ware, Wells et al. 1998).

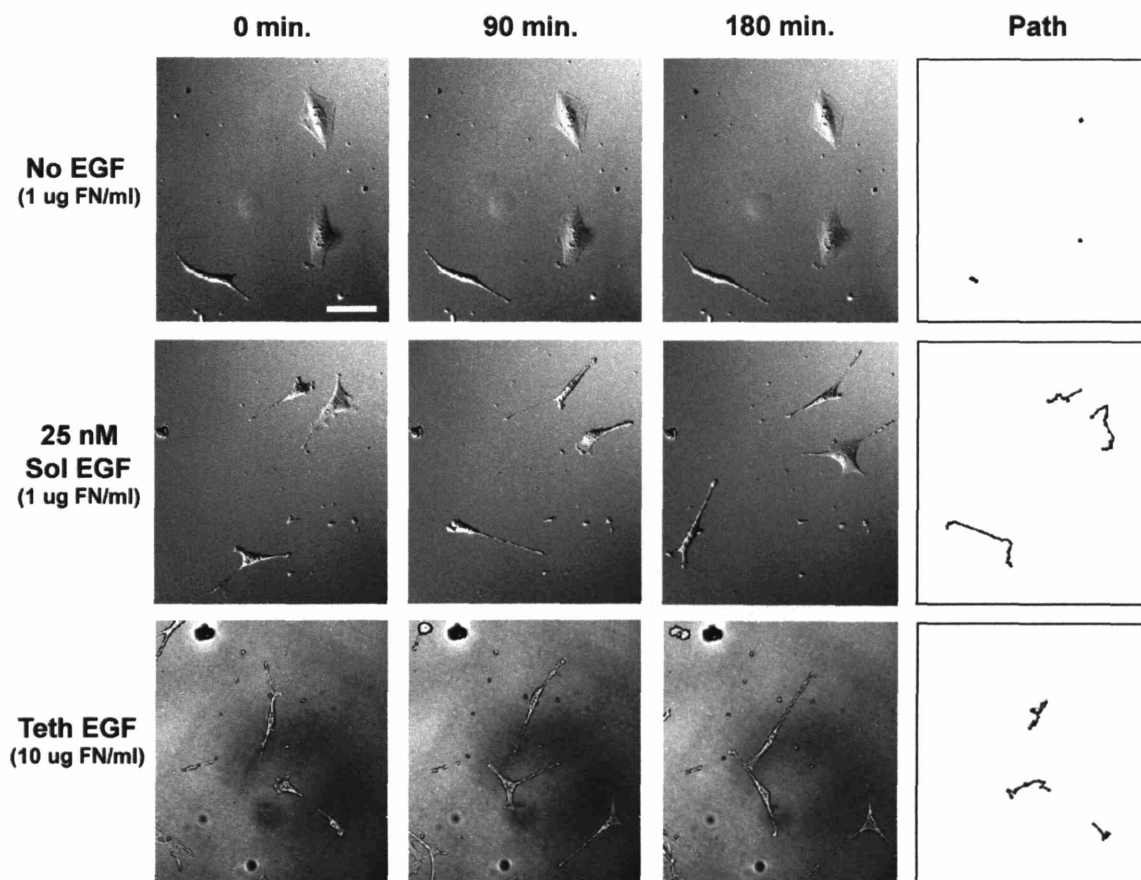


Figure 3.2 – Soluble and tethered EGF enhance motility on comb polymer substrates. 8000 quiescent WTNR6 fibroblasts/cm² were seeded in 0.5% dialyzed FBS medium onto Comb 1 polymer surfaces at peak speed adhesion conditions (no EGF + 1 ug/ml FN; 25 nM soluble EGF + 1 ug/ml FN; and tethered EGF + 10 ug/ml FN). Snapshots every hour of individually tracked cells are displayed. The path of each cell during the depicted three hour period is shown. White scale bar = 200 um.

We measured the effect of EGF presentation on fibroblast migration by varying the FN density and mapping the biphasic migration curves relating average cell speed to substrate adhesiveness for saturating 25 nM soluble EGF and tethered EGF on Comb 1 polymer substrates in addition to baseline conditions without EGF (Figure 3.3). FN coating concentrations ranged from 0.1 to 30 ug/ml, and the adsorbed FN density for a given coating concentration was equivalent with or without tethered EGF on the surface as determined in Chapter 2. Therefore, a given coating concentration yielded an equal

number of sites available for integrin binding regardless of the presence of EGF on the surface and displayed equivalent adhesive ability to the cell, but did not necessarily generate the same cell-substrate adhesion strength. Figure 3.3 demonstrates that tethered EGF elicited the same peak migration speed (~ 23 $\mu\text{m/hr}$) as 25 nM soluble EGF, but it was shifted to the right by an order of magnitude of surface-adsorbed fibronectin. Subsequently, we sought to determine the underlying mechanism responsible for the observed shift in the biphasic curve.

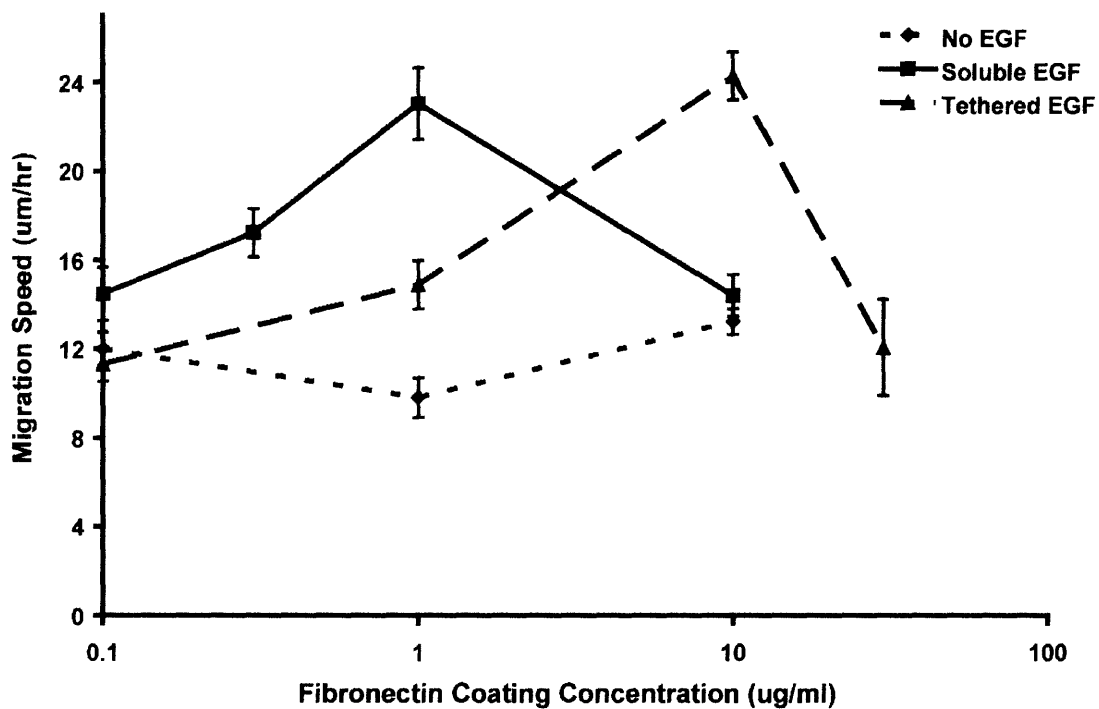


Figure 3.3 - Tethered EGF shifts the biphasic migration curve to the right relative to 25 nM soluble EGF. Average migration speed ($\mu\text{m/hr}$) is plotted versus fibronectin coating concentration ($\mu\text{g/ml}$). While peak migration speeds for tethered (\blacktriangle , dashed line) and 25 nM soluble EGF (\blacksquare , solid line) remain equivalent, the tethered EGF peak occurs at a 10-fold higher fibronectin coating concentration. Error bars represent s.e.m. for 40 – 70 individually tracked WTNR6 fibroblasts per condition.

3.3.2 Tethered EGF Reduces Cell-Substrate Adhesion Strength Relative to Soluble EGF

Based on the model of a migrating cell, the location of maximal cell speed on the biphasic curve should occur where a balance between cell-substrate adhesion strength and contraction force exists (DiMilla, Barbee et al. 1991). Therefore, a decrease in adhesion strength or an increase in contractile force could explain the observed right shift in the biphasic curve by tethered EGF. Previously, EGF was observed to reduce adhesion in fibroblasts expressing wild type EGFR (Li, Lin et al. 1999; Maheshwari, Wells et al. 1999). We hypothesized that the observed shift in the migration speed maximum might be at least partially due to a relative reduction in cell-substrate adhesion strength by tethering EGF.

We indirectly measured the effect of EGF presentation on fibroblast adhesion during migration by comparing the spread areas of cells challenged with tethered versus soluble EGF at the FN coating concentrations, 1 and 10 $\mu\text{g/ml}$, which produced FN densities responsible for their respective migration speed maxima. As expected, an increase in FN density resulted in a larger spread area for all three conditions, soluble, tethered, and no EGF (Table 3.1), which may indicate better adhesion. However, for a given FN density, tethered EGF significantly reduced spread area in comparison to soluble EGF ($p = 0.025$). It is noteworthy that the spread areas of cells migrating at peak speed for both EGF presentations were statistically the same ($\sim 2700 \mu\text{m}^2$) despite the order of magnitude difference in FN density. This implies that similar cell-substrate adhesion strength is necessary to achieve peak speed in either case. Together with the right shift we observed in the biphasic migration curve (Figure 3.3), these results indicate

a change in the effective cell-substrate adhesion strength when EGF is presented in a tethered form versus a soluble form. Cells migrating on tethered EGF require a more adhesive substrate as defined by available integrin-binding sites (FN) to create the same cell-substrate adhesion strength as in the presence of soluble EGF. This may be due to an inside-out signaling effect of EGFR on integrins, which has been observed in other EGFR and integrin-containing cell lines (Solic and Davies 1997; Pichard, Honore et al. 2001; Yamanaka, Koizumi et al. 2003). It could also be the result of increased focal adhesion disassembly by physicochemical mechanisms regulated by EGFR at the cell membrane through such downstream effectors as focal adhesion kinase (FAK) and m-calpain. These biochemical signaling pathways and their potential effects on cell motility are explored in Chapter 4.

Table 3.1 - Fibroblast spread area

	[FN] = 0.3 ug/ml	[FN] = 1 ug/ml	[FN] = 10 ug/ml	[FN] = 30 ug/ml
Soluble EGF (25 nM)	2457 ± 147 μm^2	2707 ± 224 μm^2 *†	3128 ± 115 μm^2 †	
Tethered EGF		2269 ± 141 μm^2 †	2751 ± 299 μm^2 *†	2890 ± 157 μm^2
No EGF		2438 ± 162 μm^2	2874 ± 134 μm^2	

* Conditions for peak EGF-induced migration speed

† Tethered EGF spread area at given [FN] significantly less than soluble EGF ($p = 0.025$)

3.4 References

- Chen, P., K. Gupta, et al. (1994). "Cell movement elicited by epidermal growth factor receptor requires kinase and autophosphorylation but is separable from mitogenesis." J Cell Biol **124**(4): 547-55.
- Cheresh, D. A., J. Leng, et al. (1999). "Regulation of cell contraction and membrane ruffling by distinct signals in migratory cells." J Cell Biol **146**(5): 1107-16.
- DiMilla, P. A., K. Barbee, et al. (1991). "Mathematical model for the effects of adhesion and mechanics on cell migration speed." Biophys J **60**(1): 15-37.
- DiMilla, P. A., J. A. Stone, et al. (1993). "Maximal migration of human smooth muscle cells on fibronectin and type IV collagen occurs at an intermediate attachment strength." J Cell Biol **122**(3): 729-37.
- Glading, A., D. A. Lauffenburger, et al. (2002). "Cutting to the chase: calpain proteases in cell motility." Trends Cell Biol **12**(1): 46-54.
- Li, J., M. L. Lin, et al. (1999). "Integrin-mediated migration of murine B82L fibroblasts is dependent on the expression of an intact epidermal growth factor receptor." J Biol Chem **274**(16): 11209-19.
- Maheshwari, G., A. Wells, et al. (1999). "Biophysical integration of effects of epidermal growth factor and fibronectin on fibroblast migration." Biophys J **76**(5): 2814-23.
- Pichard, V., S. Honore, et al. (2001). "Adhesion, actin cytoskeleton organisation and the spreading of colon adenocarcinoma cells induced by EGF are mediated by alpha2beta1 integrin low clustering through focal adhesion kinase." Histochem Cell Biol **116**(4): 337-48.
- Solic, N. and D. E. Davies (1997). "Differential effects of EGF and amphiregulin on adhesion molecule expression and migration of colon carcinoma cells." Exp Cell Res **234**(2): 465-76.
- Ware, M. F., A. Wells, et al. (1998). "Epidermal growth factor alters fibroblast migration speed and directional persistence reciprocally and in a matrix-dependent manner." J Cell Sci **111** (Pt 16): 2423-32.
- Wells, A., M. F. Ware, et al. (1999). "Shaping up for shipping out: PLCgamma signaling of morphology changes in EGF-stimulated fibroblast migration." Cell Motil Cytoskeleton **44**(4): 227-33.
- Yamanaka, I., M. Koizumi, et al. (2003). "Epidermal growth factor increased the expression of alpha2beta1-integrin and modulated integrin-mediated signaling in human cervical adenocarcinoma cells." Exp Cell Res **286**(2): 165-74.

4. Spatiotemporal Signal Regulation by Tethered EGF

4.1 Introduction

Previous work has demonstrated the EGFR signaling capacity of EGF-like repeats found within large ECM molecules such as laminin and tenascin (Swindle, Tran et al. 2001; Schenk, Hintermann et al. 2003). It has been proposed that such fragments of large ECM molecules might signal in a matrikine fashion, i.e. spatially restricted to the cell membrane (Swindle, Tran et al. 2001; Tran, Griffith et al. 2004). Thus, cells may discern stimulation by ligands presented in different manners via altered spatiotemporal signaling. Our goal is to understand how the cell regulates the magnitude, duration, and spatial localization of specific signals when challenged with different ligand presentations.

EGFR has been shown to act on spatially localized groups of specific signaling molecules (Haugh, Schooler et al. 1999; Burke, Schooler et al. 2001; Haugh and Meyer 2002). In Chapter 4, we use polymer-tethered EGF substrates to induce matrikine-like membrane-restricted EGFR signaling. We examine its distinct spatiotemporal regulation of EGFR activation via specific tyrosine residues and downstream signaling pathways.

In addition to varying the mode of growth factor presentation, our polymer substrates allow specific control of integrin-mediated adhesion, which synergistically regulates signaling with EGFR (Cabodi, Moro et al. 2004). We investigate the EGFR-integrin synergy to parse individual contributions to the magnitude and duration of overlapping signaling pathways, such as extracellular signal-regulated kinase (ERK) and focal adhesion kinase (FAK). These particular biochemical signals have known roles in regulating adhesion in motile cells, and we conclude with quantitative observations aimed

at determining their relevance to the difference in tethered versus soluble EGF-induced cell migration seen in Chapter 3.

4.2 Experimental Methods

4.2.1 Reagents

General cell culture reagents including minimum essential medium- α (MEM- α), fetal bovine serum (FBS), Geneticin G418, sodium pyruvate, L-glutamine, non-essential amino acids, penicillin-streptomycin, trypsin-EDTA, and Versene (EDTA) were purchased from Invitrogen. Bovine serum albumin (BSA) and lysis buffer reagents (except leupeptin, pepstatin, and aprotinin) were obtained from Sigma-Aldrich. Leupeptin, pepstatin, and aprotinin were provided by Roche. PD153035 EGFR tyrosine kinase inhibitor was purchased from Calbiochem. Primary antibodies were obtained from Cell Signaling (pY1173 EGFR, pY1068-EGFR, total EGFR, pERK 1/2, total ERK, pY887-ErbB2, total ErbB2), Biosource (pY397 FAK and total FAK), and Sigma-Aldrich (GAPDH). Secondary antibodies (anti-mouse or anti-rabbit) for Western blot were purchased from Amersham. Donkey anti-rabbit FITC conjugated secondary antibody for immunostaining was received from Jackson Immunoresearch Labs. DAPI VectaShield mounting medium was obtained from Vector Labs.

4.2.2 Cell Culture

Wild-type (WT) NR6 fibroblast cells, a murine 3T3-derived cell line that lacks endogenous EGF and EGFR synthesis and has been stably transfected with wild-type human EGFR (Chen, Gupta et al. 1994), were cultured in MEM- α supplemented with 7.5% FBS, 350 μ g/ml G418, 1 mM sodium pyruvate, 2 mM L-glutamine, 1 mM non-essential amino acids, 100 i.u./ml penicillin, and 200 μ g/ml streptomycin. For signaling

experiments, 7.5% FBS in the medium was replaced by 0.1% dialyzed FBS (dFBS) (10,000 molecular weight cut-off) with 1 mg/ml BSA and MEM- α .

4.2.3 Phospho-EGFR Immunostaining

WT NR6 fibroblasts were quiesced 4 hours in 0.1% dFBS medium and non-enzymatically suspended prior to seeding 7500 cells/cm² in 0.1% dFBS medium on 10-mm diameter Comb 1 substrates with 10 μ g/ml adsorbed FN with or without tethered EGF. Cells were permitted to attach for 30 minutes when initial signs of spreading were observed. At 30 minutes, 25 nM soluble EGF was added to appropriate wells for 15 minutes. At 45 minutes, cells were fixed in 4% paraformaldehyde for 10 minutes at room temperature, permeabilized in ice cold methanol for 15 minutes, and reduced in 0.1% sodium borohydride for 5 minutes. PBS rinses included 1 mM sodium orthovanadate to inhibit dephosphorylation. Coverslips were blocked one hour at room temperature in 10% goat serum, 1% BSA, 0.02% sodium azide, and 0.1% Tween-20 and incubated overnight at 4°C in 1:100 dilution of pY1068 EGFR rabbit polyclonal Ab followed by 45 minutes at room temperature in 5 μ g/ml of FITC-conjugated donkey anti-rabbit secondary Ab. Samples were mounted with DAPI VectaShield. FITC and DAPI channel Z-sectioned images every 0.2 μ m were acquired with a 100X oil objective on a Deltavision inverted fluorescence microscope running Softworx software. Exposure times for each channel were consistent throughout all images. A conservative deconvolution algorithm was run for the FITC channel to reduce out-of-focal-plane light. Z-sections at the cell-surface interface and through the center of the cell were isolated for comparison and FITC and DAPI channels combined into one image in Adobe Photoshop. Images are representative of two experiments, each with two to three replicates per condition.

4.2.4 Western Blot

WT NR6 fibroblasts were quiesced 4 hours in 0.1% dFBS medium and non-enzymatically suspended prior to seeding 50,000 cells/cm² onto 18-mm diameter polymer substrates in 12 well plates with or without tethered EGF and with either adsorbed FN or tethered SynKRGD to engender cell adhesion. The cells were seeded in 1 mL of 0.1% dFBS medium \pm 25 nM soluble EGF at t = 0 for the stated amount of time. At the given time point, substrates were removed and cells were lysed in 1 M Tris pH 7.5, 150 mM NaCl, 1% Triton X-100, 30 mM NaF, 10 mM Na₄P₂O₇, 50 mM β -glycerophosphate, 1 mM benzamidine, 2 mM EGTA, 1 mM dithiothreitol, 1 mM phenylmethylsulphonylfluoride, 0.1 mM Na₃VO₄, 10 ug/ml leupeptin, 10 ug/ml aprotinin, and 1 ug/ml pepstatin. BCA total protein assay was conducted to determine total protein levels so that equivalent protein (20 – 30 ug/well) was loaded in each well of the separation gel. Proteins were separated via SDS-PAGE (5% or 7.5% gels) and transferred to PVDF membranes. Membranes were blocked with 5% nonfat milk or 5% BSA in 20 mM Tris-HCl (pH 7.5), 137 mM NaCl, and 0.1% Tween 20, and probed overnight at 4°C using the following antibodies at 1:1000 dilution: pY1173 EGFR, pY1068 EGFR, total EGFR, phospho-ERK1/2, total ERK1/2, pY397 FAK, total FAK, pS473 AKT, and GAPDH. The membranes were then probed 1 hour at room temperature with a horseradish peroxidase conjugated secondary antibody to mouse or rabbit at 1:4000 dilution. Blots were imaged using enhanced chemiluminescence on a Kodak ImageStation 1000 running Kodak 1D software.

4.2.5 Densitometry

Quantitative densitometry of Western blot bands was performed using Kodak 1D software. The net intensity subtracting the background intensity was calculated for each band. Net intensities were normalized to GAPDH net intensities as GAPDH is a housekeeping protein indicative of total protein level. For the case of comparing intensities across two blots, samples from one lysate were loaded in both gels for normalization purposes. Antibodies were previously tested for linearity across 5 – 30 ug total protein loaded into gel wells. Densitometry data is the average of 3 experiments with error bars representing the standard deviation.

4.2.6 Tethered EGF Release Assay

The stability of tethered EGF substrates was determined by measuring EGF release rates under cell culture conditions. 10-mm diameter Comb1 polymer substrates presenting ~65,000 tethered ^{125}I -EGF/ μm^2 and ~6000 adsorbed FN/ μm^2 were prepared and placed in 12 well plates. They were seeded with 50,000 WTNR6 fibroblasts/ cm^2 in 1 mL of growth medium containing 7.5% FBS. After 72 hours, the medium was collected and counted for released radiolabeled EGF. Experiments were conducted in triplicate, and data were converted to average EGF release rates per cell. The stated error represents the standard deviation.

4.2.7 BOC Assay for Calpain Activity

To repeat the conditions of earlier cell motility assays, 10,000 WTNR6 fibroblasts were quiesced for 24 hours in 0.5% dFBS medium with 1 uM PD 153035 EGFR kinase inhibitor. They were non-enzymatically suspended and seeded in 1 mL of 0.5% dFBS

medium with 1 μM PD 153035 \pm 25 nM soluble EGF onto 10-mm diameter Comb 1 substrates in 12 well plates for two hours to permit attachment. The Comb 1 substrates were prepared with or without $\sim 65,000$ tethered EGF/ μm^2 and included different densities of adsorbed FN, which provided conditions for comparison of no EGF, tethered EGF, and soluble EGF. After the two-hour attachment period, the inhibitor was removed by washing the cells two times for 5 minutes each with PBS. The cells were placed in fresh 0.5% dFBS medium \pm 25 nM soluble EGF for 8 hours to allow them to reach maximal migration speed as in earlier experiments. At 8 hours, 10 μM BOC-LM-CMAC was added to the medium for 20 minutes. This reagent is a fluorescent reporter of calpain activity as calpain cleaves it to remove a fluorescence quench, resulting in an increase in fluorescence (Rosser, Powers et al. 1993). After the 20 minute incubation with BOC-LM-CMAC, images were taken at 200X magnification with constant gain and exposure time. The images were grayscale in Adobe Photoshop. Brightness is a relative indicator of calpain activity.

4.3 Results

4.3.1 Tethered EGF Spatially Restricts EGFR Activation to Cell Surface

By covalently attaching EGF to the PMMA-PEO comb polymer, we expected to inhibit EGFR internalization and spatially restrict its activation to the cell membrane. Therefore, we immunostained WTNR6 fibroblasts on tethered EGF with an antibody specific to phosphorylated EGFR tyrosine 1068, allowing us to determine the spatial distribution of activated receptors. EGFR tyrosine 1068 is heavily phosphorylated following EGF binding to the receptor and contributes to several downstream signaling pathways, including ERK, STAT, and PI-3 kinase / Akt (Batzer, Rotin et al. 1994; Rodrigues, Falasca et al. 2000; Shao, Cheng et al. 2003).

We acquired images at focal planes every 0.2 μm throughout the cell beginning at the cell-substrate interface. Images focused at the cell-substrate interface and through the center of the cell established a significant difference in activated receptor spatial localization between the tethered and 25 nM soluble EGF presentations as illustrated in Figure 4.1. Fibroblasts challenged with soluble EGF for 15 minutes demonstrated internalized perinuclear endosomal vesicles with active EGFR in addition to visible staining of pits at the cell membrane. In contrast, tethered EGF substrates elicited visible EGFR activation only at the cell membrane-substrate interface. Thus, tethered EGF restricted activated EGFR to the cell surface by preventing its internalization.

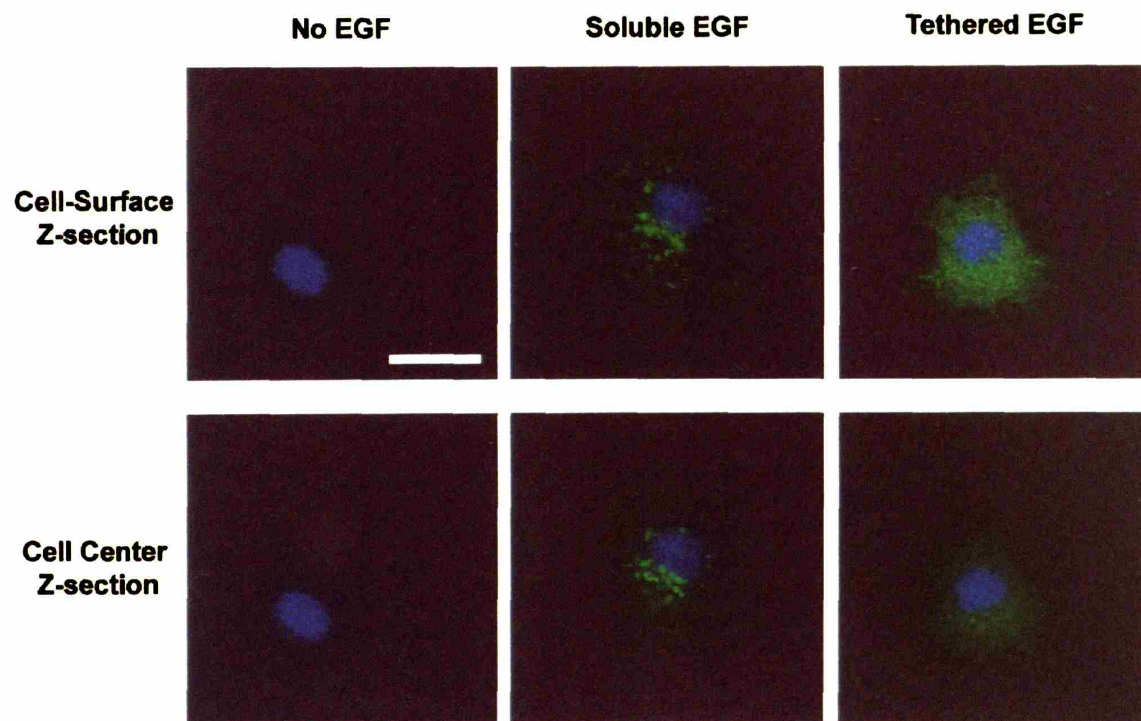


Figure 4.1 – Tethered EGF Inhibits Activated EGFR Internalization.

Tethered EGF signals via membrane-localized EGFR by inhibiting ligand-induced internalization of active EGFR. Deconvolution microscopy Z-sections were taken at the cell-substrate interface and cell center for WTNR6 fibroblasts on Comb 1 polymer substrates challenged with no EGF, tethered EGF, or 25 nM soluble EGF for 15 minutes after initial signs of spreading. Images depict FITC stained phosphorylated EGFR (pY1068) in green and DAPI stained nuclei in blue. White scale bar = 20 μm . Active EGFR in perinuclear endosomes are observed at the cell center for soluble EGF but not tethered EGF, which activates EGFR only at the cell membrane.

4.3.2 Variation in EGFR Activation by Tethered EGF Surface Density

The magnitude and duration of EGFR signaling is modulated by ligand concentration. The effective concentration for tethered EGF is governed by the ligand's surface density. Presenting tethered EGF on Comb 1 versus Comb 2 produced a 10-fold difference in EGF surface density. Comb 1 polymer resulted in a surface density of $\sim 65,000$ tethered EGF/ μm^2 , which we refer to as “high density” tethered EGF, while

Comb 2 polymer presented ~ 7000 tethered EGF/ μm^2 , our “low density” tethered EGF. It is important to note that since only 80% of the Comb 2 polymer surface contained NPC-activated chains, the effective local tethered EGF surface density encountered by the cell was ~ 8750 EGF/ μm^2 . We utilized the order of magnitude difference in EGF surface density to examine the effect of tethered EGF concentration on EGFR activation.

Via Western blot, the phosphorylation of two EGFR tyrosines, Y1068 and Y1173, was observed for high density and low density tethered EGF in comparison to no EGF and soluble EGF (Figure 4.2). Y1173 is another EGFR tyrosine residue strongly phosphorylated in response to EGF. It contributes to the activation of PLC γ -1 by direct binding as well as ERK through the binding of Shc (Batzer, Rotin et al. 1994; Chattopadhyay, Vecchi et al. 1999). While soluble EGF elicited greater tyrosine phosphorylation than both high and low density tethered EGF, EGFR activation was modulated by the tethered EGF surface density as expected. High density tethered EGF evoked relatively strong receptor phosphorylation at both Y1068 and Y1173 (Figure 4.2 A), while a low surface density resulted in only minimally visible phosphorylation when compared to soluble EGF (Figure 4.2 B). To ensure that this difference in receptor activation was not due to changes in adhesion, the density of tethered SynKRGD was modulated between high and low levels of $\sim 300,000$ SynKRGD/ μm^2 and $\sim 10,000$ SynKRGD/ μm^2 (Figures 4.2 B and C, respectively). The high density SynKRGD showed similar cell adhesion compared to FN as noted by an equivalent one-hour spreading time, while the lower density SynKRGD required two hours to achieve full spreading as demonstrated in Chapter 2. Changes in adhesion exerted no significant effect on EGFR phosphorylation.

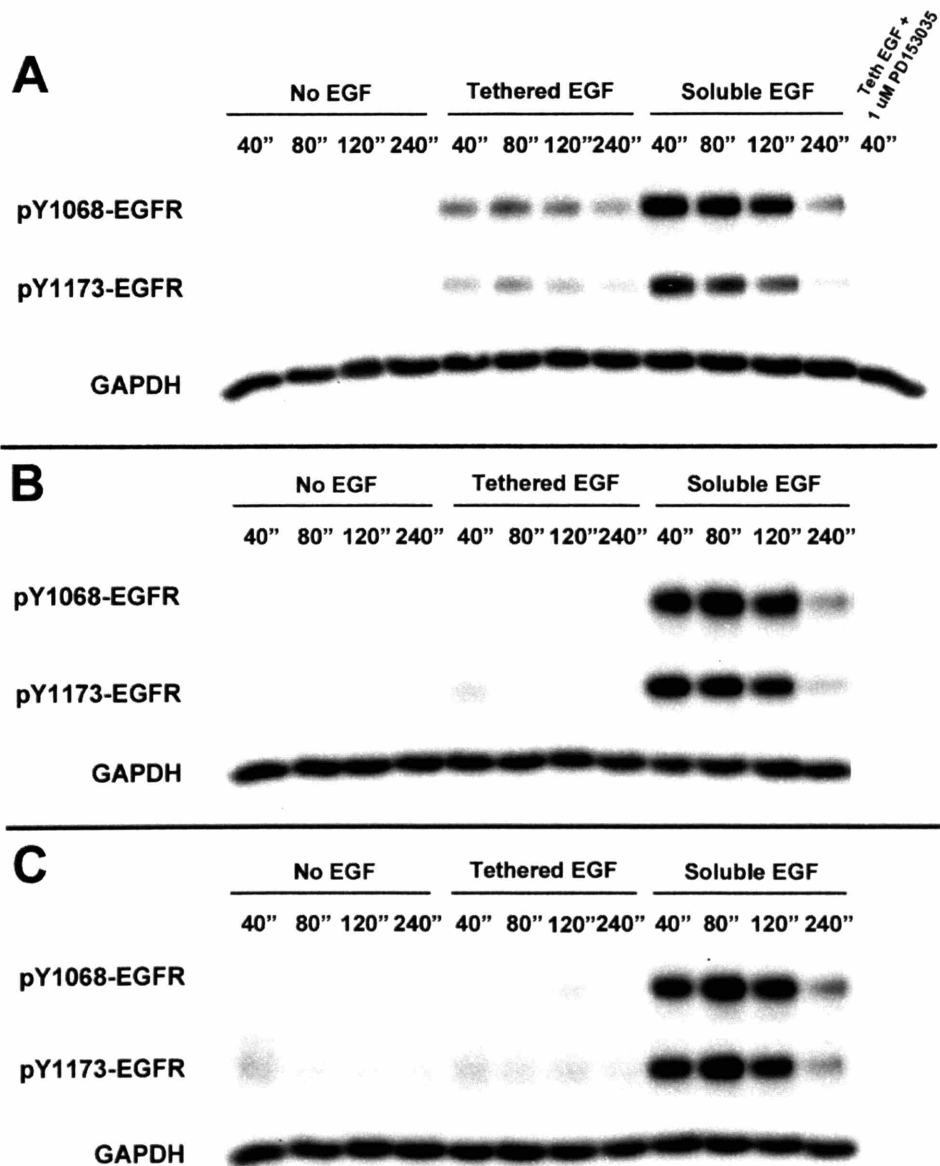


Figure 4.2 – Tethered EGF surface density modulates the magnitude of EGFR activation. Phosphorylation of EGFR tyrosines 1068 and 1173 in WTNR6 fibroblasts was compared between tethered EGF polymer substrates with (A) a high density of $\sim 65,000$ EGF/ μm^2 and (B, C) a low density of $\sim 7,000$ EGF/ μm^2 . Adhesion to substrates was engendered by (A) $\sim 6,000$ adsorbed FN/ μm^2 , (B) $\sim 300,000$ SynKRGD/ μm^2 , or (C) $\sim 10,000$ SynKRGD/ μm^2 . EGFR tyrosine phosphorylation was significantly greater on high density than low density tethered EGF but in all cases was greatest for soluble EGF. The increased activation by tethered EGF was not due to changes in cell-substrate adhesion as altering the SynKRGD density between (B) and (C) had no measurable effect on phosphorylation magnitude. Adhesion to adsorbed FN (A) and high density SynKRGD (B) was similar as observed by one-hour spreading time and morphology (data not shown). Tethered EGF activation of EGFR was abrogated by addition of $1 \mu\text{M}$ PD153035, an EGFR kinase inhibitor, as shown in (A).

To visualize the relatively low levels of EGFR phosphorylation by low density tethered EGF, we conducted timecourses comparing no EGF and low density tethered EGF without the presence of soluble EGF. This permitted longer exposure times for Western blots. Thus, we were able to determine the magnitude of Y1068 and Y1173 phosphorylation by tethered EGF over time relative to background levels without EGF. We observed differential phosphorylation of the two tyrosine residues over a 24 hour period (Figure 4.3). Phosphorylation of Y1068 persisted above background for 24 hours, while Y1173 showed initial phosphorylation at 40 minutes but was quickly dephosphorylated afterwards. Interestingly, transient EGF-independent phosphorylation of both tyrosines was observed at 40 minutes as has been previously reported during integrin-mediated adhesion (Moro, Dolce et al. 2002). However, these integrin-induced phosphorylations of Y1068 and Y1173 were enhanced two-fold by the addition of low density tethered EGF as quantified by densitometry. Therefore, while integrins contribute to the early activation of EGFR, tethered EGF increases their phosphorylation activity and also differentially activates the receptor at specific tyrosines in a time-dependent fashion.

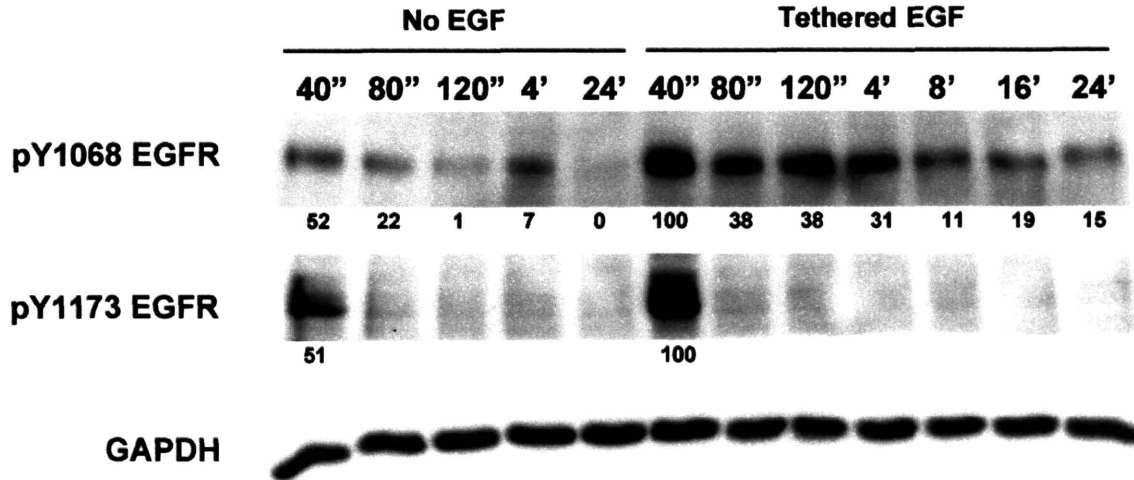


Figure 4.3 – Low density tethered EGF differentially phosphorylates EGFR tyrosines 1068 and 1173. 24-hour phosphorylation timecourses for EGFR Y1068 and Y1173 in WTNR6 fibroblasts on Comb 2 polymer substrates with $\sim 10,000$ SynKRGD/ μm^2 were observed without EGF and on low density tethered EGF (~ 7000 EGF/ μm^2). Densitometry normalized for each tyrosine is shown below the lanes. Initial integrin-mediated EGFR activation without EGF was observed at approximately half the level of tethered EGF-induced activation. Differential activation between Y1068 and Y1173 occurred as Y1068 phosphorylation persisted above background levels for 24 hours while Y1173 was rapidly dephosphorylated after 40 minutes.

4.3.3 Tethered EGF Reduces EGFR Degradation

Internalization and degradation of EGFR is a major mechanism of signal attenuation. We expected tethered EGF to inhibit receptor downregulation by preventing its endocytosis and subsequent degradation. Therefore, using Western blot we probed for total EGFR to compare receptor levels over time for tethered EGF and soluble EGF. Indeed, tethered EGF significantly reduced EGFR degradation compared to soluble EGF (Figure 4.4). When stimulated with a high concentration of soluble EGF, the fibroblasts rapidly internalized and degraded EGFR with the majority of receptors already lost at 40 minutes. In contrast, tethered EGF maintained EGFR levels for much longer periods of time. In fact, on low density tethered EGF substrates no receptor loss at all was observed

after 4 hours. However, on high density tethered EGF surfaces, we noticed a slow decrease in EGFR levels over the four-hour timecourse. These substrates contained an order of magnitude more non-specifically adsorbed EGF than the more protein resistant low density tethered EGF surfaces (from Figures 2.11 and 2.14). We suspected the slow receptor loss might be due to release of EGF from the surface sufficient to permit low levels of EGFR internalization and degradation.

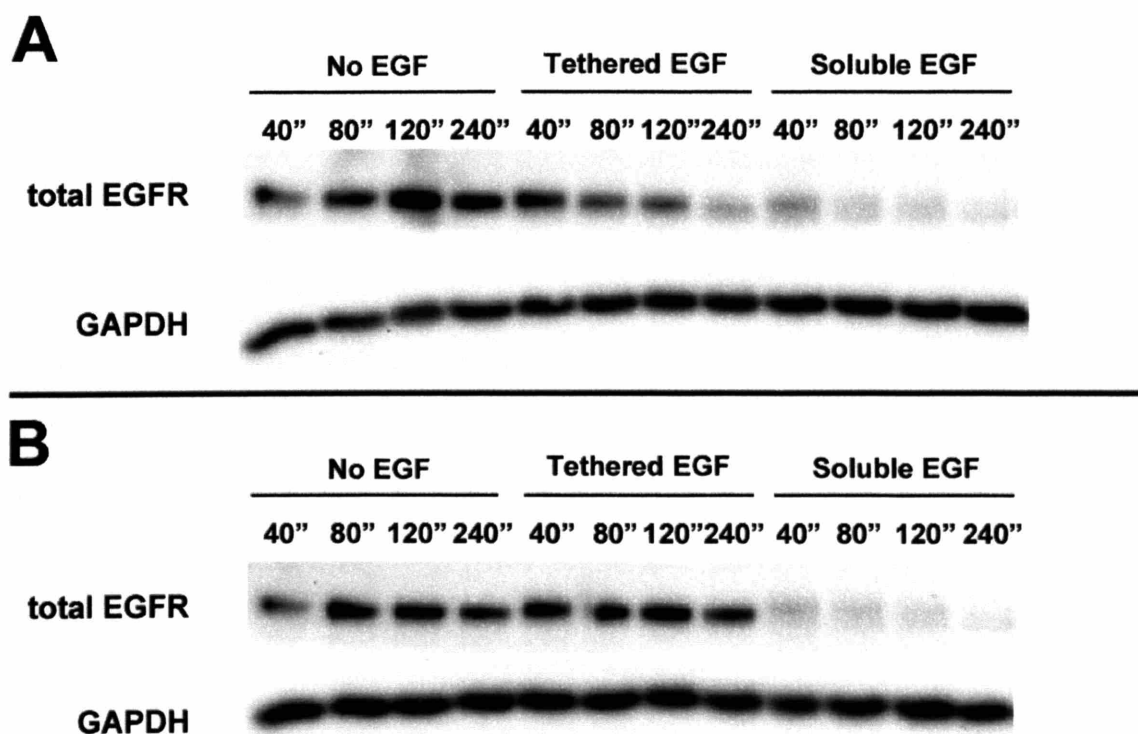


Figure 4.4 – Tethered EGF reduces EGFR degradation.

Total EGFR levels were probed for 4 hours in WTNR6 fibroblasts on polymer substrates with no EGF, different densities of tethered EGF, or 25 nM soluble EGF. Tethered EGF substrates were (A) high density tethered EGF (~65,000 EGF/um²) with ~6000 adsorbed FN/um² and (B) low density tethered EGF (~7000 EGF/um²) with ~300,000 SynKRGD/um². Cells on low density tethered EGF maintained high receptor levels even after 4 hours of exposure, while EGFR levels slowly declined over 4 hours in response to high density tethered EGF. Stimulation by soluble EGF resulted in rapid EGFR loss apparent at 40 minutes. Thus, tethered EGF inhibits EGFR degradation by spatially restricting activated EGFR to the cell surface.

To test this hypothesis, we determined the ligand release rate from high density tethered EGF substrates, assumed all ligand released was internalized, and performed a receptor balance around the cell including EGFR synthesis, internalization, and recycling (Figure 4.5) using Equation 4.1:

$$\Delta R_T = \Delta R_S - \Delta R_I + \Delta R_R \quad (\text{Eq. 4.1})$$

where ΔR_T is the change in total receptor number, ΔR_S is the EGFR synthesis rate, ΔR_I is the internalization rate, and ΔR_R is the recycling rate, all in units of EGFR/cell/min. ΔR_R is determined from ΔR_I and a recycle fraction, f_R , by Equation 4.2:

$$\Delta R_R = f_R \Delta R_I \quad (\text{Eq. 4.2})$$

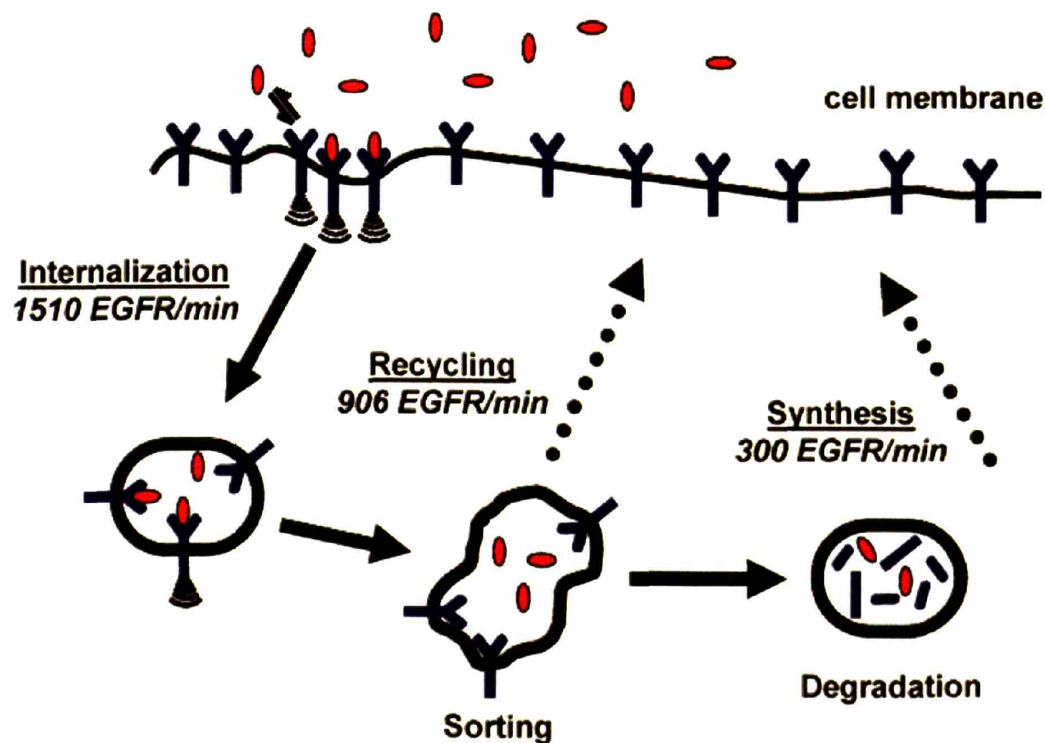


Figure 4.5 – Estimating a rate of EGFR loss on high density tethered EGF. A balance on receptor trafficking was performed using an experimentally measured value for tethered EGF release as the internalization rate and previously measured literature values for recycling and synthesis rates.

WTNR6 fibroblasts were cultured on the high density tethered EGF substrates, and radiolabeled ligand released into the medium was measured. This ligand included EGF released directly into the medium as well as EGF consumed by cells and degraded. The ligand release rate was 1510 ± 120 EGF/cell/min, which we assumed was equivalent to the internalization rate, ΔR_I . In previous work with a similar cell line of B82 murine fibroblasts expressing $\sim 200,000$ EGFR/cell, an EGFR synthesis rate, ΔR_S , of 300 EGFR/cell/min was measured under EGF stimulation (DeWitt, Dong et al. 2001). In addition, trafficking studies with those cells demonstrated that the fraction of internalized EGF-EGFR complexes recycled by the cell increased from 0.3 to 0.8 as the intracellular ligand concentration increased and the sorting machinery became saturated (French, Sudlow et al. 1994). Based on an estimate of EGFR accumulation in the cell and data from French et al., the recycled fraction might increase from 0.3 to 0.6 during the first hour of exposure. Assuming an EGFR recycling fraction of 0.6 with 1510 internalized EGFR/min and an EGFR synthesis rate of 300/min, we estimated a net EGFR loss of ~ 300 EGFR/min or $\sim 18,000$ EGFR/hr. This number is only an estimate that would vary as the recycling fraction and EGFR synthesis rate change in response to intracellular accumulation of EGF and EGFR. However, it does illustrate that a much slower rate of EGFR degradation relative to soluble EGF occurs on these high density tethered EGF surfaces. Interestingly, the 4 hour timecourse of EGFR depletion depicted in Figure 4.4A agrees qualitatively with our $\sim 18,000$ EGFR/hr rate estimate for EGFR loss since the cells initially express $\sim 100,000$ EGFR and appear to have lost more than half their receptors at 4 hours.

4.3.4 ErbB2 is Activated by Tethered EGF

ErbB2 is the second of four members of the EGFR family. While it does not have a known ligand, it heterodimerizes and is activated by bound EGFR. It also primarily is recycled to the cell surface and escapes degradation unlike EGFR (Hendriks, Wiley et al. 2003). It may be particularly important in the case of tethered EGF as it permits EGFR signaling without the two proximal EGF molecules required for homodimerization. WTNR6 fibroblasts were shown to possess detectable levels of ErbB2 (Figure 4.6).

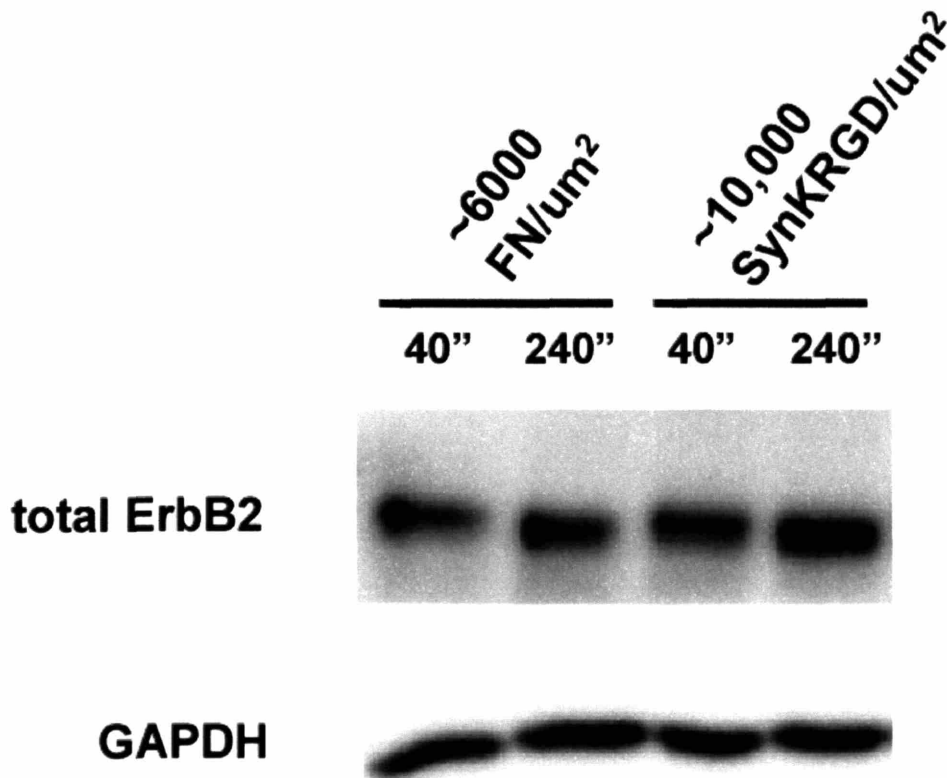


Figure 4.6 – WTNR6 fibroblasts express ErbB2.

Quiescent WTNR6 fibroblasts were seeded in 0.1% dFBS medium on Comb 1 polymer substrates with ~ 6000 adsorbed FN/ μm^2 or on Comb 2 polymer substrates with $\sim 10,000$ tethered SynKRGD/ μm^2 for 40 and 240 minutes. Lysates were probed with an antibody against total ErbB2 to demonstrate that detectable amounts of ErbB2 were present in the cell line.

Using Western blot, we probed cell lysates from high and low density tethered EGF for activation of ErbB2 at Y887 as this was the lone commercially available phospho-specific mouse ErbB2 antibody. Comparisons were made to cells in the presence of 25 nM soluble EGF (Figure 4.7).

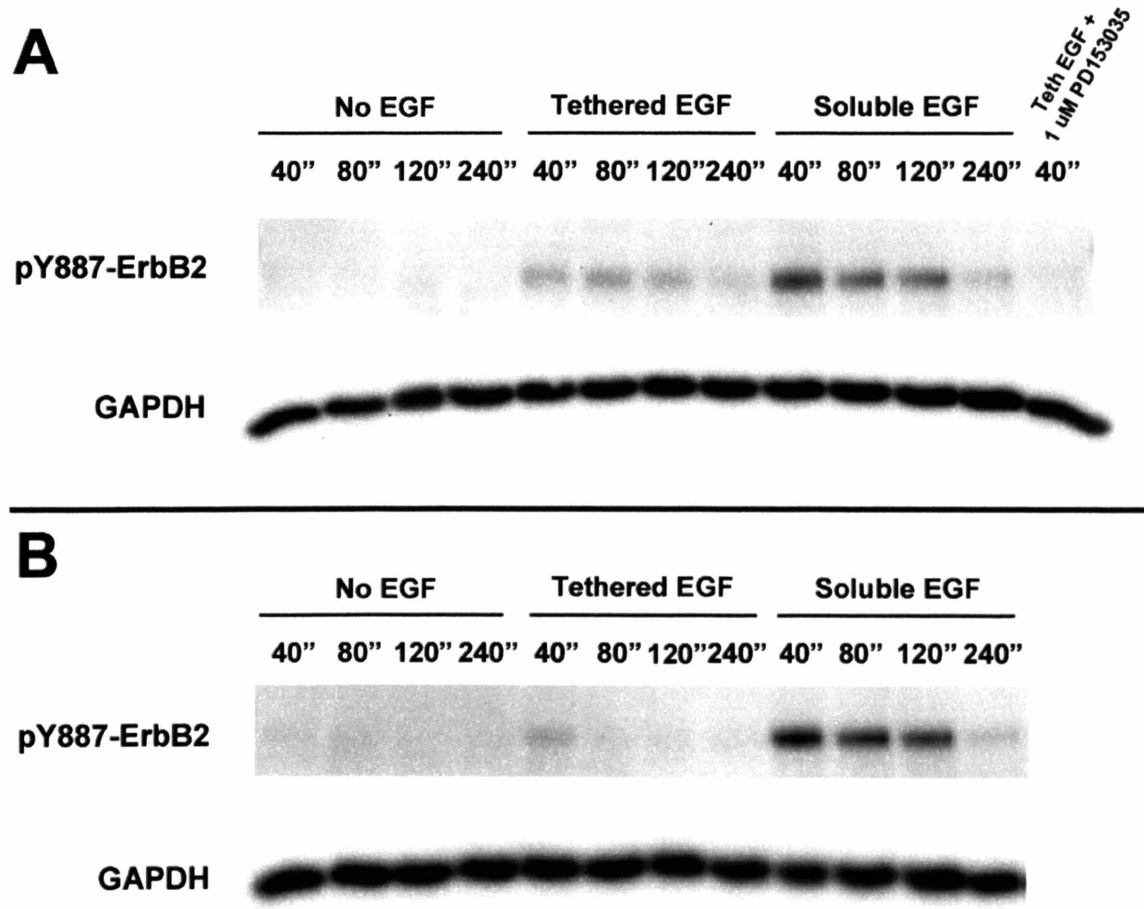


Figure 4.7 – Tethered EGF activates ErbB2.

ErbB2 activation over 4 hours was measured in WTNR6 fibroblasts on PMMA-PEO comb polymer substrates with no EGF, different densities of tethered EGF, and 25 nM soluble EGF by probing for phosphorylated Y887 in ErbB2. Comb 1 (A) and Comb 2 (B) polymer substrates consisted of (A) ~6000 adsorbed FN/ μm^2 and ~65,000 tethered EGF/ μm^2 and (B) ~300,000 tethered SynKRGD/ μm^2 and ~7000 tethered EGF/ μm^2 . Similar to EGFR phosphorylation, ErbB2 phosphorylation was strongest for soluble EGF. High density tethered EGF activated ErbB2 with greater magnitude and duration than low density tethered EGF. Tethered EGF ErbB2 activation was inhibited by 1 uM PD 153035.

Strong activation of ErbB2 was observed for 2 hours in response to soluble EGF. Weaker activation for 2 hours by high density tethered EGF also occurred and was abrogated by the EGFR kinase inhibitor, PD 153035. Decreasing the density of tethered EGF reduced phosphorylation magnitude and duration so that only a weak ErbB2 signal at 40 minutes was visible relative to the strong soluble EGF signal. Similar to EGFR activation, ErbB2 activation by tethered EGF appears to be dependent on its surface density. While we postulated an increased role for ErbB2 heterodimerization on substrates with sparser tethered EGF density, we did not observe it.

4.3.5 Tethered EGF Activates ERK and Enhances Akt and FAK Signaling

We investigated the downstream signaling consequences of spatially restricted receptor activation by tethered EGF. A significant amount of previous work has demonstrated that EGFR signals not only at the cell membrane but also from endosomes (Oksvold, Skarpen et al. 2000; Burke, Schooler et al. 2001; Sorkin and Von Zastrow 2002). In some instances, a different array of signaling molecules may be available depending on the spatial location of the activated receptor (Haugh, Huang et al. 1999; Burke, Schooler et al. 2001; Haugh and Meyer 2002).

We performed Western blot with phosphorylation specific antibodies against ERK, Akt, and FAK to determine the ability of tethered EGF to activate pathways downstream of EGFR (Figure 4.8). Although weak integrin-mediated ERK activation was visible at 40 minutes without EGF, strong and persistent ERK phosphorylation was observed for both high density tethered EGF and soluble EGF. In fact, the strong ERK phosphorylation by high density tethered EGF persisted longer than soluble EGF as

evidenced at the 120 and 240 minute marks. This might have been due to higher levels of EGFR maintained at the surface for a longer time by tethered EGF as demonstrated earlier in Figure 4.4A.

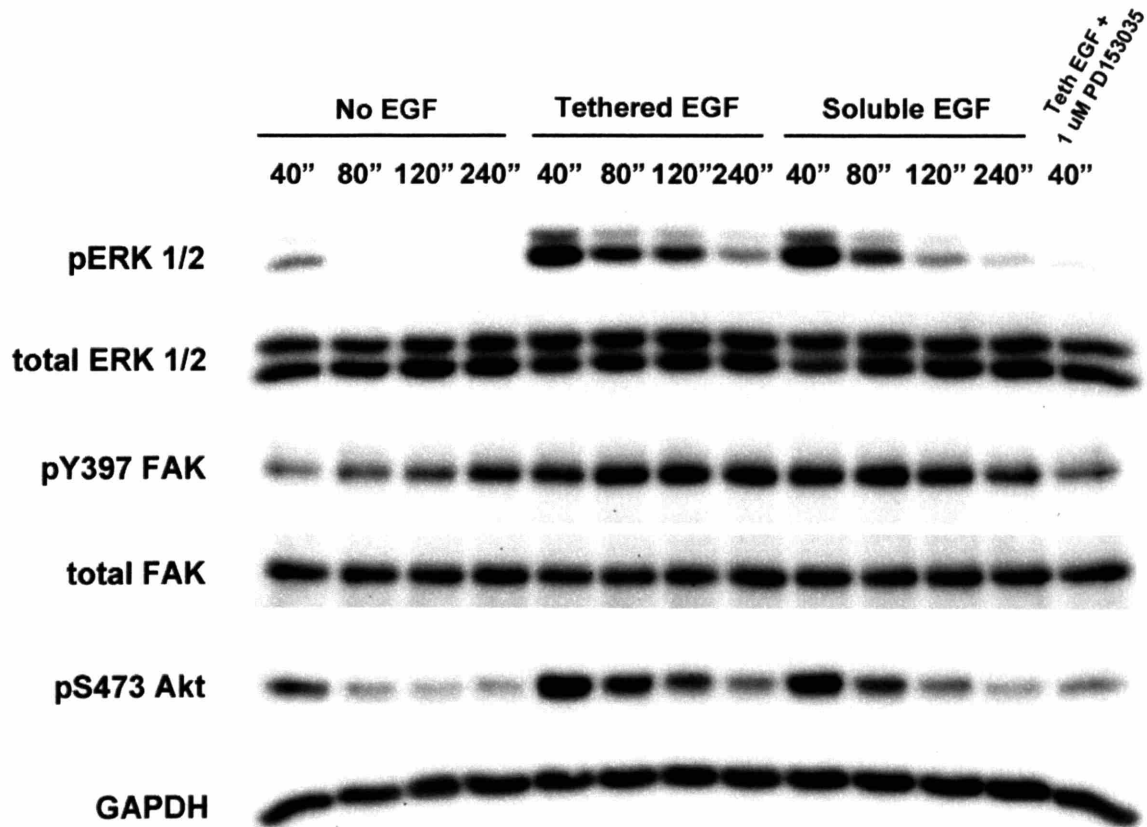


Figure 4.8 – Tethered EGF activates ERK and enhances FAK and Akt phosphorylation downstream of EGFR.

Phosphorylation of signaling molecules downstream of EGFR, including ERK, FAK, and Akt, was observed over 4 hours in WTNR6 fibroblasts on Comb 1 polymer substrates with ~6000 adsorbed FN/ μm^2 under conditions of no EGF, ~65,000 tethered EGF/ μm^2 , or 25 nM soluble EGF. ERK phosphorylation was similar in response to high density tethered EGF and soluble EGF. Low level integrin-mediated ERK activation without EGF was also visible at 40 minutes. Integrin-mediated FAK and Akt phosphorylation was significantly enhanced by high density tethered EGF and soluble EGF.

Because FAK is phosphorylated in response to integrin activation, it was activated even in the absence of EGF. Its phosphorylation levels gradually increase over time as

the cell spreads, achieves greater adhesion, and dynamically forms and turns over focal adhesions. However, stimulation by either high density tethered EGF or soluble EGF notably enhanced the early FAK phosphorylation, producing significantly greater levels during the first 2 hours on the Comb 1 substrates with adsorbed FN.

Similar early enhancement of Akt signaling was also observed. Akt is activated by PI-3 kinase at the cell membrane and acts as a survival signal for the cell. Its activation is seen in adherent cells as an integrin-mediated survival signal without the presence of growth factors. However, its phosphorylation was dramatically higher compared to integrin-mediated levels during the first 80 to 120 minutes of exposure to high density tethered EGF as well as soluble EGF.

4.3.6 ERK Phosphorylation Depends on Adhesion and EGF Presentation

We sought to more thoroughly characterize regulation of ERK signaling by adhesion and EGF presentation because it plays an important role in governing several physiological responses including cell motility. We used Comb 2 polymer substrates with low density tethered EGF and tethered SynKRGD. These surfaces displayed high affinity $\alpha_5\beta_1$ as well as $\alpha_v\beta_3$ integrin-specific adhesion via SynKRGD without additional adsorbed serum molecules. They also demonstrated dynamic adhesion control based on the wide range of attainable SynKRGD densities.

Quantitative Western blots of phosphorylated ERK in fibroblasts stimulated by tethered and soluble EGF along with unstimulated fibroblasts were conducted. Representative blots in Figure 4.9 illustrate a transient integrin-mediated ERK signal in unstimulated fibroblasts as they engage the surface during initial spreading. This transient

signal is visible during the first 80 minutes on less adhesive surfaces displaying only $\sim 10,000$ SynKRGD/ μm^2 and at the initial 40 minute time point only on the more adhesive $\sim 300,000$ SynKRGD/ μm^2 substrates. The more transient signal on surfaces with higher adhesion ligand density correlates with the more rapid integrin-mediated spreading observed (1 vs. 2 hours). In comparison, both tethered EGF and soluble EGF elicit more sustained and stronger ERK phosphorylation that remains above background levels throughout the 4 hour period measured.

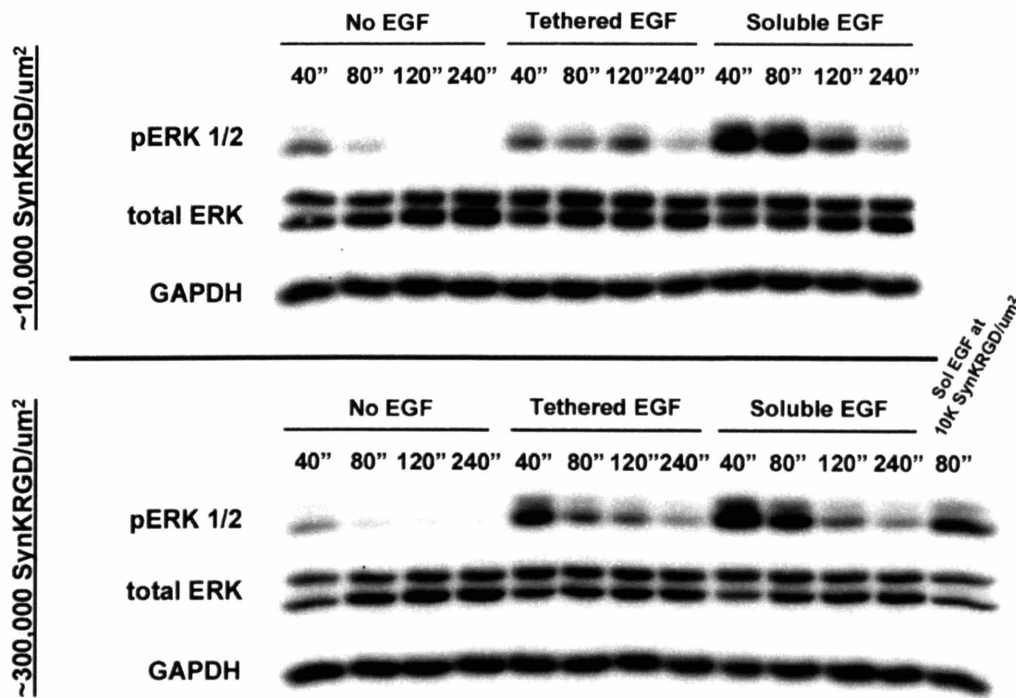


Figure 4.9 – ERK signaling is modulated by adhesion ligand density and EGF presentation.

WTNR6 fibroblasts were seeded on Comb 2 substrates presenting low density tethered EGF (~ 7000 EGF/ μm^2) with either a low adhesion ligand density of $\sim 10,000$ tethered SynKRGD/ μm^2 or a high adhesion ligand density of $\sim 300,000$ tethered SynKRGD/ μm^2 . Lysates over the course of 4 hours were probed with antibodies against phosphorylated ERK1/2, total ERK1/2, and GAPDH. Differences in ERK phosphorylation due to adhesion ligand density as well as EGF presentation (tethered vs. soluble EGF) were observed. These blots are representative of three experiments. Quantitative densitometric analysis of the three experiments is presented in Figures 4.10 and 4.11.

Quantification and comparison of ERK phosphorylation intensities at the low and high SynKRGD densities demonstrates the significant role that adhesion plays in the synergistic regulation of ERK signaling. Plots in Figure 4.10 compare phospho-ERK intensities for the two adhesion ligand densities at each of the EGF conditions.

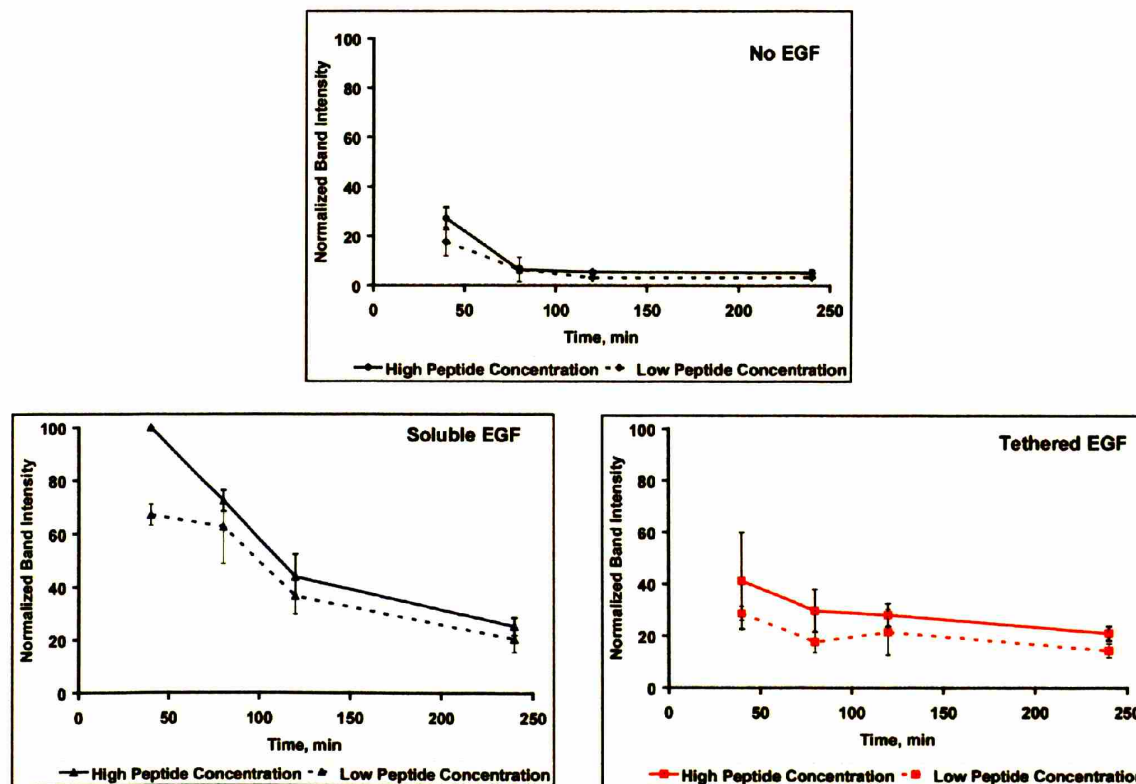


Figure 4.10 – ERK phosphorylation increases with adhesion ligand density for tethered and soluble EGF. Densitometry of three independent Western blot experiments for phosphorylated ERK represented by the blots in Figure 4.9 was performed. Net intensities of bands for no EGF, low density tethered EGF, and 25 nM soluble EGF over 4 hours were quantified at SynKRGD densities of $\sim 10,000$ and $\sim 300,000$ SynKRGD/ μm^2 . They were normalized to the maximum intensity and plotted for each condition to compare ERK phosphorylation between adhesion ligand densities. ERK phosphorylation increased significantly with higher SynKRGD density for tethered and soluble EGF. (ANOVA statistical analysis: Tethered EGF: $\sim 300,000$ SynKRGD/ μm^2 pERK intensity $>$ $\sim 10,000$ SynKRGD/ μm^2 pERK intensity with $p < 0.02$; Soluble EGF: $\sim 300,000$ SynKRGD/ μm^2 pERK intensity $>$ $\sim 10,000$ SynKRGD/ μm^2 pERK intensity with $p < 0.01$).

For both tethered and soluble EGF, an upward shift in ERK phosphorylation occurs with an increase in SynKRGD density. ANOVA statistics revealed that tethered and soluble EGF elicited significantly greater phospho-ERK intensity on the more adhesive substrates over 4 hours ($p < 0.02$ and $p < 0.01$, respectively). The data illustrate that more substantial integrin-mediated adhesion during EGF stimulation results in greater ERK signaling.

The data in Figure 4.10 were replotted in Figure 4.11 to characterize the importance of EGF presentation in regulating ERK activity by comparing EGF conditions at each adhesion ligand density. For both SynKRGD densities, the ERK phosphorylation levels for no EGF, tethered EGF, and soluble EGF were statistically distinct over the 4 hour timecourse as determined by ANOVA statistical methods ($p < 0.01$). Soluble EGF produced the greatest signal magnitude, which was particularly high during the first 80 minutes of stimulation. Tethered EGF elicited lower levels of ERK phosphorylation, but they were sustained above background levels similar to soluble EGF. ERK signaling in fibroblasts without EGF quickly returned to basal levels following initial weak adhesion-mediated ERK signaling.

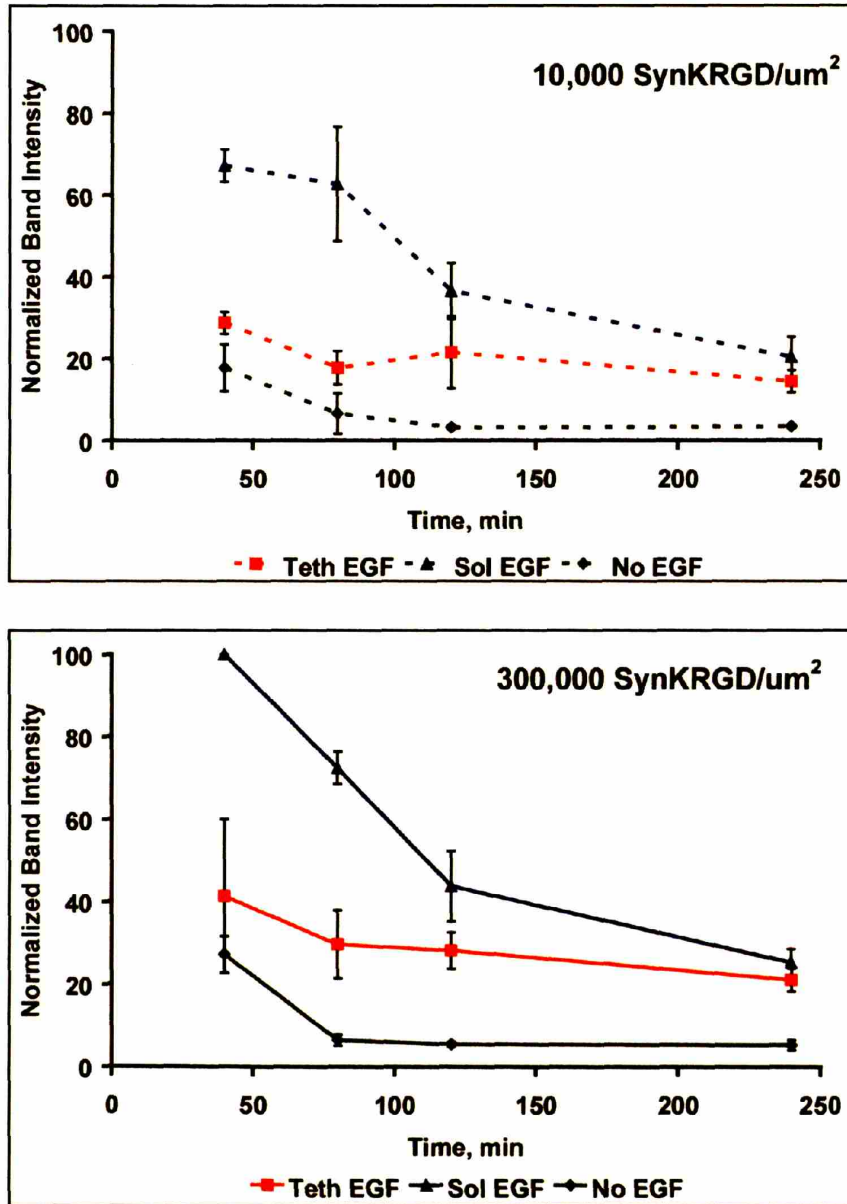


Figure 4.11 – ERK phosphorylation varies with EGF presentation as a tethered versus soluble ligand. The densitometric net intensity data in Figure 4.10 were replotted to compare ERK phosphorylation as a function of EGF presentation, i.e. no EGF vs. low density tethered EGF vs. 25 nM soluble EGF. ERK phosphorylation was significantly greater than background levels in the presence of both tethered and soluble EGF. However, soluble EGF elicited statistically greater phosphorylation than tethered EGF. These distinct phosphorylation intensities for each EGF presentation occurred at both SynKRGD densities. (*ANOVA statistical analysis: pERK intensity: Soluble EGF > Tethered EGF > No EGF for each adhesion ligand density, p < 0.01 for each pair of conditions*).

4.3.7 Tethered EGF Elicits Calpain Activity

M-calpain, or calpain II, is a protease activated by membrane-proximal ERK that cleaves focal adhesion proteins and is important in the rear release of adhesions during cell migration (Glading, Uberall et al. 2001). Because tethered EGF activates ERK and induces fibroblast motility, we wanted to determine if calpain was activated by the tethered ligand. A qualitative fluorescent reporter assay was used to compare calpain activity in unstimulated fibroblasts to those challenged with tethered EGF or soluble EGF. The assay was conducted with the same timing and conditions that elicited maximal EGF-induced migration speed.

Figure 4.12 depicts relative calpain activity in fibroblasts seeded on Comb 1 with ~1000 and ~6000 adsorbed FN/ μm^2 , the two FN densities responsible for peak migration speeds in the presence of soluble and tethered EGF, respectively. Cells on both tethered EGF and soluble EGF displayed increased calpain activity over unstimulated cells at both FN densities. Thus, tethered EGF, which activates ERK primarily through membrane-localized EGFR, upregulates calpain activity similar to soluble EGF.

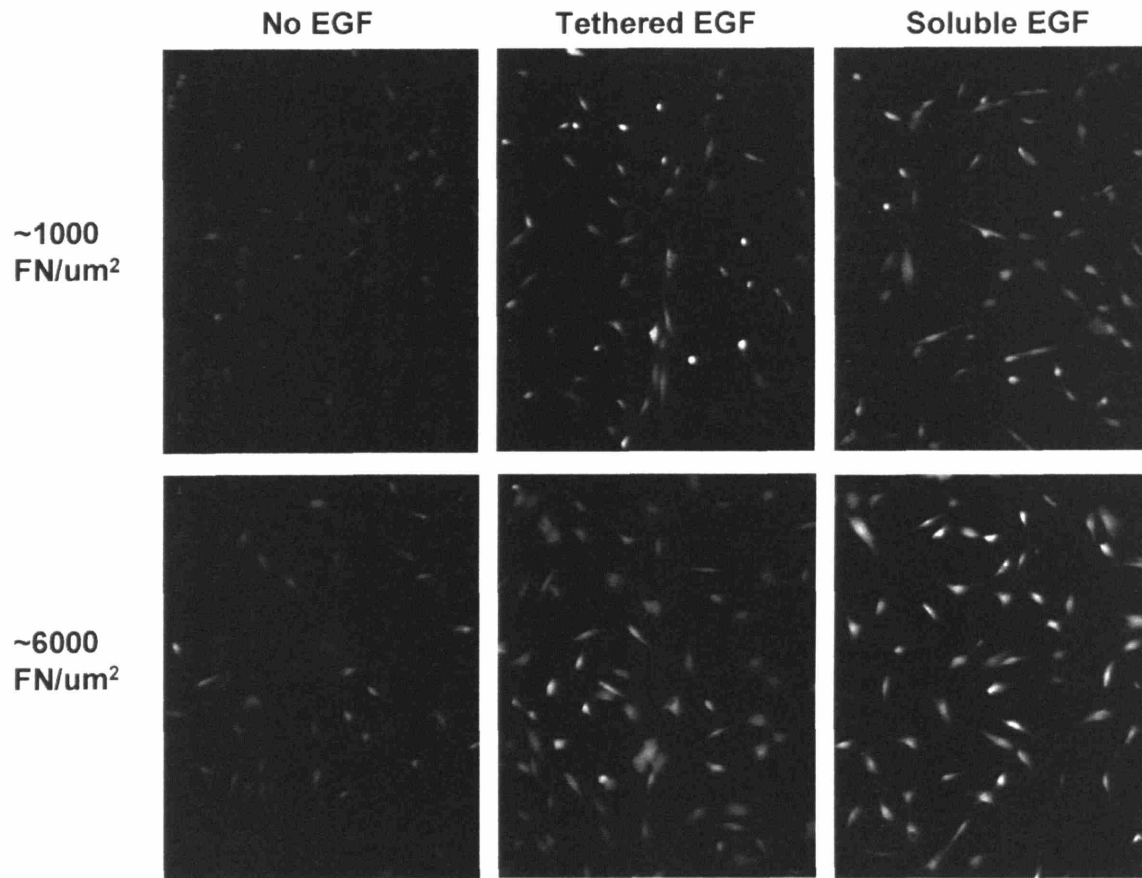


Figure 4.12 – Tethered EGF elicits calpain activity similar to soluble EGF. Calpain activity was qualitatively observed in WTNR6 fibroblasts on polymer substrates with ~1000 and ~6000 adsorbed FN/um² without EGF, on ~65,000 tethered EGF/um², or in the presence of 25 nM soluble EGF. Quiescent fibroblasts were seeded on substrates for 8 hours at which time 10 uM Boc-LM-CMAC, a calpain substrate that increases fluorescence upon cleavage by calpain, was added to the medium for 20 minutes. Fluorescence images were acquired. Relative brightness indicates level of activity at 8 hours. High density tethered EGF elicits similar calpain activity to soluble EGF.

4.3.8 FAK Phosphorylation Depends on Adhesion Ligand Density and EGF Presentation

FAK is another important signaling molecule in the regulation of cell motility as it interacts with both EGFR and integrins and is necessary for focal adhesion turnover. Similar to ERK, we quantitatively measured FAK phosphorylation via Western blot on

Comb 2 substrates with different adhesion ligand densities and EGF presentations. Phosphorylation of tyrosine 397 on FAK was probed because it is the first tyrosine phosphorylated during FAK activation and it is phosphorylated upon EGF stimulation (Sieg, Hauck et al. 2000; Schlaepfer and Mitra 2004).

FAK phosphorylation at Y397 increases with time as the fibroblasts engage integrins during spreading (Figure 4.13). Qualitatively, it appeared that differences in the magnitude and timescale of phosphorylation were due to changes in adhesion ligand density as well as the manner in which EGF was presented (tethered vs. soluble).

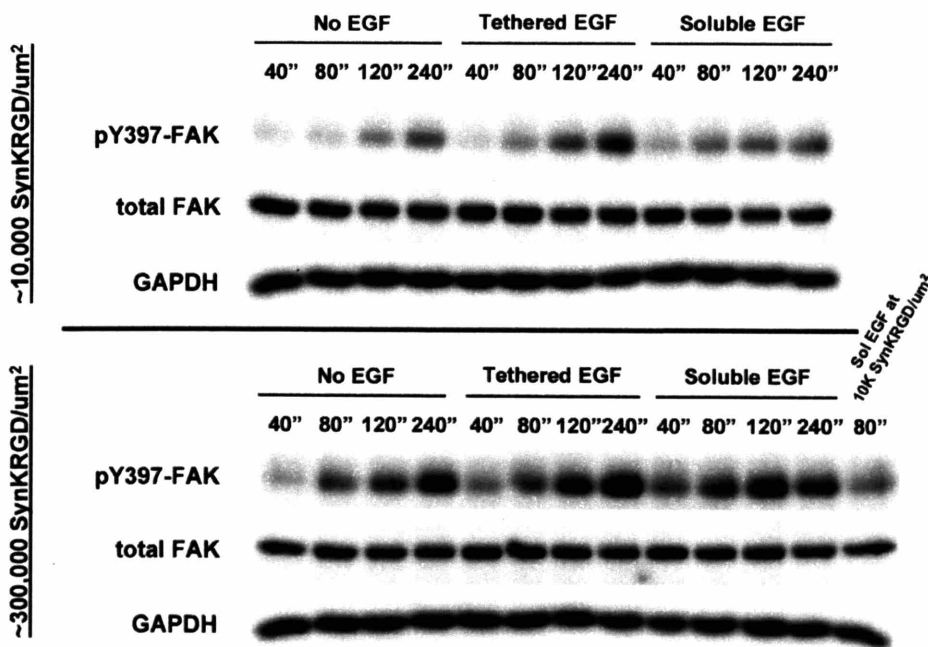


Figure 4.13 – FAK phosphorylation depends on adhesion ligand density and EGF presentation. WTNr6 fibroblasts were seeded on Comb 2 substrates presenting low density tethered EGF (~ 7000 EGF/ μm^2) with either a low adhesion ligand density of $\sim 10,000$ tethered SynKRGD/ μm^2 or a high adhesion ligand density of $\sim 300,000$ tethered SynKRGD/ μm^2 . Lysates over the course of 4 hours were probed with antibodies against phosphorylated Y397 on FAK, total FAK, and GAPDH. Differences in phosphorylated FAK due to adhesion ligand density as well as EGF presentation (tethered vs. soluble EGF) were observed. These blots are representative of three experiments. Quantitative densitometric analysis of the three experiments is presented in Figures 4.14 and 4.15.

This was quantified by plotting FAK phosphorylation intensities in Figures 4.14 and 4.15.

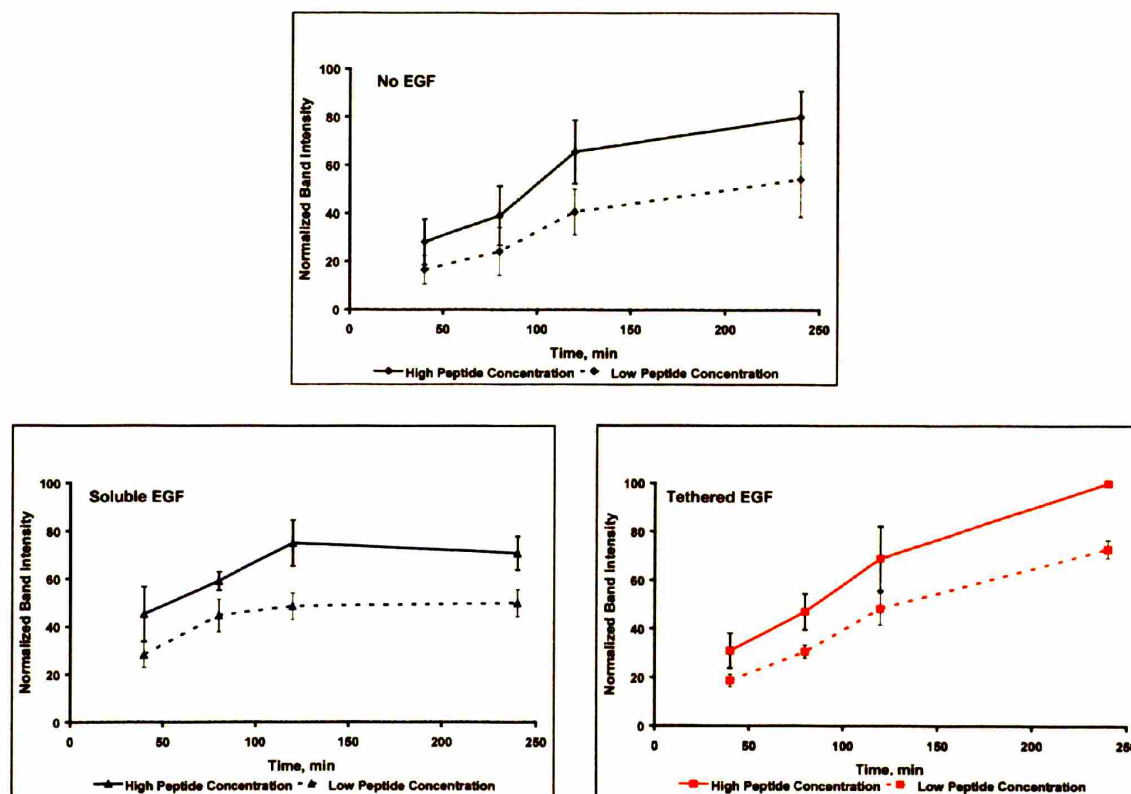


Figure 4.14 – FAK phosphorylation increases with adhesion ligand density.

Densitometry of three independent Western blot experiments for phosphorylated Y397 on FAK represented by the blots in Figure 4.13 was performed. Net intensities of bands for no EGF, low density tethered EGF, and 25 nM soluble EGF over 4 hours were quantified at SynKRGD densities of $\sim 10,000$ and $\sim 300,000$ SynKRGD/ μm^2 . They were normalized to the maximum intensity and plotted for each condition to compare FAK phosphorylation between adhesion ligand densities. FAK phosphorylation increased significantly with higher SynKRGD density independent of EGF presentation. (ANOVA statistical analysis: $\sim 300,000$ SynKRGD/ μm^2 pY397-FAK intensity $>$ $\sim 10,000$ SynKRGD/ μm^2 pY397-FAK intensity with $p << 0.01$ for no EGF, tethered EGF, and soluble EGF conditions).

Indeed, adhesion ligand density significantly influences FAK activation for all EGF presentations as an upward shift in phosphorylation intensity is observed with increased SynKRGD density (Figure 4.14). ANOVA statistics confirm this shift with $p << 0.01$ for no EGF, tethered EGF, and soluble EGF. EGF presentation does not have a statistical

impact on FAK phosphorylation when considering all time points, but the trends of soluble and tethered EGF are qualitatively different. As depicted in Figure 4.14, tethered EGF increases FAK phosphorylation monotonically over the first four hours, whereas soluble EGF plateaus earlier. This time-dependent phenomenon is noticeable at high densities of tethered EGF with $\sim 6000 \text{ FN}/\mu\text{m}^2$ present such as in Figure 4.8. There, FAK phosphorylation is obviously enhanced by both soluble EGF and tethered EGF. However, the enhancement appears earlier for soluble EGF with strong FAK phosphorylation at 40 minutes and a substantial decrease at 4 hours whereas it is delayed for tethered EGF as the fibroblast spreads but it persists at high levels through 4 hours.

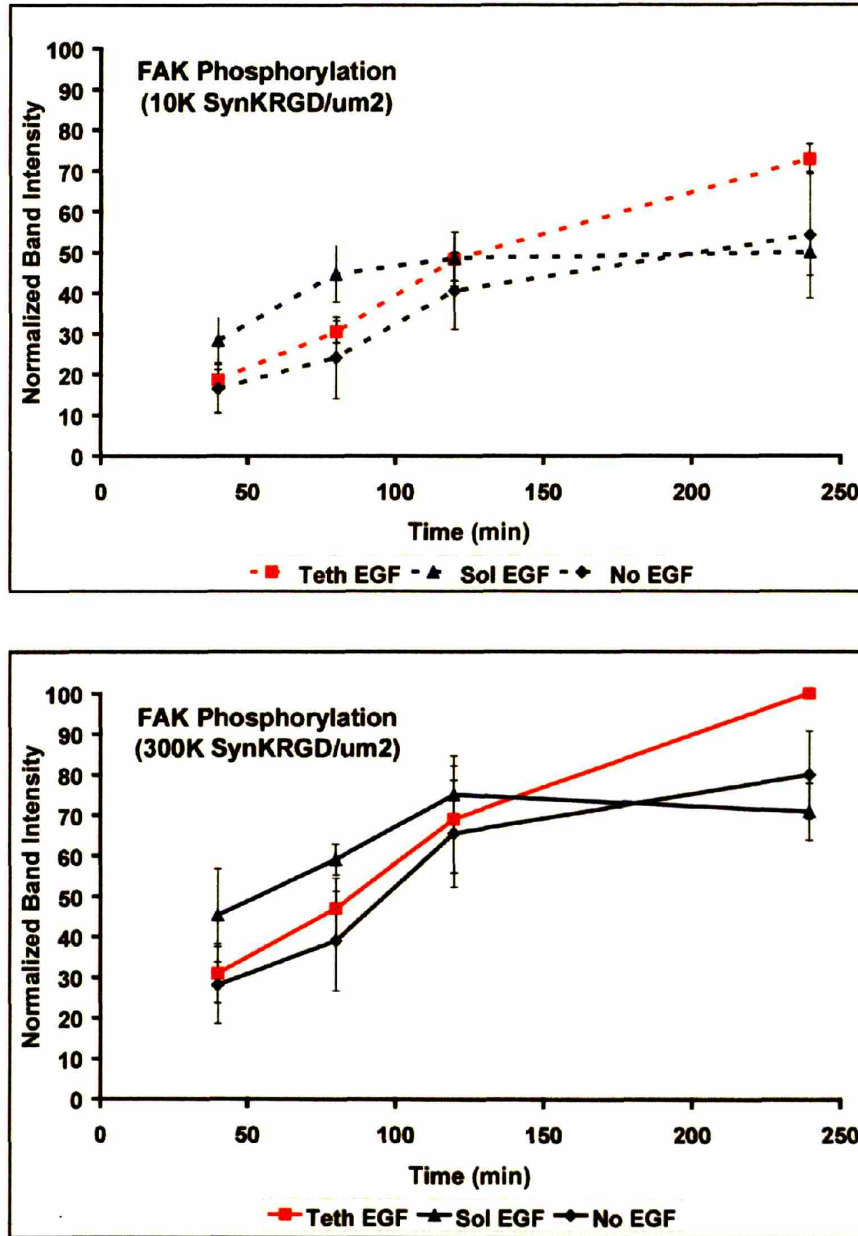


Figure 4.15 – FAK phosphorylation as a function of EGF presentation.

The densitometric net intensity data in Figure 4.14 were replotted to compare FAK phosphorylation as a function of EGF presentation, i.e. no EGF vs. low density tethered EGF vs. 25 nM soluble EGF. Comparing FAK phosphorylations between different EGF presentations did not reveal statistical significance over the entire 4 hour period, although FAK phosphorylation by tethered EGF was statistically greater than no EGF and soluble EGF at the 4-hour time point (*Two-tailed t-test at 4 hours*: Tethered EGF > Soluble EGF for 10,000 and 300,000 SynKRGD/um², $p < 0.01$ in each case; Tethered EGF > No EGF for 300,000 SynKRGD/um², $p < 0.04$). Qualitative time-dependent patterns were different as tethered EGF FAK phosphorylation increased monotonically and soluble EGF phospho-FAK intensity reached a plateau prior to 4 hours.

4.3.9 Variation in FAK and ERK Phosphorylation on EGF-FN Substrates

The combination of adhesion-dependent and EGF presentation-dependent regulation of FAK and ERK seen on Comb 2 substrates and observed qualitatively on initial blots on Comb 1 substrates with ~ 6000 FN/ μm^2 rendered the two molecules interesting candidates for further study as potentially significant regulators of cell motility on the Comb 1 EGF-FN substrates. FAK has been shown to be necessary for cell migration as FAK-null fibroblasts display motility defects that can be eliminated by reconstitution of FAK expression (Sieg, Hauck et al. 1999). FAK is localized to the cell front during focal contact formation (Zaidel-Bar, Ballestrem et al. 2003). It has also been connected to focal contact disassembly by rate limitation in FAK-null cells (Webb, Donais et al. 2004) and due to its ability to complex with ERK and m-calpain for increased protease activity at focal adhesion sites (Carragher, Westhoff et al. 2003). In addition, overexpression of FAK has been noted in invasive tumor cells (Slack, Adams et al. 2001; Hauck, Hsia et al. 2002). Meanwhile, ERK signaling is also necessary for EGF-induced cell migration and mediates rear de-adhesion of the cell through m-calpain (Glading, Chang et al. 2000).

To determine if either FAK or ERK might contribute to the biphasic curve shift between soluble and tethered EGF seen in Chapter 3, we quantified their phosphorylation intensities on Comb 1 substrates with varying FN coating concentrations via densitometric Western blot (Figures 4.16, 4.17, and 4.18). These substrates were prepared in the same manner as those used in the motility experiments.

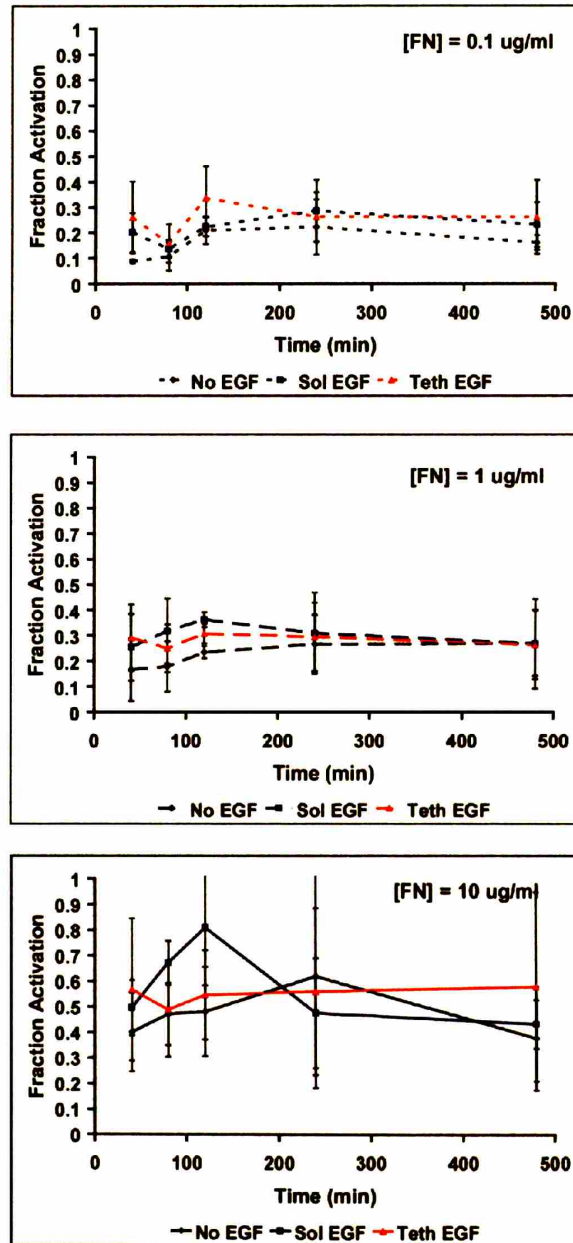


Figure 4.16 – FAK phosphorylation on Comb 1 EGF-FN substrates as a function of EGF presentation at different FN coating concentrations. Densitometry of three independent Western blot experiments for phosphorylated Y397 on FAK was performed on lysates from Comb 1 EGF-FN substrates prepared in the same manner as the motility experiments in Chapter 3. Net intensities of bands for no EGF, high density tethered EGF, and 25 nM soluble EGF over 8 hours were quantified at FN coating concentrations of 0.1, 1, and 10 ug/ml. Intensities in each experiment were first normalized to a reference lysate loaded in all gels and then normalized to the maximum intensity in the experiment to report “Fraction Activation”. Data are plotted here to compare FAK phosphorylation as a function of EGF presentation at each FN coating concentration. No statistically significant differences were observed between EGF presentations.

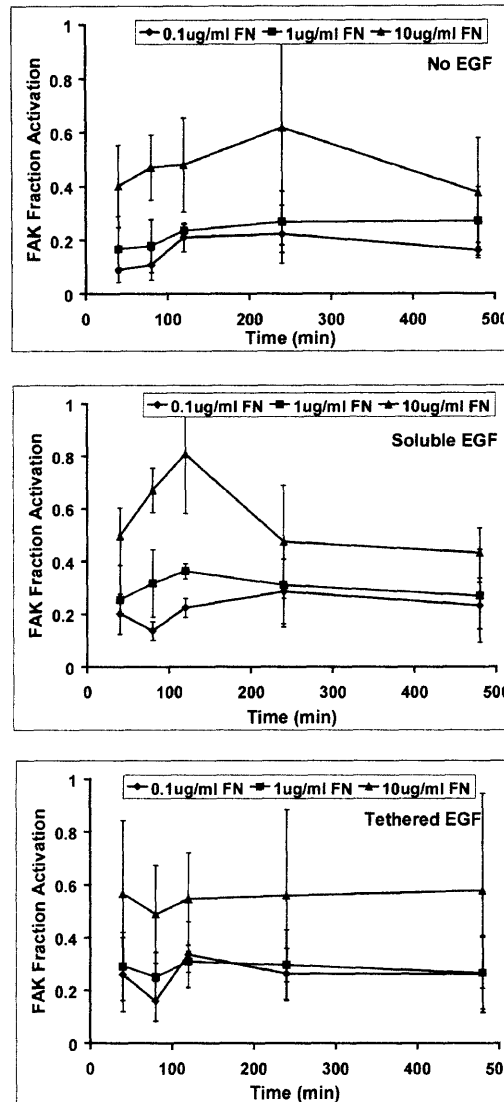


Figure 4.17 - FAK phosphorylation on Comb 1 EGF-FN substrates increases with FN coating concentration for all EGF presentations. Densitometry of three independent Western blot experiments for phosphorylated Y397 on FAK was performed on lysates from Comb 1 EGF-FN substrates prepared in the same manner as the motility experiments in Chapter 3. Net intensities of bands for no EGF, high density tethered EGF, and 25 nM soluble EGF over 8 hours were quantified at FN coating concentrations of 0.1, 1, and 10 $\mu\text{g}/\text{ml}$. Intensities in each experiment were first normalized to a reference lysate loaded in all gels and then normalized to the maximum intensity in the experiment to report “Fraction Activation”. Data are plotted here to compare FAK phosphorylation as a function of FN coating concentration for each EGF presentation. FAK phosphorylation increased significantly as FN density increased for all EGF presentations. (*ANOVA statistical analysis: No EGF: [FN]=1 $\mu\text{g}/\text{ml}$ > [FN]=0.1 $\mu\text{g}/\text{ml}$, $p < 0.05$; [FN]=10 $\mu\text{g}/\text{ml}$ > [FN]=1 $\mu\text{g}/\text{ml}$, $p < 0.002$; Soluble EGF: [FN]=1 $\mu\text{g}/\text{ml}$ > [FN]=0.1 $\mu\text{g}/\text{ml}$, $p < 0.05$; [FN]=10 $\mu\text{g}/\text{ml}$ > [FN]=1 $\mu\text{g}/\text{ml}$, $p < 0.001$; Tethered EGF: No significant difference between [FN]=1 $\mu\text{g}/\text{ml}$ and [FN]=0.1 $\mu\text{g}/\text{ml}$; [FN]=10 $\mu\text{g}/\text{ml}$ > [FN]=1 $\mu\text{g}/\text{ml}$, $p < 0.003$).*)

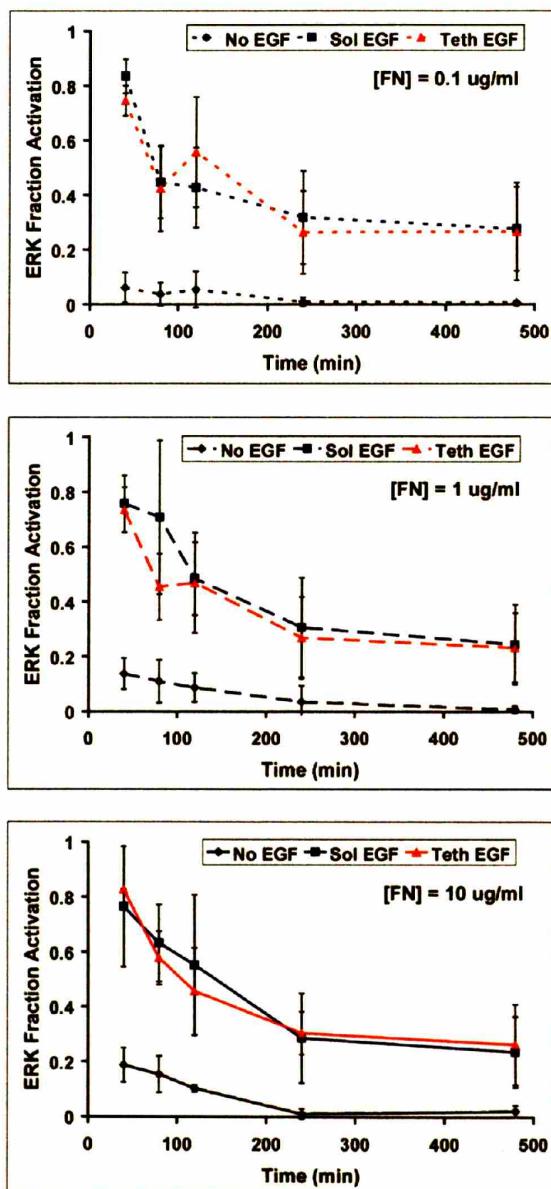


Figure 4.18 – ERK phosphorylation over time on tethered EGF-FN substrates is similar to soluble EGF independent of FN density.

Densitometry of three independent Western blot experiments for phosphorylated ERK 1/2 was performed on lysates from Comb 1 EGF-FN substrates prepared in the same manner as the motility experiments in Chapter 3. Net intensities of bands for no EGF, high density tethered EGF, and 25 nM soluble EGF over 8 hours were quantified at FN coating concentrations of 0.1, 1, and 10 ug/ml. Intensities in each experiment were first normalized to a reference lysate loaded in all gels and then normalized to the maximum intensity in the experiment to report “Fraction Activation”. Data are plotted here to compare ERK phosphorylation as a function of EGF presentation at each FN coating concentration. No statistically significant differences were observed between tethered or soluble EGF. Both EGF presentations significantly increased ERK phosphorylation over the unstimulated condition.

Unfortunately, no statistically significant differences in FAK or ERK phosphorylation were observed between tethered EGF and soluble EGF that might dictate the biphasic curve shift (Figures 4.16 and 4.18). FAK phosphorylation appeared more variable on Comb 1 EGF-FN substrates than on the Comb 2 EGF-SynKRGD substrates making statistical differences difficult to achieve (Figure 4.16). ERK phosphorylation, however, was less variable and displayed significant increases for both tethered and soluble EGF in comparison to no EGF.

Despite the relatively noisy observations of FAK phosphorylation on EGF-FN substrates, it was apparent that FAK activity increased with greater FN density across all EGF conditions (Figure 4.17). ANOVA statistics support this observation with statistical differences between each of three FN coating concentrations for all EGF conditions with one exception. The difference in FAK phosphorylation intensity between the FN coating concentrations 0.1 ug/ml and 1 ug/ml for tethered EGF was not significant.

Unlike our earlier studies of ERK activity on Comb 2 substrates with low density tethered EGF and SynKRGD, we did not see any differences in ERK phosphorylation due to changes in Comb 1 substrate adhesiveness. It can be seen in Figure 4.18 that the phospho-ERK curves for both tethered and soluble EGF at different FN densities are the same qualitatively and quantitatively.

From this data, we cannot conclusively contribute regulation of the biphasic curve by EGF presentation to changes in the magnitude or duration of ERK or FAK signaling.

4.4 Discussion

4.4.1 Matrikine Growth Factors: Avidity Signaling Via Spatially Restricted EGFR

Matrix-embedded signaling molecules have an inherent barrier in that they must be present in spatially localized densities that permit receptor dimerization to achieve receptor activation. Physiologically this is accomplished because large molecules like tenascin have multiple EGF-like repeats. While these repeats have lower affinity for EGFR, their avidity allows them to initiate intracellular signals (Swindle, Tran et al. 2001) while their spatial restriction maintains their presence at the cell membrane.

We recognized early in our work with tethered EGF that despite our presentation of high surface densities that should theoretically saturate cell surface receptors (Figure 4.5), the magnitude of EGFR phosphorylation achieved on these substrates was consistently less than when cells were presented with high concentrations of soluble EGF (Figure 4.2 A). This observation might be attributed to a reduction in affinity for the receptor because of the artificial N-terminal tether addition, a phenomenon seen with the addition of certain membrane-anchoring ligand domains (Dong, Opresko et al. 2005). However, in spite of the relatively weak EGFR phosphorylation, we still observed strong downstream signaling in ERK, FAK, and Akt (Figure 4.8).

Therefore, the potential existed that ErbB2, the EGFR family member not requiring a ligand, could contribute to this downstream signaling. Our cells express ErbB2 (Figure 4.6), which heterodimerizes with bound EGFR and signals in a similar fashion. Indeed, we did observe ErbB2 phosphorylation on tethered EGF surfaces (Figure

4.7), but it was not as strong as with soluble EGF. The strong downstream signals achieved with relatively low receptor phosphorylation provide evidence that saturating EGFR is not necessary for strong signal propagation and illustrate the importance of cascade amplification in signaling pathways. Thus, less affine matrikine ligands without the ability to strongly activate EGFR as modeled by our tethered EGF constructs may still elicit consequential intracellular signals.

The underlying assumption of matrikine growth factors is that matrix-tethered molecules signal from the cell surface. We showed that tethered EGF indeed restricts EGFR activation to the cell-substrate interface by inhibiting ligand-induced internalization (Figure 4.1). This phenomenon has implications in spatiotemporal regulation of EGFR-mediated signaling. It ultimately prevents degradation of receptors as demonstrated in Figure 4.4. Cells internalize and degrade activated EGFR as a means of signal attenuation, depleting receptors at the cell surface to desensitize themselves from further ligand stimulation (Wiley 2003). It is therefore possible that certain signals may be prolonged by maintaining EGFR at the cell membrane. On tethered EGF surfaces, we observed above background phosphorylation of EGFR Y1068 even after 24 hours (Figure 4.3). However, the difference between a matrikine factor and a soluble one is not as simple as a global on-off signal switch regulated by EGFR activation, internalization, and degradation.

4.4.2 Spatiotemporal Governance of Specific Signals

Internalization has also been shown to play a key role in transferring specific signals to the cell interior (Wiley and Burke 2001). While EGFR's are phosphorylated both at the cell membrane and within endosomes, experimental work has shown that they

act on different pools of spatially localized substrates, a particularly relevant observation for the cell surface-restricted matrikine ligands modeled by tethered EGF. Some signaling molecules like PLC γ act primarily at the cell surface (Haugh, Schooler et al. 1999; Haugh and Meyer 2002), while others, such as Eps8 and c-Cbl, associate with internalized EGFR (Burke, Schooler et al. 2001). Then there are still other molecules, like ERK, that are active throughout the cell, but their balance of membrane versus cytosolic signaling may be influenced by internalization or lack thereof (Vieira, Lamaze et al. 1996; Haugh, Huang et al. 1999; Burke, Schooler et al. 2001). Ubiquitous molecules may even serve different functions dependent upon their spatial localization, such as the regulation of m-calpain by a membrane-proximal ERK pool (Glading, Uberall et al. 2001).

An interesting question is how the numerous distinct signals referred to here are generated by one receptor with such diverse spatiotemporal control. In addition to compartmentalizing particular signaling substrates, such as the membrane-localized phosphoinositides acted on by PLC γ (Haugh and Meyer 2002), cells may also induce certain signals by selectively phosphorylating particular EGFR tyrosine residues. Constituents of downstream signaling pathways generally bind the receptor at specific phosphorylated tyrosines such as PLC γ at Y992 and Y1173, Grb2 at Y1068 and Y1086, and Shc at multiple sites (Batzer, Rotin et al. 1994; Chattopadhyay, Vecchi et al. 1999). Redundancy may allow graduated control of the strength of specific signals. We observed for the case of low density tethered EGF that membrane-restricted EGFR activated by the tethered ligand caused differential receptor tyrosine phosphorylation. Figure 4.3 illustrates how Y1068 displayed sustained phosphorylation while Y1173 was rapidly dephosphorylated shortly after activation by tethered EGF. This particular

phosphorylation pattern was not observed for the soluble EGF case (Figure 4.2). Previous work has shown that integrins also induce a different pattern of EGFR tyrosine phosphorylations from soluble EGF (Moro, Dolce et al. 2002). Thus, dynamic patterns of receptor tyrosine phosphorylation in response to different ligands, concentrations, or presentation modes may provide molecule-specific spatiotemporal control of multiple signals.

But how does the cell modulate individual tyrosine phosphorylations such as turning off Y1173 while maintaining phosphorylation of other tyrosines? Evidence suggests that it does so via residue-specific phosphatases. For our case of rapid Y1173 dephosphorylation, we suspect that it occurs by SHP-1, a phosphatase that specifically binds to Y1173 (Keilhack, Tenev et al. 1998). Because rapid Y1173 dephosphorylation happens only in the instance of membrane-restricted EGFR activation, SHP-1 phosphatase regulation may occur preferentially at the cell membrane. In support of this argument, Haugh et al. have presented models suggesting the importance of spatially localized phosphatase regulation (Haugh, Schneider et al. 2004). If this is indeed the case, our observation of differential tyrosine phosphorylation illustrates how the cell governs both the spatial and temporal distributions of individual signals through a competition of localized and specific positive and negative regulators.

4.4.3 Signal Regulation By Adhesion and EGF Presentation

With a better understanding of how EGFR regulates specific signals, we investigated the synergistic effects of adhesion modulation and EGF presentation on signaling molecules downstream of EGFR. Particular interest was given to regulators of biophysical mechanisms involved in the cell adhesion and motility responses studied

during the course of this work. While their functions are not completely understood, ERK, FAK and m-calpain are known to play important EGFR and integrin-governed roles in cell adhesion and migration. Akt was also examined as it is an adhesion-dependent survival signal synergistically governed by integrins and EGFR.

As expected, we observed significant adhesion-mediated influences on both ERK and FAK signaling using our $\alpha_5\beta_1$ and $\alpha_v\beta_3$ integrin-specific Comb 2 SynKRGD substrates. As integrins engage adhesion ligands during attachment and spreading, a transient ERK signal occurs via a corresponding EGFR phosphorylation. This happens even without the presence of EGF (Figures 4.3 and 4.9), although the phosphorylations are significantly weaker than an initial activation by EGF. This integrin-mediated EGFR and ERK activation has been studied previously and is a necessary contributor to EGF-stimulated transcription and the resultant cell survival and proliferation responses, which are intrinsically anchorage-dependent (Moro, Venturino et al. 1998; Short, Talbott et al. 1998; Cabodi, Moro et al. 2004). Interestingly, quantification of phosphorylation levels revealed that tethered and soluble EGF-induced ERK phosphorylation in addition to EGF-independent ERK activity was modulated by adhesion ligand density (Figure 4.10). Despite the fact that EGF presented in either form elicits significantly stronger ERK phosphorylation than integrins alone, ERK activity in the presence of tethered or soluble EGF is still synergistically modulated by cell-matrix adhesions. Thus, integrin activation is a required contributor to EGF-induced ERK activity and modulates its signal strength.

Similar to ERK, FAK phosphorylation, which is crucial for focal adhesion turnover in migrating cells (Sieg, Hauck et al. 2000), showed modulation by adhesion ligand density. Because FAK binds to and is activated by integrins, it displays increasing

phosphorylation over time as cells adhere and spread on a substrate (Figure 4.13). FAK phosphorylation levels also increase with greater adhesion ligand density at any given time independent of EGF because more integrins are engaged (Figure 4.14). Since FAK phosphorylation is necessary for cell migration, this is an expected but important finding in considering the biochemical regulation of cell motility.

We hoped to see similar statistically significant differences in ERK or FAK signaling on the Comb 1 FN substrates used in our cell motility experiments that might explain the shift in the biphasic curve from soluble to tethered EGF. Interestingly, previous work suggests that ERK and FAK, which provide divergent pathways downstream of EGFR and integrins, may later converge to collaboratively regulate the the dynamics of adhesion in motility. ERK and m-calpain have been shown to form a complex with FAK at the cell membrane (Carragher, Westhoff et al. 2003). Thus, in addition to its involvement in focal contact maturation (Sieg, Hauck et al. 1999; Zaidel-Bar, Ballestrem et al. 2003), a role exists for FAK in recruiting m-calpain and its upstream activator, ERK, to focal adhesion sites, spatially localizing the protease and its activator to promote cleavage of focal adhesion proteins and subsequent focal adhesion disassembly (Mitra, Hanson et al. 2005).

Unfortunately, our quantitative signaling studies on the Comb 1 substrates did not yield any significant differences in ERK or FAK signaling between soluble and tethered EGF presentations. While the FAK phosphorylation measurements were particularly noisy (Figure 4.16), the ERK intensities displayed less variance and demonstrated a marked increase between conditions with and without EGF, albeit no difference between soluble and tethered EGF (Figure 4.18). Despite the fact that we could not discern

differences in FAK signaling due to EGF presentation, our finding that FAK phosphorylation increased statistically with FN density on these substrates is similar to our observation on the Comb 2 SynKRGD surfaces. This underscores the importance of FAK in regulating cell-matrix connections, which increase with FN or adhesion ligand density and contribute to the modulation of cell migration speed.

Even though we cannot yet explain biochemically our observed difference in cell migration speed between tethered and soluble EGF, portions of this work support the assertion that EGF presentation plays a role in synergistically regulating intracellular signals. EGF was necessary for prolonged ERK phosphorylation, and it enhanced FAK phosphorylation relative to the integrin-mediated signal. Phosphorylation of Akt, an important signal for anchorage-dependent survival (Kauffmann-Zeh, Rodriguez-Viciana et al. 1997; Fujio and Walsh 1999), was also enhanced by the addition of EGF. Differences in the magnitude and duration of these three signals were observed between tethered and soluble EGF (Figures 4.8, 4.9, 4.11, 4.13, and 4.15), some of which may also be influenced by effective concentrations of EGF and levels of cell-substrate adhesion. It is not known whether signal magnitude, duration, or a combination of the two exhibits the greatest influence in governing biophysical mechanisms; it is likely specific to each signal and mechanism. However, the findings here illustrate that cells can discern different ligand presentations via various changes in signal transduction that subsequently manifest themselves in biophysical phenomena as evidenced in our study of cell migration speed in Chapter 3.

Ultimately, cell responses such as motility, proliferation, and survival are governed by a complex set of synergistic signals derived from multiple cues as

demonstrated by the collaborative contributions of EGFR, integrins, and their downstream signaling molecules. The manner in which ligands are presented to cells provides yet another means of biological diversity in their regulation of cell response.

4.5 References

- Batzer, A. G., D. Rotin, et al. (1994). "Hierarchy of binding sites for Grb2 and Shc on the epidermal growth factor receptor." *Mol Cell Biol* **14**(8): 5192-201.
- Burke, P., K. Schooler, et al. (2001). "Regulation of epidermal growth factor receptor signaling by endocytosis and intracellular trafficking." *Mol Biol Cell* **12**(6): 1897-910.
- Cabodi, S., L. Moro, et al. (2004). "Integrin regulation of epidermal growth factor (EGF) receptor and of EGF-dependent responses." *Biochem Soc Trans* **32**(Pt3): 438-42.
- Carragher, N. O., M. A. Westhoff, et al. (2003). "A novel role for FAK as a protease-targeting adaptor protein: regulation by p42 ERK and Src." *Curr Biol* **13**(16): 1442-50.
- Chattopadhyay, A., M. Vecchi, et al. (1999). "The role of individual SH2 domains in mediating association of phospholipase C-gamma 1 with the activated EGF receptor." *J Biol Chem* **274**(37): 26091-7.
- Chen, P., K. Gupta, et al. (1994). "Cell movement elicited by epidermal growth factor receptor requires kinase and autophosphorylation but is separable from mitogenesis." *J Cell Biol* **124**(4): 547-55.
- DeWitt, A. E., J. Y. Dong, et al. (2001). "Quantitative analysis of the EGF receptor autocrine system reveals cryptic regulation of cell response by ligand capture." *J Cell Sci* **114**(Pt 12): 2301-13.
- Dong, J., L. K. Opresko, et al. (2005). "The membrane-anchoring domain of epidermal growth factor receptor ligands dictates their ability to operate in juxtacrine mode." *Mol Biol Cell* **16**(6): 2984-98.
- French, A. R., G. P. Sudlow, et al. (1994). "Postendocytic trafficking of epidermal growth factor-receptor complexes is mediated through saturable and specific endosomal interactions." *J Biol Chem* **269**(22): 15749-55.
- Fujio, Y. and K. Walsh (1999). "Akt mediates cytoprotection of endothelial cells by vascular endothelial growth factor in an anchorage-dependent manner." *J Biol Chem* **274**(23): 16349-54.
- Glading, A., P. Chang, et al. (2000). "Epidermal growth factor receptor activation of calpain is required for fibroblast motility and occurs via an ERK/MAP kinase signaling pathway." *J Biol Chem* **275**(4): 2390-8.
- Glading, A., F. Uberall, et al. (2001). "Membrane proximal ERK signaling is required for M-calpain activation downstream of epidermal growth factor receptor signaling." *J Biol Chem* **276**(26): 23341-8.
- Hauck, C. R., D. A. Hsia, et al. (2002). "The focal adhesion kinase--a regulator of cell migration and invasion." *IUBMB Life* **53**(2): 115-9.
- Haugh, J. M., A. C. Huang, et al. (1999). "Internalized epidermal growth factor receptors participate in the activation of p21(ras) in fibroblasts." *J Biol Chem* **274**(48): 34350-60.
- Haugh, J. M. and T. Meyer (2002). "Active EGF receptors have limited access to PtdIns(4,5)P(2) in endosomes: implications for phospholipase C and PI 3-kinase signaling." *J Cell Sci* **115**(Pt 2): 303-10.

- Haugh, J. M., I. C. Schneider, et al. (2004). "On the cross-regulation of protein tyrosine phosphatases and receptor tyrosine kinases in intracellular signaling." J Theor Biol **230**(1): 119-32.
- Haugh, J. M., K. Schooler, et al. (1999). "Effect of epidermal growth factor receptor internalization on regulation of the phospholipase C-gamma1 signaling pathway." J Biol Chem **274**(13): 8958-65.
- Hendriks, B. S., H. S. Wiley, et al. (2003). "HER2-mediated effects on EGFR endosomal sorting: analysis of biophysical mechanisms." Biophys J **85**(4): 2732-45.
- Kauffmann-Zeh, A., P. Rodriguez-Viciana, et al. (1997). "Suppression of c-Myc-induced apoptosis by Ras signalling through PI(3)K and PKB." Nature **385**(6616): 544-8.
- Keilhack, H., T. Tenev, et al. (1998). "Phosphotyrosine 1173 mediates binding of the protein-tyrosine phosphatase SHP-1 to the epidermal growth factor receptor and attenuation of receptor signaling." J Biol Chem **273**(38): 24839-46.
- Mitra, S. K., D. A. Hanson, et al. (2005). "Focal adhesion kinase: in command and control of cell motility." Nat Rev Mol Cell Biol **6**(1): 56-68.
- Moro, L., L. Dolce, et al. (2002). "Integrin-induced epidermal growth factor (EGF) receptor activation requires c-Src and p130Cas and leads to phosphorylation of specific EGF receptor tyrosines." J Biol Chem **277**(11): 9405-14.
- Moro, L., M. Venturino, et al. (1998). "Integrins induce activation of EGF receptor: role in MAP kinase induction and adhesion-dependent cell survival." Embo J **17**(22): 6622-32.
- Oksvold, M. P., E. Skarpen, et al. (2000). "Immunocytochemical localization of Shc and activated EGF receptor in early endosomes after EGF stimulation of HeLa cells." J Histochem Cytochem **48**(1): 21-33.
- Rodrigues, G. A., M. Falasca, et al. (2000). "A novel positive feedback loop mediated by the docking protein Gab1 and phosphatidylinositol 3-kinase in epidermal growth factor receptor signaling." Mol Cell Biol **20**(4): 1448-59.
- Rosser, B. G., S. P. Powers, et al. (1993). "Calpain activity increases in hepatocytes following addition of ATP. Demonstration by a novel fluorescent approach." J Biol Chem **268**(31): 23593-600.
- Schenk, S., E. Hintermann, et al. (2003). "Binding to EGF receptor of a laminin-5 EGF-like fragment liberated during MMP-dependent mammary gland involution." J Cell Biol **161**(1): 197-209.
- Schlaepfer, D. D. and S. K. Mitra (2004). "Multiple connections link FAK to cell motility and invasion." Curr Opin Genet Dev **14**(1): 92-101.
- Shao, H., H. Y. Cheng, et al. (2003). "Identification and characterization of signal transducer and activator of transcription 3 recruitment sites within the epidermal growth factor receptor." Cancer Res **63**(14): 3923-30.
- Short, S. M., G. A. Talbott, et al. (1998). "Integrin-mediated signaling events in human endothelial cells." Mol Biol Cell **9**(8): 1969-80.
- Sieg, D. J., C. R. Hauck, et al. (2000). "FAK integrates growth-factor and integrin signals to promote cell migration." Nat Cell Biol **2**(5): 249-56.
- Sieg, D. J., C. R. Hauck, et al. (1999). "Required role of focal adhesion kinase (FAK) for integrin-stimulated cell migration." J Cell Sci **112** (Pt 16): 2677-91.

- Slack, J. K., R. B. Adams, et al. (2001). "Alterations in the focal adhesion kinase/Src signal transduction pathway correlate with increased migratory capacity of prostate carcinoma cells." *Oncogene* **20**(10): 1152-63.
- Sorkin, A. and M. Von Zastrow (2002). "Signal transduction and endocytosis: close encounters of many kinds." *Nat Rev Mol Cell Biol* **3**(8): 600-14.
- Swindle, C. S., K. T. Tran, et al. (2001). "Epidermal growth factor (EGF)-like repeats of human tenascin-C as ligands for EGF receptor." *J Cell Biol* **154**(2): 459-68.
- Tran, K. T., L. Griffith, et al. (2004). "Extracellular matrix signaling through growth factor receptors during wound healing." *Wound Repair Regen* **12**(3): 262-8.
- Vieira, A. V., C. Lamaze, et al. (1996). "Control of EGF receptor signaling by clathrin-mediated endocytosis." *Science* **274**(5295): 2086-9.
- Webb, D. J., K. Donais, et al. (2004). "FAK-Src signalling through paxillin, ERK and MLCK regulates adhesion disassembly." *Nat Cell Biol* **6**(2): 154-61.
- Wiley, H. S. (2003). "Trafficking of the ErbB receptors and its influence on signaling." *Experimental Cell Research* **284**(1): 78-88.
- Wiley, H. S. and P. M. Burke (2001). "Regulation of receptor tyrosine kinase signaling by endocytic trafficking." *Traffic* **2**(1): 12-8.
- Zaidel-Bar, R., C. Ballestrem, et al. (2003). "Early molecular events in the assembly of matrix adhesions at the leading edge of migrating cells." *J Cell Sci* **116**(Pt 22): 4605-13.

5 Conclusion and Future Direction

5.1 Conclusion

The goal of tissue engineering is to develop organized tissue structures for use in the repair or replacement of organs. At its core is the necessity to organize cells and their extracellular matrix to recapitulate normal physiology. This involves providing the cells with spatially controlled extracellular biochemical and mechanical stimuli to promote desired signals and responses. Many tissue engineering approaches aim to accomplish this using synthetic substrates with controllable ligand presentations. In this dissertation, we have developed and characterized synthetic substrates that model matrix-restricted ligand presentation, which has been proposed to induce a new mode of spatially specific signaling called matrikine signaling.

In matrikine signaling, signaling moieties bound or embedded in the ECM signal cells primarily from their surface (Swindle, Tran et al. 2001; Tran, Griffith et al. 2004). Our PMMA-g-PEO comb polymer substrates simultaneously present tethered growth factors and adhesion ligands to cells with nanoscale spatial control such that receptor activation is restricted to the cell surface. Using a model EGFR-expressing fibroblast cell line with these artificial ECM's, we demonstrated significant differences in the regulation of signal transduction and in the motility response by EGF presentation, i.e. a matrikine factor-like tethered EGF as opposed to the canonical soluble molecule. As a result of the cell membrane-restricted EGFR activation by tethered EGF, we observed different EGFR phosphorylation patterns and inhibited receptor trafficking and degradation. This altered both the magnitude and timescale of the cell motility-regulating downstream signals ERK

and FAK. We determined, however, that an important contributing factor was the synergistic role that integrins play with EGFR.

While we found that soluble and tethered EGF elicited the same enhanced migration speed, it occurred at different substrate adhesion conditions for each. This suggested that the spatial differences in matrikine EGFR-mediated signaling significantly altered from within the cell the integrin-mediated adhesion that regulates cell motility. Indeed, similar adhesion to tethered EGF substrates required greater FN densities than in the presence of soluble EGF. While we could not specifically attribute this phenotypic phenomenon to ERK or FAK signaling differences as a result of EGF presentation on FN substrates, we did observe modulation of the magnitude of ERK and FAK phosphorylation downstream of EGFR by altering adhesion ligand density on SynKRGD surfaces. In total, we illustrated that EGFR and integrins regulate each other's activities by both inside-out and outside-in means.

The previously demonstrated roles of membrane-localized ERK and FAK in focal adhesion turnover together with our measurements of EGF-induced motility and adhesion indicate that spatial control of cell signaling is an important governing factor in cell motility. This is most likely a basic tenet in dictating and regulating many cell responses. As such, artificial matrix substrates with nanoscale spatial ligand control will grow in their importance both as tools for revealing the intricacies of cell-matrix interactions and ultimately as successful platforms for directed tissue growth and repair in medicine.

5.2 Future Direction

The well characterized PMMA-g-PEO comb polymer system presenting both growth factors and adhesion ligands is a promising platform for further studies of integrin and growth factor receptor synergy. The ability to control both global and local ligand densities of multiple ligands provides the opportunity to investigate how integrins and EGFR interact in response to different spatially localized extracellular ligands. One interesting phenomenon that begs further study is the clustering of integrins and EGFR (Miyamoto, Teramoto et al. 1996). Quantitative microscopy techniques such as image correlation spectroscopy (ICS) offer the ability to examine aggregates of receptors on a sub-cellular scale. They have been utilized to look at integrin clustering (Koo 2003) and could provide insight into the integrin-EGFR co-clustering phenomenon.

In addition, the use of techniques for subcellular localization of signaling molecules would further the study of spatially localized signal transduction with respect to tethered ligands. These biology intensive types of approaches were outside the scope of this thesis, but they might provide a more conclusive explanation of why we observe the phenomenological change in the biphasic motility curve.

As a promising candidate for tissue engineering scaffolds, the comb polymer may some day be used to direct cell growth and organization for the creation of whole tissue structures. The lessons learned here and insights gained in the future will aid in the design of nanoscale features within scaffolds that guide the placement and activity of individual cells contributing to the development of tissue structures. Thus, this polymer system holds continued promise as a cell biology tool and as a platform for the medical advancement of engineered tissues.

5.3 References

- Koo, L. Y. (2003). "Cell Adhesion Regulated Through Nanoscale Ligand Clustering." MIT Ph.D. Thesis.
- Miyamoto, S., H. Teramoto, et al. (1996). "Integrins can collaborate with growth factors for phosphorylation of receptor tyrosine kinases and MAP kinase activation: roles of integrin aggregation and occupancy of receptors." J Cell Biol **135**(6 Pt 1): 1633-42.
- Swindle, C. S., K. T. Tran, et al. (2001). "Epidermal growth factor (EGF)-like repeats of human tenascin-C as ligands for EGF receptor." J Cell Biol **154**(2): 459-68.
- Tran, K. T., L. Griffith, et al. (2004). "Extracellular matrix signaling through growth factor receptors during wound healing." Wound Repair Regen **12**(3): 262-8.



Room 14-0551
77 Massachusetts Avenue
Cambridge, MA 02139
Ph: 617.253.5668 Fax: 617.253.1690
Email: docs@mit.edu
<http://libraries.mit.edu/docs>

DISCLAIMER OF QUALITY

Due to the condition of the original material, there are unavoidable flaws in this reproduction. We have made every effort possible to provide you with the best copy available. If you are dissatisfied with this product and find it unusable, please contact Document Services as soon as possible.

Thank you.

Some pages in the original document contain color pictures or graphics that will not scan or reproduce well.